university of groningen / faculty of mathematics and natural sciences

# Study to the characteristics of HMF autoxidation with a Co/Mn/Br catalyst

Determination of the important parameters for process intensification in a capillary microreactor

MASTER THESIS

Minke Janssens
1879774

Groningen, August 2015

Supervisor: dr. J. Yue
Second supervisor: prof. dr. ir. H.J. Heeres
Daily supervisor: ir. A. Hommes

University of Groningen
Department of Chemical Engineering

# TABLE OF CONTENTS

# ABSTRACT

In this research the characteristics of the autoxidation reaction of HMF in acetic acid with a homogeneous Co/Mn/Br catalyst and acetaldehyde as initiator were explored. The aim was to investigate its potential to be intensified using a capillary microreactor. Three important topics in current green chemistry field are in that way addressed: HMF is a highly valued platform chemical that can readily be produced from biomass. Homogeneous catalysis is considered to be very promising for biomass conversion and the highly efficient microreaction technology is a sustainable engineering tool for process intensification. The behaviour of the reaction was primarily investigated in a semi-batch reactor (SB) at atmospheric pressure and in an autoclave (A) at high pressure. These results were compared to data obtained from preliminary experiments in the capillary microreactor (M). The parameters that were varied in the performed reactions were acetaldehyde (A, SB), catalyst (SB) and HMF concentration (SB), temperature (A, M, SB), pressure (A) and flow rate (M, SB). Although the reaction rate was not assumed to be limited by oxygen mass transfer, experimental data showed the contrary. If oxygen supply is low, the reaction rate is limited by mass transfer and the reaction is suitable for process intensification. The performance of the reaction was enhanced upon operation in a microreactor: for similar reaction time and conditions the DFF and FFCA yield showed an increase of respectively 34% and 94% at medium temperature (70°C), compared to the semi-batch reactor. Compared to the autoclave, operated at higher pressure and furthermore similar conditions, this increase was even 328% and 578%, respectively.

# ACKNOWLEDGEMENTS

First of all I would like to thank Arne Hommes and Jun Yue for their great help during my research. Arne for the very pleasant collaboration, his daily supervision and for always being open to discussion. Jun for sharing his knowledge and for his helpful input during our weekly meetings. Many thanks for your daily supervision on the experiments with the microreactor and your very extensive and adequate feedback on previous versions of this thesis.
Next to that I want to thankfully acknowledge prof. Erik Heeres for being my second supervisor and giving good suggestions on how to improve my research. Thanks to the analytical department as well: Jan-Henk Marsman and Léon Rohrbach, for helping me to find a suitable analytical method, providing guidance on how to use this method and helping me with the troubleshooting. I would also like to thank the technical department: Anne, Erwin and Marcel, for their willingness to help if something was missing from my set-up. Ria, Angela and Zheng, I want to thank for sharing the HPLC-troubles and making the best out of it.

I wouldn't have had as much fun in doing my research as I had, if the atmosphere at the department wasn't so pleasant as it was. Thanks to everyone from the Chemical Engineering department for creating such a nice working atmosphere, with special thanks to Henk, Marte, Marc and Erik. And last but not least, thanks to my roommate Marloes for putting up with the fact that I claimed the living room during the whole summer for writing my thesis.

# LIST OF ABBREVIATIONS

| | |
|---|---|
| A | Autoclave |
| AMF | 5-acetoxymethylfurfural |
| DFF | 2,5-diformylfuran |
| FDCA | 2,5-furandicarboxylic acid |
| FFCA | 5-formylfuran-2-carboxylic acid |
| HMF | 5-hydroxymethyl-2-furancarboxaldehyde; 5-(hydroxymethyl)furfural |
| HMFCA | 5-hydroxymethyl-2-furancarboxylic acid |
| HPLC | High performance liquid chromatography |
| IS | Internal standard |
| M | Microreactor |
| OBMF | 5,5-oxy(bis-meth-ylene)-2-furaldehyde |
| RID | Refraction index detector |
| RM | Reaction mixture |
| RT | Retention time |
| SB | Semi-batch reactor |
| STP | Standard temperature and pressure (0°C; 1 bar) |
| UV | Ultra violet |

# LIST OF SYMBOLS

The parameters that were used in this report are listed below. The units given are SI units; if other units are used, this is clearly stated in the report.

| | | |
|---|---|---|
| $\alpha,\beta,\gamma$ | - | reaction order |
| $\eta_i$ | mol % | yield of compound i |
| $\sigma_i$ | mol% | selectivity of compound i |
| $\varphi$ | - | void fraction |
| [i] | mol $L^{-1}$ | concentration of compound i |
| $[i]_0$ | mol $L^{-1}$ | initial concentration of compound i |
| a | $m^2\ m^{-3}$ | interfacial area |
| $A_i$ | - | area of peak of compound i in chromatogram |
| $E_A$ | J $mol^{-1}$ | activation energy |
| $F_i$ | - | response factor of compound i |
| $k_L$ | m $s^{-1}$ | mass transfer coefficient |
| $k_{m,n}$ | $mol^{1-(m+n)}.L^{(m+n)-1}.s^{-1}$ | reaction rate constant of order (m+n) |
| M | mol $L^{-1}$ | molarity |
| p | Pa | pressure |
| Q | $m^3/s$ | flow rate |

| | | |
|---|---|---|
| $r_{1,2}$ | mol $L^{-1}$ $s^{-1}$ | reaction rate of pathway 1 or 2 |
| R | 8,31 J $K^{-1}$ $mol^{-1}$ | gas constant |
| t | s | reaction time |
| T | K | temperature |
| V | $m^3$ | volume |
| X | - | side products |
| $X_i$ | mol % | conversion of compound i |

# 1. INTRODUCTION

Finding new resources is a trending topic for research at the moment since oil demand is increasing enormously while the oil reserves are being depleted (van Putten, et al. 2013). Therefore, it becomes more and more difficult to meet this demand in the future. Oil is mostly known as the number one source of energy, but it also serves as a very important feedstock for the chemical industry (van Putten, et al. 2013). A transition is inevitable: next to renewable energy resources such as solar and wind energy, sustainable sources for chemicals must be found. Biomass is an extensively investigated example of such a source because it is widely available and renewable (Teong, Yi and Zhang 2014). If biomass is used that does not compete with the food production, it is also a very sustainable source for chemicals (Deuss, Barta and de Vries 2014). Biomass consists of mostly carbohydrates that forms the largest feedstock of natural carbon on earth, next to fossil fuels (van Putten, et al. 2013). Already quite some products have been developed from biomass such as packaging material, fibres, resins, fuels etc. (Werpy, et al. 2004). This is either done by a drop-in strategy or an emerging strategy, i.e. production of common bulk chemicals from biomass or development of completely new structures respectively (Deuss, Barta and de Vries 2014).

## 1.1 Background information

Three important topics in current green chemistry field are combined in this research. Homogeneous catalysis is chosen to oxidise HMF with air under different process conditions. The reaction of converting HMF to valuable products is explored to determine the parameters important for process intensification and the tool that is used for intensification is a capillary microreactor. These topics will be further introduced below.

### 1.1.1 Homogeneous catalysis promising for biomass conversion

Converting biomass into valuable chemicals and building blocks can be done by gasification to e.g. syngas (a mixture of $H_2$ and CO) or by extraction of sugars (Werpy, et al. 2004) that form the basis for a wide range of chemicals. Selective defunctionalisation and subsequently refunctionalisation is key to allow the complex structures present in biomass to be converted to the versatile, valuable chemicals needed for the transition. Homogeneous catalysis enables us to design the catalyst in a very detailed manner, making it highly selective (Deuss, Barta and de Vries 2014). The type of active metal species, as well as the choice of ligands and ionic substitutes are some examples of parameters that can be influenced to enhance the performance of the catalyst (Geilen, et al. 2010). In addition to that, analogous to the oxidation of biomass as it happens in nature, multiple metal ions can be used in one catalyst system as well as several types of catalysts together (Collinsona and Thielemans 2010). Homogeneous catalysts are very promising for biomass conversion since “the platform chemicals and intermediates of a biomass-derived supply chain are not yet fixed as firmly

as in petrochemistry" (Geilen, et al. 2010). Due to the diversity of homogeneous catalysts the design of the complex can be adjusted to the desired synthesis route. Furthermore metals salts are cheap resulting in low catalyst costs per amount of product.
A much heard counterargument of the application of homogeneous catalysis in industry is that regeneration of the catalyst requires additional steps compared to heterogeneous catalysis. This however should not be seen as an inevitable difficulty, but as a subject for creative process solutions. The process can be designed in a way such that separation of the catalyst does not form a problem upon isolation of the desired products. Two-phasic systems with the catalyst in one phase and the reagents and products in the other or membranes that separate the catalyst from the process stream are two possibilities (Deuss, Barta and de Vries 2014).

### 1.1.2 HMF as a key platform chemical

Extensive research is performed to the most valuable chemicals that can be derived from biomass. Furan derivatives show a lot of potential to substitute the petro-based chemicals. A few first-generation furan compounds can readily be prepared from sugars derived from biomass. These compounds form the basis of the majority of current bio-based macromolecules where the aromatic units of their petro-based counterparts are replaced by furan rings (Gandini 2011).
Some furan compounds are "listed as the top 10 value-added bio-based chemicals by the US department of Energy" (Teong, Yi and Zhang 2014) and thus extensive research is done throughout the world to the identify the optimal conditions for synthesis of these compounds. One of these furan compounds is 5-hydroxymethylfurfural (HMF), a compound that has wide applications such as monomer, surfactant, in pharmaceuticals and in plant protection agents (Sanborn 2013). Further conversion of HMF gives even more valuable chemicals. It is therefore a key compound in the production of useful materials from biomass, as is displayed in Figure 1.

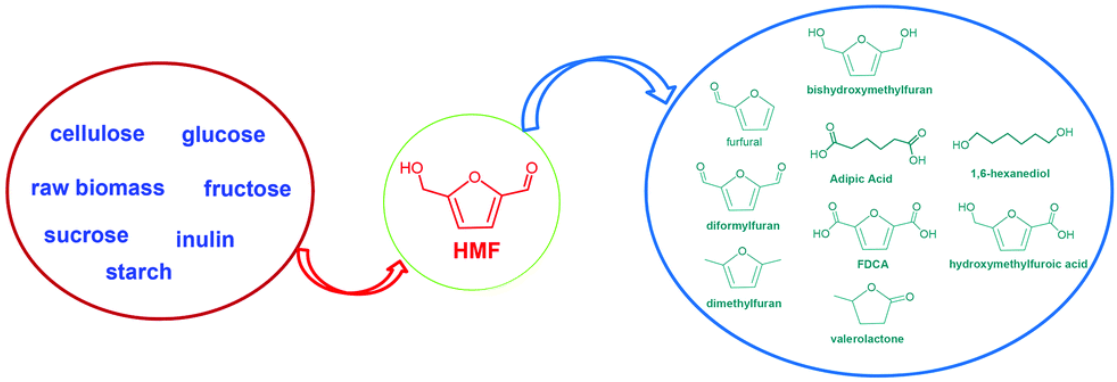


*Figure 1 HMF as a key intermediate in the conversion of biomass to valuable chemicals. Adapted from (Teong, Yi and Zhang 2014).*

Oxidation of HMF gives products that have great value (Sanborn 2013), such as 2,5-furandicarboxylic acid (FDCA) that was already selected by Werpy et al. in 2004 as one of the top 10 chemical opportunities from carbohydrates (Bozell and Petersen 2010). This oxidation reaction has two

intermediate products: 2,5-diformylfuran (DFF) and 5-formylfuran-2-carboxylic acid (FFCA) that have wide applications as well. The reaction scheme is given below if air is used as oxidising agent (r1 – r3). Air is "the ultimate green oxidant" (Vanoye, et al. 2013) because it is sustainable due to its abundant presence in the atmosphere. The reaction equation is displayed in Figure 2.

$$2\ \mathrm{HMF} + \mathrm{O_2} \rightarrow 2\ \mathrm{DFF} + 2\ \mathrm{H_2O} \quad \text{(r1)}$$

$$2\ \mathrm{DFF} + \mathrm{O_2} \rightarrow 2\ \mathrm{FFCA} \quad \text{(r2)}$$

$$2\ \mathrm{FFCA} + \mathrm{O_2} \rightarrow 2\ \mathrm{FDCA} \quad \text{(r3)}$$

$$2\ \mathrm{HMF} + 3\ \mathrm{O_2} \rightarrow 2\ \mathrm{FDCA} + 2\ \mathrm{H_2O} \quad \text{(r4)}$$

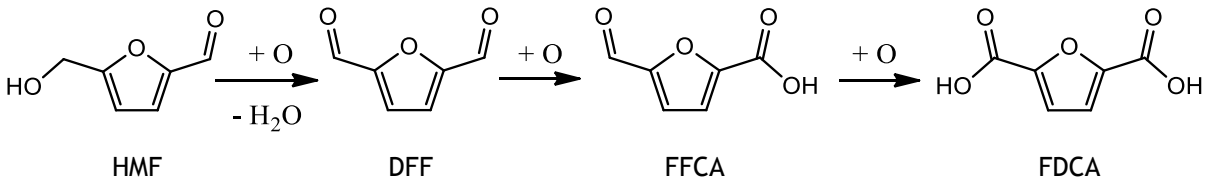


*Figure 2 Reaction equation from HMF to FDCA.*

Most of the oxidation products of HMF have a high potential as a biofuel or polymer (van Putten, et al. 2013). DFF finds its application in pharmaceuticals, photography and macrocyclic ligands. It can also serve as a crosslinking agent, a monomer for many types of polymers, such as polyvinyl or urea-resin and as a starting material for antifungal agents (Ma, et al. 2011, Sanborn 2013, van Putten, et al. 2013). FDCA has high value and is mainly used as a monomer in polyesters or polyamides. The polyesters can be used as packaging material and polyamides to produce new types of nylons (Werpy, et al. 2004, van Putten, et al. 2013). The company Avantium has recently built a pilot plant to produce PEF (poly-2,5-ethylene furancarboxylate), a biobased substitute of PET (polyethylene terephthalate), a widely used polymer for packaging material (van Putten, et al. 2013). It is designed in such a way that process conditions can be changed easily to synthesise and test new products (Dam, et al. 2012). The applications of FFCA are not extensively described, but it can be used as a monomer (van Putten, et al. 2013).

Three other oxidation products are worth addressing are HMFCA, OBMF and AMF, see Figure 3. They belong to the oxidation products with high potential as monomer or biofuel. HMFCA is formed when the aldehyde group of HMF is oxidised. This compound is used as a monomer (Gandini 2011, van Putten, et al. 2013), OBMF is the dimeric ether of HMF and is used for the production of imine-based polymers with glass transition temperatures at 300°C and as hepatitis antiviral precursor (Resasco, et al. 2011). AMF is the ester of HMF with acetic acid and might be used as a biodiesel, but it is mainly investigated as an alternative to HMF for industrial applications. It is just as versatile as a platform chemical as HMF, while AMF is more stable due to the acetoxymethyl group instead of the hydroxymethyl group. Isolation from an aqueous solution is therefore easier (Kang, et al. 2015).

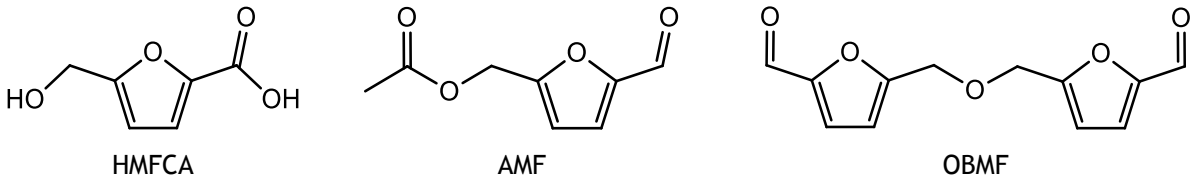


*Figure 3 Structures of important HMF oxidation products.*

### 1.1.3 Autoxidation by a Co/Mn/Br catalyst

In this research the characteristics of homogeneous aerobic HMF oxidation are examined and its potential to be intensified. The catalyst used is the Co/Mn/Br complex, a widely used homogeneous catalyst that is selective and efficient in autoxidation of especially aromatic hydrocarbons (Partenheimer 1995).

#### Structure of the catalyst

By dissolving the metal acetates with NaBr in acetic acid the catalyst complex forms. It can exist in different orientations and structures; either monomeric or dimeric. The orientation of the ligands is dependent on several factors, such as the amount of water present in the mixture. When the hydrated forms of the metal acetates is used, crystallisation water is present in the mixture and different coordination compounds exist. Figure 4 gives some suggested structures for the Co/Mn/Br mixture in acetic acid (Partenheimer 2001).

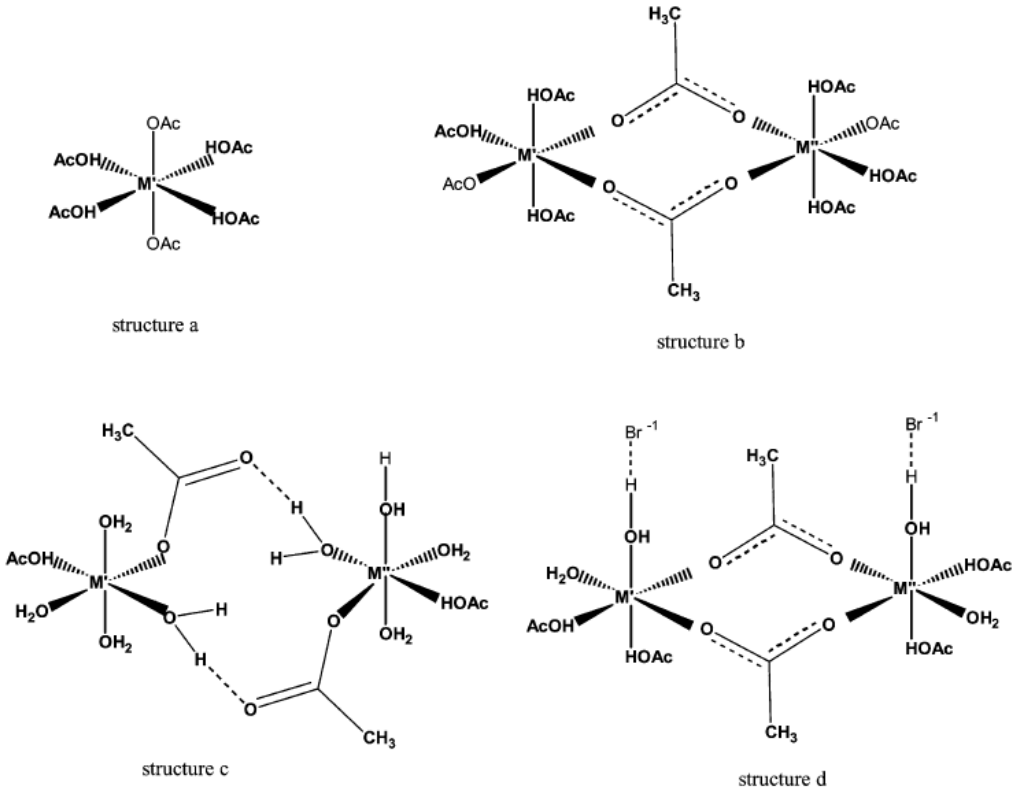


*Figure 4 Suggested structures for Co/Mn/Br mixtures in acetic acid/water mixtures. M = Co(II, III), Mn(II, III). Adapted from (Partenheimer 2001)*

This catalyst works best in carboxylic acid solvents, since the acetic acid ligands are weakly bonded to the metal and can therefore easily be displaced by a peroxo radical, a peroxide or a peracid. Such a structure still exists when acetic acid/water mixtures are used, although to a lesser extent since there are a more complex catalyst structures present due to water-rich microphases (Partenheimer and Grushin 2000). Presence of water inhibits the metal catalysed reactions for HMF oxidation (Partenheimer 2005), since performance of the catalyst then becomes worse. It decreases the rate of the redox cascade in Figure 5. The oxidation rate reduction is already 35% for a water concentration increase of only 5% (Partenheimer 1995). The performance of acetaldehyde oxidation also becomes worse with increase of water concentration (Bawn and Williamson 1950). Catalyst deactivation can also be caused by anti-oxidants, catalyst metal precipitation by aromatic acids, deactivation by aromatic acids, formation of organic bromides, presence of strong acids that inhibit the reaction, specific metals such as vanadium and copper and insufficient oxygen diffusion rates (Partenheimer 1995).

### The working of acetaldehyde oxidation

The Co/Mn/Br catalyst is active in a temperature range between 25°C and 260°C (Partenheimer 1995). It is proven to work better than a mixture of Co/Br which in turn works better than Co as the sole catalyst (Partenheimer 1995, 2000). Addition of bromide decreases the steady state concentration of Co(III) (and Mn(III) if this is present) because bromide is able to oxidise it to Co(II) (or Mn(II)). This is beneficial since decarboxylation of the compounds present during the reaction is in this way reduced, making the catalyst more selective. If manganese is added to the mixture, oxidation of Co(III) is accelerated even more (Partenheimer 1995, 2005).

The catalyst compound that is formed by dissolving, is not yet active for autoxidation. Activation happens when a peroxide or a peroxo radical is formed (Partenheimer 2001). The cobalt then changes oxidation state from Co(II) to Co(III) and a redox cascade is initiated, which is shown in Figure 5. Through this chain of reactions the selective bromide atom is generated that is able to radicalise an alcohol or aldehyde group (Partenheimer and Grushin 2000).


*Figure 5 Summary of the chemistry of Co/Mn/Br autoxidation catalyst. Half-lives are at 60°C in 10% water/acetic acid mixture. Adapted from (Partenheimer and Grushin 2000)*

The peroxide species that oxidises cobalt can be originated from acetaldehyde, because this compound is oxidised more easily than either the hydroxymethyl or aldehyde group of HMF (Partenheimer and Grushin 2000). The initiation of acetaldehyde radical oxidation can be caused by

various reactions (Bawn and Williamson 1950). The exact character of the initiation reaction is difficult to determine, since it has a turbulent character and is highly exothermic (Kagan and Lubarsky 1934). It was experimentally proven however that initiation is induced by a trace of trivalent metal (Kagan and Lubarsky 1934, Bawn and Williamson 1950). In the case of the Co/Mn/Br catalyst this trivalent metal is manganese. Although the steady-state concentration of Mn(III) in solution is as said greatly reduced by use of a Co/Mn/Br mixture (Partenheimer 2005), initiation is possible since only a trace is necessary. The trivalent manganese can form the selective bromide that can radicalise an alcohol or aldehyde group through reaction (r5). This is the rate determining step (Bawn and Williamson 1950).
Once initiation of acetaldehyde has occurred high reaction rates take place (Kagan and Lubarsky 1934); the peracetic acid is formed and the catalyst is further activated by oxidation of Co. The reaction of the acetaldehyde radical is fast with sufficient oxygen supply, as was concluded by Bawn and Williamson (1950). The oxygen uptake that was measured here was higher than would have been expected if the reaction rate depended on oxygen solvation alone (Bawn and Williamson 1950) and thus oxygen is consumed by chemical reaction. The reaction scheme is given below in (r5) to (r10) where Ac is short for $CH_3CO$. Upon dissolving the bromide atoms present in the mixture coordinate to the outer sphere of the metal and can therefore be rapidly reduced by Mn(III) (Partenheimer 2001).

*Initiation*

$$\mathrm{Mn(III) + Br^{-} \rightarrow [Mn(II) - Br^{\cdot}]} \quad \textit{trace} \quad \text{(r5)}$$

$$\mathrm{[Mn(II) - Br\cdot] + AcH \rightarrow Mn(III) + HBr + Ac\cdot} \quad \text{(r6)}$$

*Propagation*

$$\mathrm{Ac\cdot + O_2 \rightarrow AcOO\cdot} \quad \text{(r7)}$$

$$\mathrm{AcOO\cdot + AcH \rightarrow AcOOH + Ac\cdot} \quad \text{(r8)}$$

*Termination*

$$\mathrm{AcOO\cdot + AcOOH \rightarrow \text{inactive products}} \quad \text{(r9)}$$

$$\mathrm{2\ AcOO\cdot \rightarrow \text{inactive products}} \quad \text{(r10)}$$

In the work of Bawn and Williamson (1950) the rate of autoxidation of acetaldehyde with an anhydrous $Co(OAc)_2$ catalyst was proven to be independent of the oxygen pressure within a range of 0.73 to 1.3 bar and directly proportional to the acetaldehyde concentration, which was varied between 0.1 and 0.5 M. It also showed a linear dependence of the catalyst concentration.

Mechanism HMF autoxidation

When propagation of the acetaldehyde mechanism has started, the free radical chain mechanism of HMF oxidation is initiated. A peroxide radical of acetaldehyde radicalises either the alcohol or the aldehyde group of HMF. The work of Partenheimer (2001, 2006) teaches us that the alcohol group of HMF is preferentially oxidised to the aldehyde group to yield DFF. For benzaldehyde it is even true that the compound will not significantly react to the carboxylic acid until almost all benzyl alcohol is converted. The mechanistic cycle of the oxidation of the aldehyde group to the carboxylic acid is shown in Figure 6. A similar cycle for the alcohol can be found in Appendix I: Autoxidation of an aromatic alcohol. The reactions depicted inside the yellow ellipse are accelerated by the catalyst as is shown by the pink arrows. Reaction 14 is e.g. 400,000 times faster than reaction 9. Increasing the catalyst concentration is therefore beneficial to the selectivity of the reaction towards the desired products (Partenheimer 2001, Grushin, Ernest Manzer and Partenheimer 2014). These reactions are inhibited by water that is a side product of the reaction unfortunately, resulting in deactivation of the catalyst during the reaction.

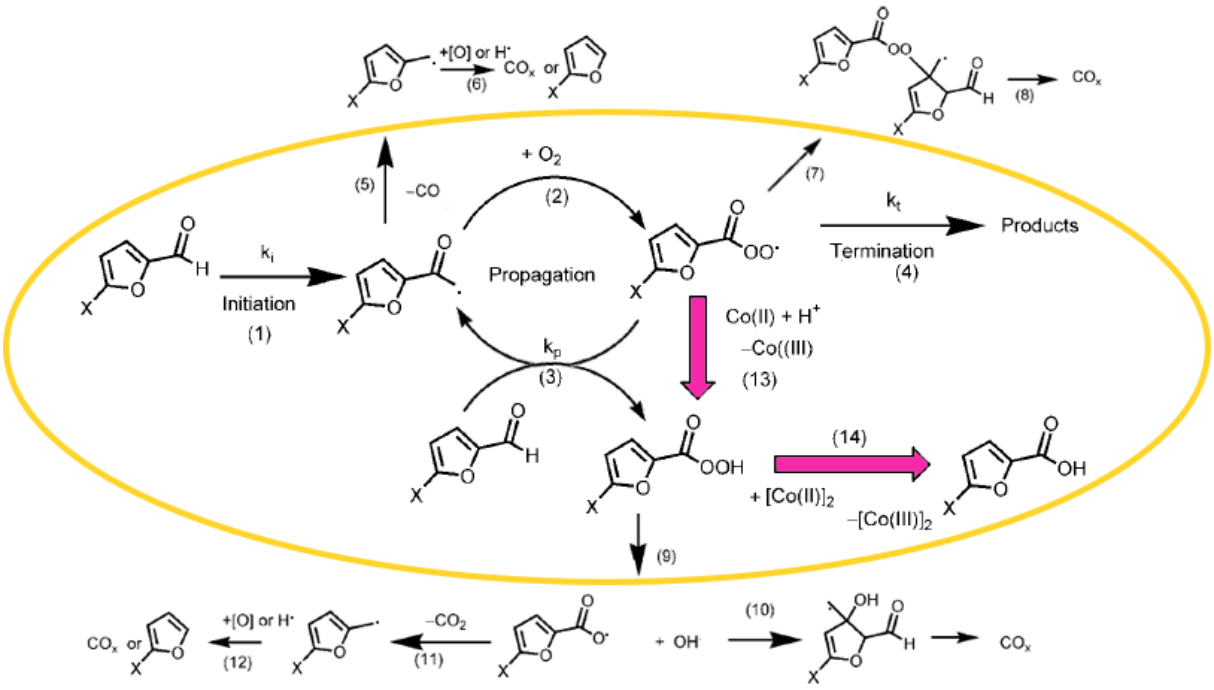


*Figure 6 Overview of the important pathways in HMF oxidation by a radical chain mechanism. Adapted from (Partenheimer and Grushin 2000)*

### 1.1.4 Microreactors as a green tool for process intensification

Continuous flow technology is a very sustainable and efficient way to perform research to new types of reactions or enhanced reaction conditions. The amount of materials needed, the reaction time and waste production is reduced when using flow chemistry; safety is improved, scale up is easier and it is energy and cost efficient. High throughputs per unit volume per unit time can be reached, resulting in reduced screening time for the best reaction conditions compared to batch operation (Vaccaro, et al. 2014). When small reaction volumes are used process conditions such as

temperature, pressure, residence time and flow rate are easily controlled. Safety is increased at operation at high pressure with small volumes (Jähnisch, et al. 2004). In addition to that, small reaction volumes are a great advantage if the starting materials are costly or toxic materials (Jähnisch, et al. 2004, Vaccaro, et al. 2014).
The use of microreaction technology experienced a boost worldwide for application in chemical and biological reactions since a workshop in 1995 in Germany. It was praised for its high surface area to volume ratio, that lies between 10,000 and 50,000 $m^2m^{-3}$ where traditional reactors scarcely offer an interfacial area of 1,000 $m^2m^{-3}$. Thanks to this efficient heat transfer is possible, enabling safe operation of explosive or highly exothermic reactions. A microreactor offers operation with laminar, directed and highly symmetric flow. Further intensification of the reaction is improved by enhanced mass transport. All these features enable rational design of the microsystem (Jähnisch, et al. 2004).
The sustainability of a process is enhanced if this process can be intensified, i.e. higher productivity in grams produced per hour per reactor volume or shorter reaction times. Flow technology is a tool that is currently much used for this purpose (Vaccaro, et al. 2014) because of the advantages described above. Next to that it is a great engineering tool to gain information about a process in short time and with greater safety before the transfer to pilot and production scale is made (Jähnisch, et al. 2004). Scale-up is achieved easily by parallel operation of the microreactors (Vaccaro, et al. 2014).

## 1.2 Objective

In this research the homogeneously catalysed autoxidation reaction of HMF is chosen to investigate for intensification. As stated before three important topics in current green chemistry field are combined by the aim of this research: homogeneous catalysis for biomass conversion, HMF as a platform chemical and the highly efficient microreaction technology as an engineering tool to intensify the process and perform research in a sustainable manner.

This research is an inventory research to gain knowledge about the characteristics and limitations of the reaction in batch and semi-batch operation. Fundamental knowledge can be gained on how to perform the reaction, such as kinetics and mass transfer behaviour. With this knowledge first steps to process intensification were made and to enable further research towards optimal intensification.

## 1.3 Approach

In order to determine the limitations of the autoxidation reaction of HMF catalysed by a Co/Mn/Br catalyst, it was performed at atmospheric pressure in a semi-batch operation and at high pressure in a batch operation. In the semi-batch operation the liquid flow was in batch and the air flow was continuous. The work of Saha (2012) provided guidance on the reaction conditions, including the concentrations of the starting material and catalysts. Soon after that however this research turned out to be irreproducible and a switch was made to the conditions as described by Partenheimer and

Grushin (2000). This work also provided a more extensive explanation of the theory behind the reaction.

Once the reaction gave results like described in literature, several parameters were modified to examine the influence hereof. The experimental procedure that was followed is described in paragraphs 2.2.1 and 2.2.2, as well as the parameters that were investigated. Before starting the experiments the most suitable analytical method was determined and an internal standard was chosen to be able to monitor the conversion of starting material and yield of products formed. To get a first idea of the performance in flow operation a few experiments were performed with different air and liquid flow rates at different temperatures in a capillary microreactor. Due to the intensification of mass transfer, higher product yields were obtained in this set of experiments, compared to semi-batch and batch operation.

With all the data that was generated, some nice conclusions were drawn on the kinetics and the mass transfer behaviour of the reaction that are of value for further intensification of the autoxidation reaction of HMF.

# 2. MATERIALS AND METHODS

## 2.1 Chemicals

HMF (97%) was ordered from Hangzhou Dayangchem Co. Ltd. The catalysts $Mn(OAc)_2$ (≥ 99.0 %) and $Co(OAc)_2$ (reagent grade), the internal standard 2,5-pentanedione (≥ 99.5%), the initiator acetaldehyde (≥ 99.5%) and pure products for calibration (DFF (97%), FDCA (97%) and AMF (97%)) were received from Sigma-Aldrich. Catalyst NaBr (extra pure) was obtained from Merck. Pure FFCA (90.3%) for calibration and acetic acid (≥ 99.5%) were purchased at Acros. The percentages in brackets are the purities.
If water was used, it was exclusively milli-Q water from the tap at the faculty. Compressed air at 3 bar was used for the experiments in the semi-batch reactor. For the reactions in the autoclave and the microreactor dry air from a cylinder of Linde Gas (200 bar) was used.

## 2.2 Experimental setup

### 2.2.1 Procedure semi-batch reactor

A three necked round-bottom flask was used for performing HMF oxidation with air at atmospheric pressure. It was equipped with a reflux condenser, an air inlet and a stopper, see Figure 7 and 8. A magnetic stirrer was used to mix the reaction mixture before starting the reaction; it was not used during the reaction. Heating of the reactor took place through an oil bath on a hotplate. The temperature of the oil was constantly measured and was assumed to be equal to the reaction temperature due to good heat transfer via an oil bath. The air flow into the flask was regulated via a mass flow controller (Bronkhorst high-tech, serial number 930044A, type F-201D-FA-22-P). It was calibrated at 353.9 mL/min air at full range before entering the reactor. The inlet could be adjusted from 0% to 100% of this 353.9 mL/min.

A typical experimental procedure is as follows: first, the mass of the empty flask was determined. Then the catalyst materials $Co(OAc)_2$, $Mn(OAc)_2$ and NaBr were weighted and dissolved in acetic acid. The molar ratio that was used in all reactions was (Co + Mn)/Br = 1:1. HMF was dissolved separately in acetic acid and then added to the catalyst solution. After addition of acetaldehyde as the initiator for the reaction, the flask with reaction mixture (total volume: 50 mL) was weighted. The reaction was started by heating up the mixture and introducing a constant air flow. Aliquots were taken in duplicate at set times by removing the stopper and taking around 0.3 mL from the reaction mixture with a syringe. The weight of each aliquot was measured. The syringe was washed in the reaction mixture every time before taking a new aliquot. The method to further work with these aliquots for HPLC analysis is described below. After the reaction was stopped, the flask was weighted again to determine if weight loss occurred in the course of the reaction.

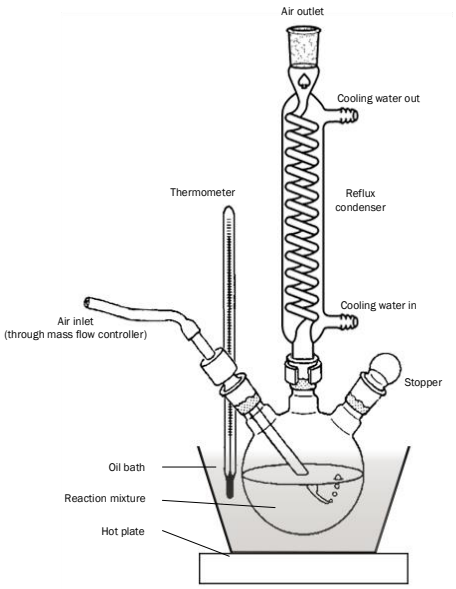


*Figure 7 Schematics of the experimental setup for semi-batch reactor study.*

*Figure 8 Photo of the experimental setup for semi-batch reactor study.*

In this research, several parameters were adjusted to investigate whether these influenced the reaction performance. The parameters and how they were changed are displayed in Table 1; the starting concentrations of HMF are given as measured by HPLC.

*Table 1 Overview of the performed reactions in the semi-batch reactor with different parameters that were changed. The initial concentrations are given as well as reaction temperature and time and air flow rate. This flow rate is expressed as a percentage of 353.9 mL/min. The concentration of bromide in some cases differed from the ideal (Co + Mn)/Br = 1:1 ratio and is therefore given separately.*

| NO. | $[HMF]_0$ (M) | [Co] (M) | [Br] (M) | $[ACETALDEHYDE]_0$ (M) | T (°C) | TIME (H) | AIR FLOW RATE |
|---|---|---|---|---|---|---|---|
| **SB1** | 0.216 | 0 | 0 | 0 | 90 | 5 | 100% |
| **SB2**[†] | 0.155 | 0.030 | 0.062 | 0 | 90 | 8 | >100% |
| **SB3** | 0.185 | 0.030 | 0.061 | 0.226 | 90 | 8 | 100% |
| **SB4** | 0.141 | 0.030 | 0.068 | 0.119 | 90 | 3 | 100% |
| **SB5** | 0.158 | 0.030 | 0.060 | 0.061 | 90 | 3 | 100% |
| **SB6** | 0.190 | 0.030 | 0.068 | 0.245 | 90 | 8 | 50% |
| **SB7** | 0.192 | 0.030 | 0.060 | 0.232 | 90 | 8 | 25% |
| **SB8** | 0.183 | 0.030 | 0.060 | 0.243 | 90 | 8 | 10% |
| **SB9** | 0.201 | 0.030 | 0.060 | 0.239 | 70 | 8 | 25% |
| **SB10** | 0.205 | 0.030 | 0.060 | 0.231 | 50 | 8 | 25% |
| **SB11** | 0.175 | 0.010 | 0.021 | 0.225 | 90 | 8 | 25% |
| **SB12** | 0.180 | 0.002 | 0.004 | 0.234 | 90 | 8 | 25% |
| **SB13** | 0.373 | 0.010 | 0.022 | 0.234 | 90 | 8 | 25% |
| **SB14** | 0.096 | 0.010 | 0.025 | 0.236 | 90 | 8 | 25% |

[†]No data is available of this reaction due to absence of the internal standard in the HPLC samples.

### 2.2.2 Procedure autoclave

The autoclave (stainless steel, volume: 100mL) was equipped with a pressure meter, a sampling tube (volume: 0.35 mL) and an air in- and outlet, see Figure 9 and 10. Insulation material was wrapped around the reactor to prevent significant heat loss to the environment. The air inlet was connected to a pressure regulator which was connected to a cylinder that contained compressed air at 200 bar. The sampling tube and the air in- and outlet were all closed with a valve. To heat the reactor, it was placed on a hot plate.

Preparation of the reaction was performed in the same manner as for the semi-batch reactor. To start the reaction, the reaction mixture (total volume: 50 mL) was poured in the autoclave which was then securely closed and placed on the hot plate. Air was introduced until the pressure in the vessel was sufficient. Aliquots were taken in duplicate at set times by opening the valve of the sampling tube to enable the liquid to come out. For each sampling, the first aliquot taken was considered unreliable because the sampling tube still contained reaction mixture from the previous sampling. The weight of each aliquot was measured. The HPLC sample preparation method is described in paragraph 2.2.4. After the reaction was stopped and cooled down close to room temperature, the reaction mixture was poured back into the flask and this was weighted to determine if weight loss had occurred during the process.

The parameters that were adjusted to investigate their influence on the performance of the reaction are displayed in Table 2; the starting concentrations of HMF are given as they were measured by the HPLC.

*Table 2 Overview of the performed reactions in the autoclave with different parameters that were changed. The initial concentrations are given as well as set temperature, reaction time and pressure in the autoclave. The concentration of bromide in some cases differed from the ideal (Co + Mn)/Br = 1:1 ratio and is therefore given separately.*

| NO. | $[HMF]_0$ (M) | [Co] (M) | [Br] (M) | $[ACETALDEHYDE]_0$ (M) | $T_{SET}$ (°C) | TIME (H) | PRESSURE (BAR) |
|---|---|---|---|---|---|---|---|
| **A15** | 0.200 | 0.011 | 0.021 | 0 | 125 | 6.0 | 20 |
| **A16** | 0.197 | 0.010 | 0.022 | 0.237 | 125 | 6.75 | 20 |
| **A17** | 0.222 | 0.010 | 0.021 | 0.132 | 125 | 6.5 | 20 |
| **A18** | 0.187 | 0.010 | 0.021 | 0.227 | 75 | 6.5 | 20 |
| **A19** | 0.181 | 0.010 | 0.021 | 0.237 | 75 | 6.5 | 40 |

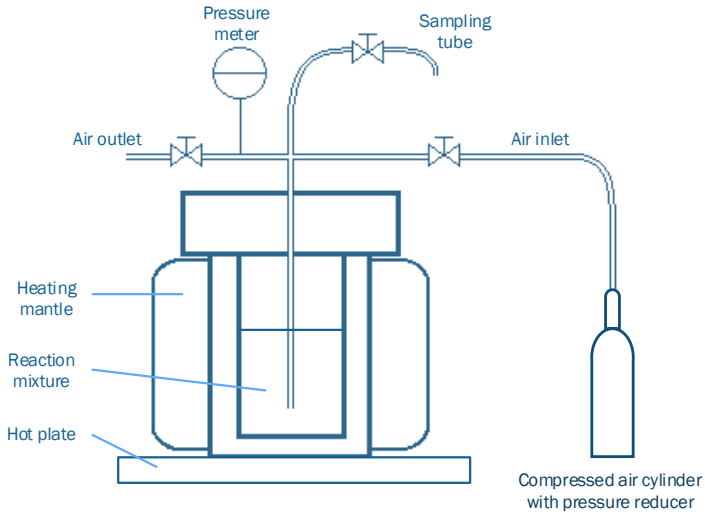


*Figure 9 Schematics of the experimental setup for reaction test in the autoclave.*

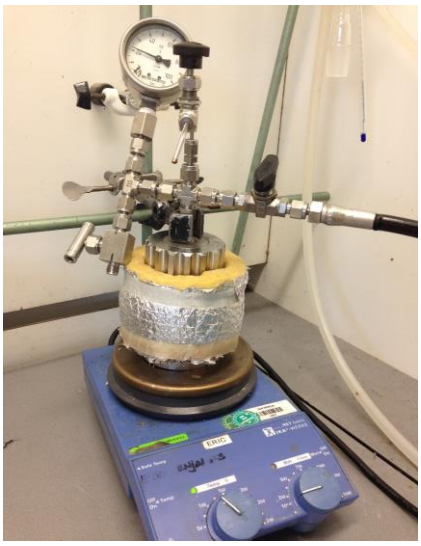

*Figure 10 Photo of the experimental setup for reaction test in the autoclave.*

Since the temperature inside the autoclave was not directly the set temperature, the heating profile was determined at 20 bar with water inside the autoclave, as is displayed in Figure 11. It is assumed that heating of acetic acid follows a similar profile. For reactions 15 to 17 in Table 2 the temperature was set on 125°C and the desired temperature was reached after 1 hour; for reactions 18 and 19 the temperature was set on 75°C and the desired temperature was reached after 35 minutes.

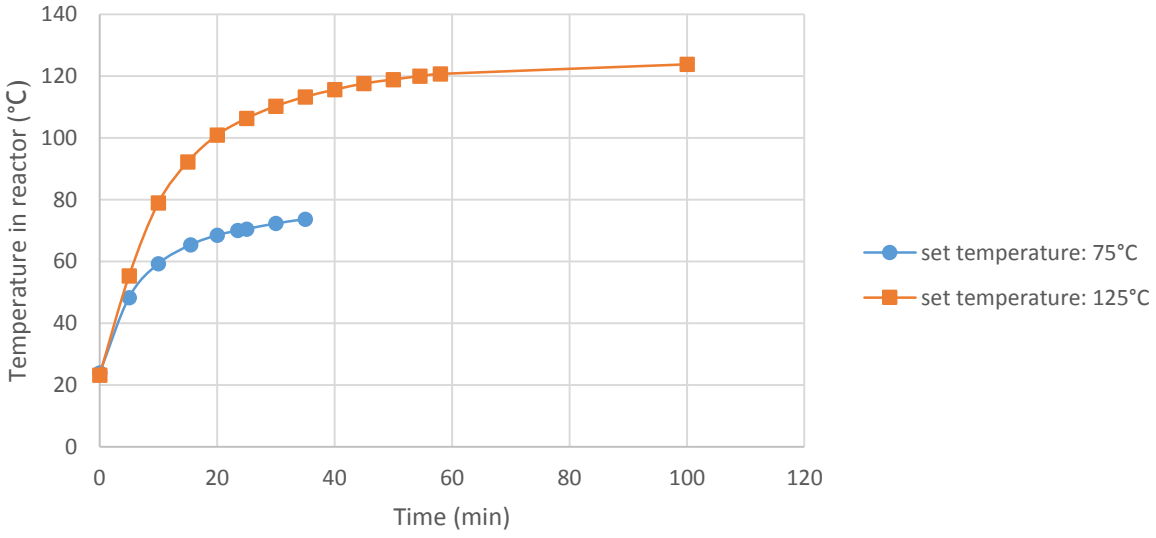


*Figure 11 Heating profile in the autoclave.*

### 2.2.3 Procedure microreactor

The experimental setup is shown schematically in Figure 12 with some photos given in Figure 13. A PTFE capillary of 10 m length and 0.8 mm internal diameter served as the microreactor (volume: 5.03 mL). The capillary was coiled to be able to put it in a water bath, that was heated on a hot plate. Aliquots could be collected by placing a vial under the outlet of the microreactor. To prevent the solvent (acetic acid) in the aliquot to evaporate, the vial was placed in an ice bath.
The gas and liquid flows were introduced to the microreactor through a T-junction. Air was provided from a compressed air cylinder with a pressure regulator that was set at 20 bar. Air was first led through a mass flow controller (5 mL/min air STP of supplier Bronkhorst high-tech, serial number: 940201C, type: F-200C-FA-11V) to regulate its flow rate and was then introduced to the T-junction. A small diameter capillary tubing to connect the mass flow controller with the T-junction was chosen such that the pressure drop in this tubing was sufficient to create a reproducible slug flow in the reactor. The liquid was pumped from a vessel to the T-junction and subsequently to the capillary microreactor by an automatic dual syringe pump (Pharmacia Biotech P-500). A purge tube with a valve was installed to enable quick removal of the reaction mixture out of the pump.

Preparation of the liquid reaction mixture for the reaction test was done in the same manner as for the semi-batch reactor and the autoclave. An aliquot was taken from this mixture before each reaction test to serve as a starting point. The complete setup (pump, microreactor and tubings in the liquid feeding line) was first flushed with the reaction mixture. The microreactor was completely filled with reaction mixture before starting a reaction test under slug flow operation to avoid unwanted high pressure drop fluctuation in the system. This pressure drop could otherwise be significant due to the friction of small liquid droplets on the inner surface of the microreactor from a previous experiment.
The reaction was started by leaving the liquid flow on when the microreactor was completely filled with liquid and then introducing the air flow. After the first slug flow had reached the end of the microreactor, the flow was left running for 4 hours. Aliquots were taken every half an hour from the moment the slug flow had reached the end of the microreactor. See paragraph 2.2.4 below for the further preparation of HPLC samples from these aliquots.
The reaction conditions performed in the microreactor are displayed in Table 3; the starting concentrations of HMF are given measured by HPLC. The air flow rate is given under standard conditions; in paragraph 3.2.3 the actual flow rate and reaction time in the microreactor are calculated.

*Table 3 Overview of the performed reactions in the microreactor with the different parameters that were changed. The initial concentrations are given as well as reaction temperature and time and air and liquid flow rate. The concentration of bromide in some cases differed from the ideal (Co + Mn)/Br = 1:1 ratio and is therefore given separately.*

| NO. | $[HMF]_0$ (M) | [Co] (M) | [Br] (M) | $[ACETALDEHYDE]_0$ (M) | T (°C) | TIME (MIN) | $Q_{AIR}$ (ML/MIN) | $Q_{LIQ.}$ (ML/MIN) |
|---|---|---|---|---|---|---|---|---|
| **M20** | 0.189 | 0.010 | 0.020 | 0.227 | 70 | 24.7 | 0.200 | 0.033 |
| **M21** | 0.198 | 0.010 | 0.026 | 0.227 | 70 | 35.1 | 0.150 | 0.033 |
| **M22** | 0.211 | 0.010 | 0.026 | 0.227 | 70 | 34.8 | 0.150 | 0.017 |
| **M23** | 0.185 | 0.010 | 0.020 | 0.245 | 90 | 24.6 | 0.200 | 0.033 |

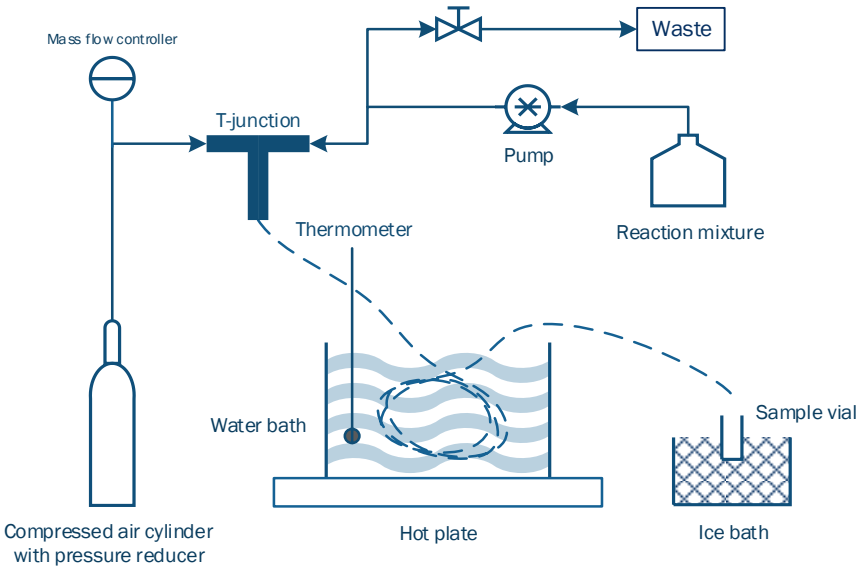


*Figure 12 Schematics of the microreactor setup.*

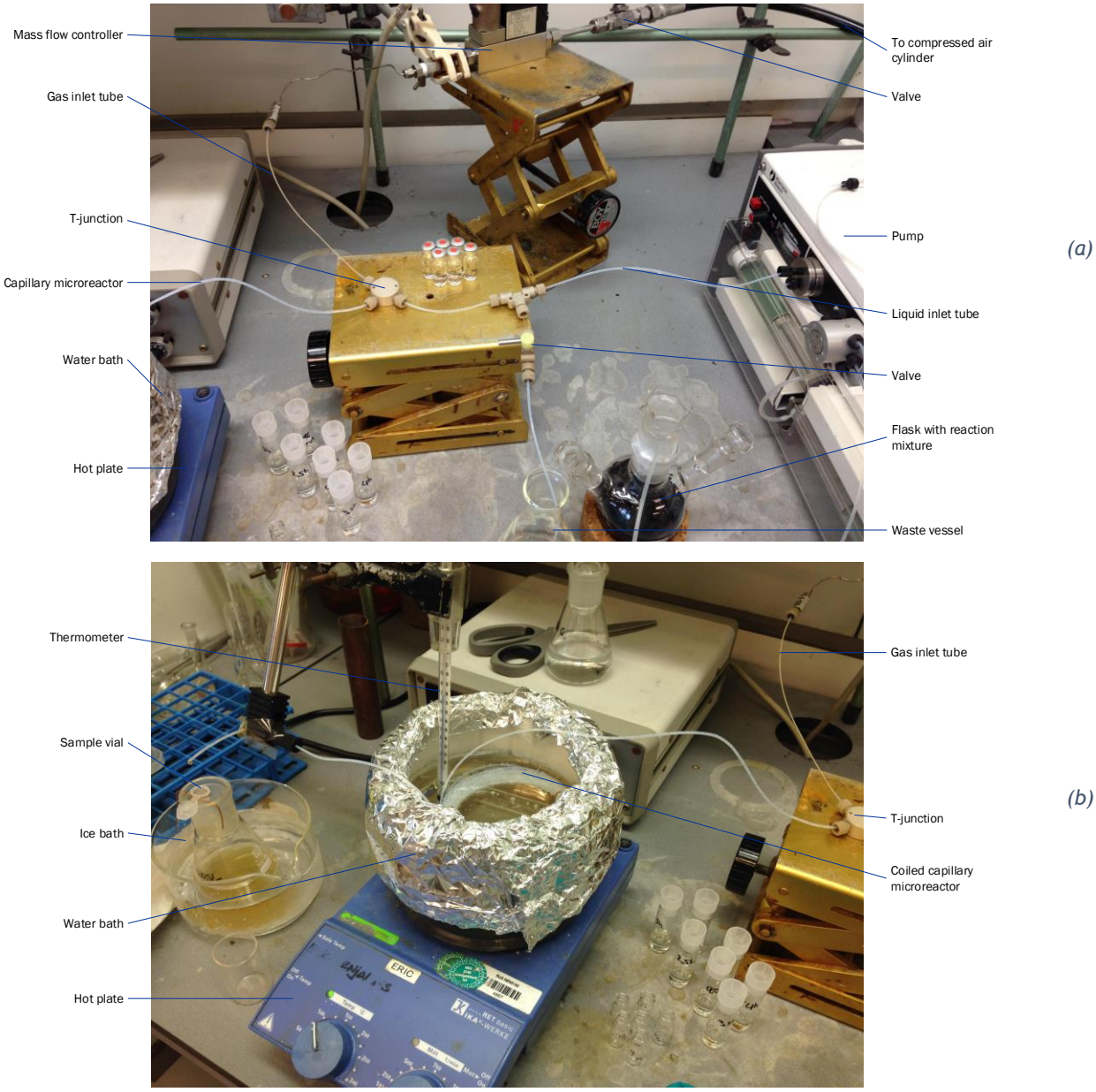


*Figure 13 Photos of the microreactor setup.*

### 2.2.4 Sample preparation

As mentioned above aliquots from the semi-batch reactor, the autoclave and the microreactor were taken from the reaction mixture at set times. From each of these aliquots 100 µL was used to prepare a sample for HPLC. Together with 100 µL of the internal standard solution and 1.8 mL water the mixture was filtered through a 0.45 µm PTFE syringe filter and injected in a HPLC vial of 2 mL. The internal standard solution consisted of 20 g/L 2,5-pentanedione in water.

## 2.3 Analytics

For analysis an HPLC system from Agilent Technologies 1200 was used, equipped with an ion exchange column from Biorad (type: HPX-87H) of 30 cm length and 7.8 mm internal diameter operated at 60°C. The column consists of a polystyrene/divinylbenzene matrix with side groups of sulfonic acid. 0.005 M $H_2SO_4$ was used as eluent. After the column, the compounds in the sample were detected by an RID and a UV-detector. The measuring time was set at 70 minutes and UV response was measured at 280 nm, where all the expected products as well as the internal standard were visible. In this way, the compounds could be calibrated by two different methods. Measuring time of 70 minutes assured us that most of the unidentified reaction products were released from the column before measuring a new sample. Still this was not always the case, but there seemed no obvious hindrance from compounds that were left from a previous measurement on detecting the desired products in the next run. Integration of the desired peaks was performed manually using Agilent ChemStation followed by calculations in Excel to convert the data to molar concentrations.

The peaks of all the desired products from the oxidation reaction of HMF (DFF, FFCA and FDCA) and HMF itself were identified and calibrated. Calibration of AMF gave information about the response deviation for HMF since these compounds had the same retention time.
For each calibration a concentration range of the compound was chosen close to the range that would be reached during a reaction. HPLC standard samples with set concentrations were achieved by diluting a stock solution of the pure compound with water in such a way that the right concentration was reached. The stock solution was prepared by dissolving the right amount of the pure compound into solvent using weighing method. The solvent was either acetic acid or an acetic acid/water mixture, dependent on the solubility of the compound in water. A duplicate of this solution was prepared in the same manner to preclude weighing errors. Since there were two stock solutions, HPLC standard samples for each set concentration were prepared in duplicate.
An HPLC standard sample of 2 mL contained 100 μL internal standard solution of 20 g/L and a variable amount of the stock solution. The sample was filled up with water. The exact amount that was used can be found in Appendix II: Experimental data for calibration and calibration curves.

# 3. RESULTS

## 3.1 Sample analysis

### 3.1.1 Peak identification

To determine the retention times of the important compounds that are present in the reaction mixture, pure components dissolved in a 10% acetic acid/water mixture were run through the HPLC, to simulate the conditions in the collected reaction samples. In this way, impurities could be identified as well. The retention times of these compounds are tabulated in Table 4. The retention times of AMF and HMF are almost the same, meaning that the two peaks overlap if they are both present in a sample. The effect hereof is discussed in paragraph 4.2.1. A typical UV chromatogram of a sample from one of the reactions is shown in Figure 14.

Throughout the time period of this research, the retention times tended to vary slightly. This can be caused by a change in mobile phase composition (Dolan 2012) which is in this case a feasible explanation since the eluent was renewed quite often. For that reason, little notice was paid to this.

*Table 4 Overview of the retention times of the important compounds for this research.*

| COMPOUND | RETENTION TIME (MIN) | |
|---|---|---|
| | RID | UV |
| **ACETIC ACID** | 17.2 | |
| **FDCA** | 18.8 | 18.5 |
| **ACETALDEHYDE** | 20.1 | |
| **FFCA** | 24.9 | 24.6 |
| **2,4-PENTANEDIONE (I.S.)** | 27.1 | 26.8 |
| **HMF** | 34.5 | 34.2 |
| **AMF** | 34.9 | 34.6 |
| **DFF** | 42.6 | 42.3 |

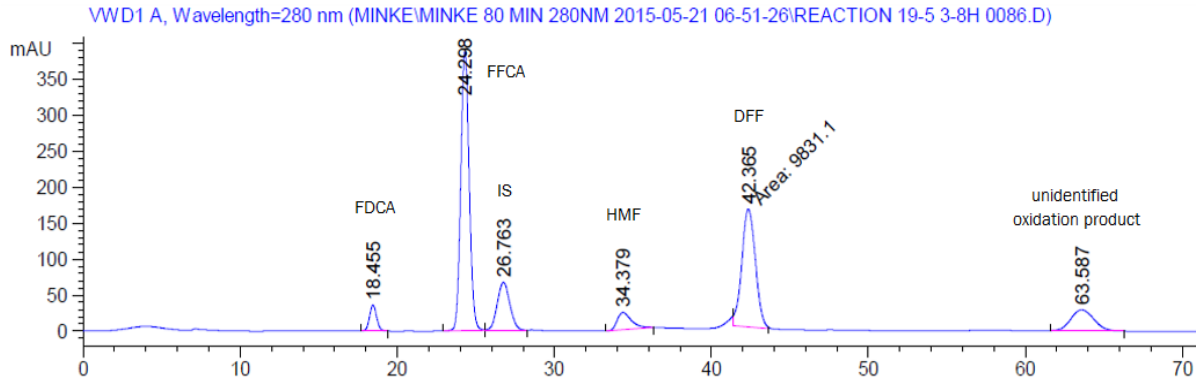


*Figure 14 A typical chromatogram from the UV detector showing the retention times of the product and reactant peaks.*

Figure 14 shows peaks of the compounds that are all nicely visible and distinct. In some of the samples, however, the desired peaks were not that easy to distinguish. Especially in early stages of the reaction several peaks appeared at RT 40-44 in the RID chromatogram, around the DFF peak. These peaks also gave a UV signal, see Figure 15 for an example. As the reaction proceeded the actual DFF peak grew over these little peaks to a form similar to that in Figure 14, making it easier to recognise and integrate the actual DFF peak. This phenomenon was observed in all reactions in all reactor types. The low DFF concentrations reported are therefore less reliable than the higher values. In some of the tables with experimental data, a DFF concentration is given for zero reaction time. It is unlikely that a reaction has taken place at room temperature, as will be explained in paragraph 4.1. Due to retention time shifting and the character of the DFF peak at low HMF conversion, it is most likely that this "DFF" at zero reaction time is another compound.
The RID-peak of FFCA at low HMF conversions sometimes had two tops, indicating different compounds. The UV signal gave only one top, therefore it was chosen to integrate both the peaks in the RID chromatogram together and use this value to calculate the concentrations, see Figure 16 for an example.

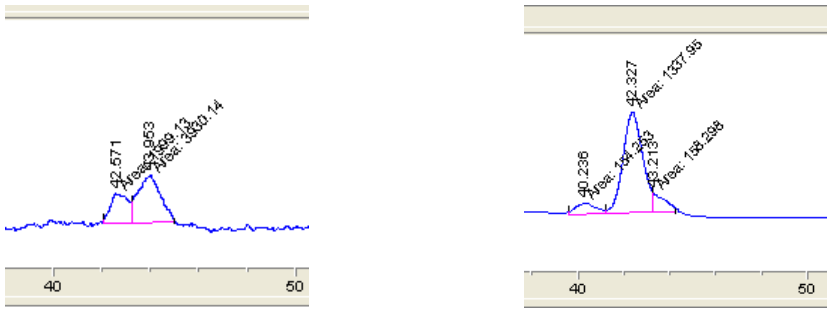


*(a)* *(b)*

*Figure 15 RID (a) and UV (b) chromatogram between RT 40-50 min at low HMF conversion (reaction 20)*

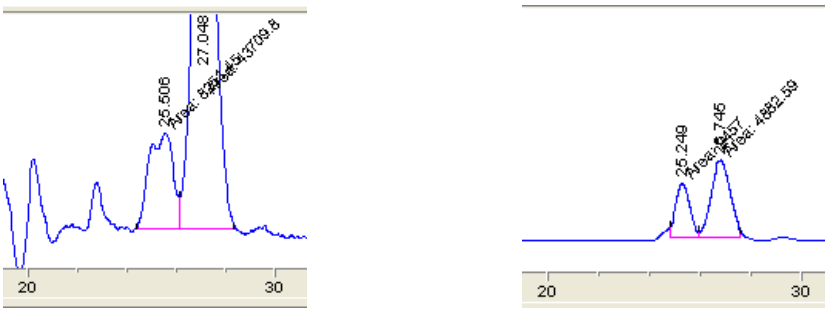


*(a)* *(b)*

*Figure 16 RID (a) and UV (b) chromatogram between RT 20-30 min at low HMF conversion (reaction 17; t = 0.5h)*

### 3.1.2 Response factor determination

Each component gives a different signal intensity, dependent on molecular structure. To be able to compare the peaks of the compounds, an internal standard was added to the mixture that enabled to calibrate the signals of the reaction products. The internal standard was chosen such that the compounds could be calibrated on two different detection methods: RID and UV.

Upon calibration, the response factor of the compound i is determined compared with that of the internal standard. This response factor is dependent on the concentration ratio of the compound to the internal standard and the ratio of the peak areas between the compound and IS, as is shown in formula (f1) that can be rewritten into formula (f2). The latter gives the format for the calibration curve.

$$F_i = F_{IS} \frac{A_i}{A_{IS}} \frac{[IS]}{[i]} \qquad \text{(f1)}$$

$$\frac{A_i}{A_{IS}} = \frac{F_i}{F_{IS}} \frac{[i]}{[IS]} \qquad \text{(f2)}$$

In which *F* is the response factor for compound *i* or the internal standard (IS). *A* is the area of the peak of the component in the chromatogram. [*i*] is the concentration of compound *i*.

Carefully prepared samples provided the data for the calibration curves that are displayed in Appendix II: Experimental data for calibration and calibration curves. The experimental procedure for preparing these samples was described earlier in paragraph 2.2.4. The determined response factors are given in Table 5.

*Table 5 Response factors compared to 2,4-pentanedione for various compounds that might be present in the reaction mixture.*

| COMPOUND | RESPONSE FACTOR | |
|---|---|---|
| | RID | UV |
| **2,4-PENTANEDIONE (I.S.)** | 1 | 1 |
| **HMF** | 1.25 | 5.87 |
| **DFF** | 2.11 | 8.73 |
| **FFCA** | 3.37 | 16.00 |
| **FDCA** | 1.85 | 3.47 |
| **AMF** | 0.98 | 2.55 |

## 3.2 Experimental data

An overview of reactions that were performed in the three different reactor types was given in the previous chapter (Table 1, 2 and 3).

Two different pathways are considered for the autoxidation reaction of HMF:

1) $\mathrm{HMF} \rightarrow \mathrm{DFF} \rightarrow \mathrm{FFCA} \rightarrow \mathrm{FDCA}$
2) $\mathrm{HMF} \rightarrow \text{side products (X)}$

In the previous paragraph, one could read that all the products of pathway 1 were calibrated. Of the products of pathway 2, however, only AMF was calibrated since this was the only side product that was identified. A lot of different side products can form during this reaction, therefore these were compiled and are referred to as X hereafter. The experimental data of all the reactions that were performed are summarised in Table 6-23 and Table 25-28 listed in this paragraph. From these tables, the information on the progress of the reaction can be derived. The reaction entries are marked with SB, A or M for easy recognition of the reactor type if the results are discussed. SB indicates operation in the semi-batch reactor; A, operation in the autoclave and M stands for microreactor.

The concentrations and selectivities of the compounds according to pathway 1 are given separately for all the times at which aliquots were taken. In the semi-batch reactor and autoclave, these times are equal to the reaction time. The concentrations were corrected for the weight loss that was measured in the reactions in the semi-batch reactor and the autoclave, assuming this weight loss occurred linearly with time. A calculation example can be found in Appendix III: Calculation example for weight loss compensation. From the concentrations obtained for each compound ($[i]$), the conversion of HMF and the yields ($\eta_i$) and selectivities ($\sigma_i$) of the products can be calculated by equations (f3) and (f4).

$$\eta_i = \frac{[\mathrm{i}]}{[\mathrm{i}]_{\max}} \cdot 100\% \quad \text{(f3)}$$

$$\sigma_{\mathrm{i}} = \frac{\eta_i}{\mathrm{X}} \quad \text{(f4)}$$

Since the mass balance could not be closed due to the unidentified side products X according to pathway 2, the gap in the mass balance at different reaction times are also given as concentration of X. The last column of the tables with experimental data mentioned above displays the selectivity towards X; this can be seen as the ratio of the gap in the mass balance in percentage towards the HMF conversion. Further explanation on the gap is given below in paragraph 4.2.

### 3.2.1 Results semi-batch reactor

In Table 6 to 18 below the results of the reactions in the semi-batch reactor are displayed. Per reaction the experimental conditions are presented in short. Only the concentration of Co is given; the catalyst molar ratio that was used in all reactions was (Co + Mn)/Br = 1:1.

*Table 6 Experimental data of reaction SB1. T = 90°C, $Q_{air}$ = 353.9 mL/min, $[Co]_0$ = 0 M, $[HMF]_0$ = 0.216 M, $[acetaldehyde]_0$ = 0 M, t = 5 h, weight loss = 14.7 wt%.*

| TIME (h) | HMF (mmol/L) | [X] (mmol/L) |
|---|---|---|
| **0** | 215.62 | 0.00 |
| **0.25** | 212.56 | 3.07 |
| **0.50** | 205.28 | 10.34 |
| **1** | 215.77 | -0.15 |
| **2** | 206.49 | 9.14 |
| **3** | 204.72 | 10.90 |
| **4** | 210.67 | 4.95 |
| **5** | 194.07 | 21.55 |

*Table 7 Experimental data of reaction SB3. T = 90°C, $Q_{air}$ = 353.9 mL/min, $[Co]_0$ = 0.03 M, $[HMF]_0$ = 0.185 M, $[acetaldehyde]_0$ = 0.226 M, t = 8 h, weight loss = 18.2 wt%.*

| TIME (h) | [HMF] (mmol/L) | [DFF] (mmol/L) | $\sigma_{DFF}$ (%) | [FFCA] (mmol/L) | $\sigma_{FFCA}$ (%) | [FDCA] (mmol/L) | $\sigma_{FDCA}$ (%) | [X] (mmol/L) | $\sigma_X$ (%) |
|---|---|---|---|---|---|---|---|---|---|
| **0** | 185.42 | 0.00 | - | 0.00 | - | 0.00 | - | 0.00 | - |
| **0.17** | 202.80 | 1.25 | -7.2 | 0.00 | - | 0.00 | - | -18.64 | 107.2 |
| **0.33** | 179.41 | 5.73 | 95.4 | 0.72 | 12.0 | 0.00 | - | -0.44 | -7.4 |
| **0.5** | 171.43 | 9.48 | 67.8 | 1.13 | 8.1 | 0.00 | - | 3.39 | 24.2 |
| **0.75** | 165.53 | 15.48 | 77.8 | 2.31 | 11.6 | 0.00 | - | 2.10 | 10.5 |
| **1** | 149.90 | 18.94 | 53.3 | 3.57 | 10.1 | 0.00 | - | 13.01 | 36.6 |
| **3** | 82.80 | 49.79 | 48.5 | 13.12 | 12.8 | 2.47 | 2.4 | 37.23 | 36.3 |
| **5** | 40.26 | 66.67 | 45.9 | 22.52 | 15.5 | 3.26 | 2.2 | 52.71 | 36.3 |
| **6** | 32.44 | 76.53 | 50.0 | 27.79 | 18.2 | 3.32 | 2.2 | 45.33 | 29.6 |
| **8** | 22.48 | 85.52 | 52.5 | 35.66 | 21.9 | 5.43 | 3.3 | 36.34 | 22.3 |

*Table 8 Experimental data of reaction SB4. T = 90°C, $Q_{air}$ = 353.9 mL/min, $[Co]_0$ = 0.03 M, $[HMF]_0$ = 0.141 M, $[acetaldehyde]_0$ = 0.119 M, t = 3 h, weight loss = 7.2 wt%.*

| TIME (h) | [HMF] (mmol/L) | [DFF] (mmol/L) | $\sigma_{DFF}$ (%) | [FFCA] (mmol/L) | $\sigma_{FFCA}$ (%) | [X] (mmol/L) | $\sigma_X$ (%) |
|---|---|---|---|---|---|---|---|
| **0** | 142.90 | 0.00 | - | 0.00 | - | 0.00 | - |
| **0.17** | 140.87 | 0.00 | - | 0.00 | - | 2.03 | 100.0 |
| **0.33** | 141.57 | 0.00 | - | 0.00 | - | 1.33 | 100.0 |
| **0.5** | 136.19 | 5.58 | 83.1 | 1.1 | 16.4 | 0.03 | 0.5 |
| **0.75** | 126.49 | 8.11 | 49.4 | 1.9 | 11.5 | 6.42 | 39.1 |
| **1** | 119.94 | 11.03 | 48.0 | 2.8 | 12.0 | 9.17 | 39.9 |
| **3** | 67.01 | 28.52 | 37.6 | 12.1 | 14.8 | 36.11 | 47.6 |

*Table 9 Experimental data of reaction SB5. T = 90°C, $Q_{air}$ = 353.9 mL/min, $[Co]_0$ = 0.03 M, $[HMF]_0$ = 0.158 M, $[acetaldehyde]_0$ = 0.061 M, t = 3 h, weight loss = 6.4 wt%.*

| TIME (h) | [HMF] (mmol/L) | [X] (mmol/L) |
|---|---|---|
| **0** | 158.44 | 0.00 |
| **0.17** | 162.29 | -3.85 |
| **0.33** | 161.25 | -2.80 |
| **0.5** | 161.28 | -2.84 |
| **0.75** | 159.91 | -1.47 |
| **1** | 155.08 | 3.36 |
| **3** | 154.85 | 3.60 |

*Table 10 Experimental data of reaction SB6. T = 90°C, $Q_{air}$ = 176.97 mL/min, $[Co]_0$ = 0.03 M, $[HMF]_0$ = 0.190 M, $[acetaldehyde]_0$ = 0.245 M, t = 8 h, weight loss = 9.9 wt%.*

| TIME (h) | [HMF] (mmol/L) | [DFF] (mmol/L) | $\sigma_{DFF}$ (%) | [FFCA] (mmol/L) | $\sigma_{FFCA}$ (%) | [FDCA] (mmol/L) | $\sigma_{FDCA}$ (%) | [X] (mmol/L) | $\sigma_X$ (%) |
|---|---|---|---|---|---|---|---|---|---|
| **0** | 189.60 | 0.00 | - | 0.00 | - | 0.00 | - | 0.00 | - |
| **0.17** | 186.13 | 2.52 | 72.6 | 0.00 | - | 0.00 | - | 0.95 | 27.4 |
| **0.33** | 171.78 | 7.01 | 39.4 | 0.80 | 4.5 | 0.00 | - | 10.00 | 56.1 |
| **0.5** | 161.18 | 11.37 | 40.0 | 1.28 | 4.5 | 0.00 | - | 15.77 | 55.5 |
| **0.75** | 148.01 | 17.61 | 42.3 | 2.57 | 6.2 | 0.00 | - | 21.40 | 51.5 |
| **1** | 138.43 | 24.05 | 47.0 | 3.94 | 7.7 | 0.00 | - | 23.18 | 45.3 |
| **3** | 49.92 | 61.63 | 44.1 | 13.21 | 9.5 | 0.50 | 0.4 | 64.35 | 46.1 |
| **6** | 15.51 | 66.14 | 38.0 | 22.17 | 12.7 | 5.64 | 3.2 | 80.15 | 46.0 |
| **8** | 9.62 | 64.47 | 35.8 | 26.46 | 14.7 | 6.21 | 3.4 | 82.84 | 46.0 |

*Table 11 Experimental data of reaction SB7. T = 90°C, $Q_{air}$ = 88.49 mL/min, $[Co]_0$ = 0.03 M, $[HMF]_0$ = 0.192 M, $[acetaldehyde]_0$ = 0.232 M, t = 8 h, weight loss = 8.0 wt%.*

| TIME (h) | [HMF] (mmol/L) | [DFF] (mmol/L) | $\sigma_{DFF}$ (%) | [FFCA] (mmol/L) | $\sigma_{FFCA}$ (%) | [FDCA] (mmol/L) | $\sigma_{FDCA}$ (%) | [X] (mmol/L) | $\sigma_X$ (%) |
|---|---|---|---|---|---|---|---|---|---|
| **0** | 192.34 | 0.00 | - | 0.00 | - | 0.00 | - | 0.00 | - |
| **0.17** | 197.50 | 0.26 | -5.1 | 0.00 | - | 0.00 | - | -5.42 | 105.1 |
| **0.33** | 190.39 | 0.83 | 42.3 | 0.39 | 19.7 | 0.00 | - | 0.74 | 38.0 |
| **0.5** | 183.30 | 3.21 | 35.5 | 0.66 | 7.3 | 0.00 | - | 5.17 | 57.2 |
| **0.75** | 175.68 | 5.75 | 34.5 | 1.16 | 7.0 | 0.00 | - | 9.76 | 58.6 |
| **1** | 158.97 | 9.49 | 28.4 | 2.29 | 6.9 | 0.00 | - | 21.59 | 64.7 |
| **3** | 54.82 | 47.65 | 34.6 | 15.76 | 11.5 | 0.77 | 0.6 | 73.34 | 53.9 |
| **6** | 14.44 | 53.41 | 30.0 | 27.06 | 15.2 | 7.65 | 4.3 | 89.78 | 50.5 |
| **8** | 9.80 | 53.48 | 29.3 | 33.36 | 18.3 | 10.05 | 5.5 | 85.66 | 46.9 |

*Table 12 Experimental data of reaction SB8. T = 90°C, $Q_{air}$ = 35.39 mL/min, $[Co]_0$ = 0.03 M, $[HMF]_0$ = 0.183 M, $[acetaldehyde]_0$ = 0.243 M, t = 8 h, weight loss = 3.6 wt%.*

| TIME (h) | [HMF] (mmol/L) | [DFF] (mmol/L) | $\sigma_{DFF}$ (%) | [FFCA] (mmol/L) | $\sigma_{FFCA}$ (%) | [FDCA] (mmol/L) | $\sigma_{FDCA}$ (%) | [X] (mmol/L) | $\sigma_X$ (%) |
|---|---|---|---|---|---|---|---|---|---|
| **0** | 182.55 | 0.05 | | 0.00 | - | 0.00 | - | -0.05 | |
| **0.17** | 206.67 | 0.18 | -0.8 | 0.00 | - | 0.00 | - | -24.30 | 100.8 |
| **0.33** | 186.81 | 0.29 | -6.9 | 0.00 | - | 0.00 | - | -4.55 | 106.9 |
| **0.5** | 177.95 | 0.48 | 10.4 | 0.00 | - | 0.00 | - | 4.12 | 89.6 |
| **0.75** | 175.03 | 1.97 | 26.1 | 0.00 | - | 0.00 | - | 5.56 | 73.9 |
| **1** | 167.81 | 1.69 | 11.5 | 0.05 | 0.3 | 0.00 | - | 13.01 | 88.2 |
| **2** | 146.06 | 6.52 | 17.9 | 1.16 | 3.2 | 0.00 | - | 28.80 | 78.9 |
| **4** | 91.11 | 23.36 | 25.5 | 6.31 | 6.9 | 0.00 | - | 61.77 | 67.5 |
| **6** | 38.70 | 40.68 | 28.3 | 14.02 | 9.7 | 0.00 | - | 89.16 | 62.0 |
| **8** | 21.44 | 43.71 | 27.1 | 20.02 | 12.4 | 2.44 | 1.5 | 94.94 | 58.9 |

*Table 13 Experimental data of reaction SB9. T = 70°C, $Q_{air}$ = 88.49 mL/min, $[Co]_0$ = 0.03 M, $[HMF]_0$ = 0.200 M, $[acetaldehyde]_0$ = 0.239 M, t = 8 h, weight loss = 5.3 wt%.*

| TIME (h) | [HMF] (mmol/L) | [DFF] (mmol/L) | $\sigma_{DFF}$ (%) | [FFCA] (mmol/L) | $\sigma_{FFCA}$ (%) | [FDCA] (mmol/L) | $\sigma_{FDCA}$ (%) | [X] (mmol/L) | $\sigma_X$ (%) |
|---|---|---|---|---|---|---|---|---|---|
| **0** | 200.74 | 0.00 | - | 0.00 | - | 0.00 | - | 0.00 | - |
| **0.17** | 199.57 | 0.26 | 22.1 | 0.00 | - | 0.00 | - | 0.91 | 77.9 |
| **0.33** | 196.60 | 0.71 | 17.2 | 0.00 | - | 0.00 | - | 3.42 | 82.8 |
| **0.5** | 179.83 | 2.55 | 12.2 | 0.41 | 2.0 | 0.00 | - | 17.94 | 85.8 |
| **0.75** | 168.50 | 5.57 | 17.3 | 0.49 | 1.5 | 0.00 | - | 26.17 | 81.2 |
| **1** | 161.40 | 8.20 | 20.9 | 0.83 | 2.1 | 0.00 | - | 30.30 | 77.0 |
| **2** | 141.63 | 20.80 | 35.2 | 1.88 | 3.2 | 0.00 | - | 36.43 | 61.6 |
| **4** | 121.24 | 29.97 | 37.7 | 3.40 | 4.3 | 0.00 | - | 46.13 | 58.0 |
| **6** | 104.69 | 34.30 | 35.7 | 4.37 | 4.6 | 0.00 | - | 57.37 | 59.7 |
| **8** | 90.68 | 39.58 | 36.0 | 6.04 | 5.5 | 0.00 | - | 64.44 | 58.6 |

*Table 14 Experimental data of reaction SB10. T = 50°C, $Q_{air}$ = 88.49 mL/min, $[Co]_0$ = 0.03 M, $[HMF]_0$ = 0.205 M, $[acetaldehyde]_0$ = 0.231 M, t = 8 h, weight loss = 6.6 wt%.*

| TIME (h) | [HMF] (mmol/L) | [DFF] (mmol/L) | $\sigma_{DFF}$ (%) | [FFCA] (mmol/L) | $\sigma_{FFCA}$ (%) | [FDCA] (mmol/L) | $\sigma_{FDCA}$ (%) | [X] (mmol/L) | $\sigma_X$ (%) |
|---|---|---|---|---|---|---|---|---|---|
| **0** | 205.47 | 0.00 | - | 0.00 | - | 0.00 | - | 0.00 | - |
| **0.17** | 215.56 | 0.21 | -2.1 | 0.00 | - | 0.00 | - | -10.30 | 102.1 |
| **0.33** | 216.67 | 1.69 | -15.1 | 0.00 | - | 0.00 | - | -12.90 | 115.1 |
| **0.5** | 223.66 | 3.41 | -18.7 | 0.00 | - | 0.00 | - | -21.60 | 118.7 |
| **0.75** | 226.48 | 3.57 | -17.0 | 0.38 | -1.8 | 0.00 | - | -24.97 | 118.8 |
| **1** | 219.99 | 5.39 | -37.1 | 0.64 | -4.4 | 0.00 | - | -20.56 | 141.5 |
| **2** | 195.79 | 7.23 | 74.8 | 0.66 | 6.8 | 0.00 | - | 0.08 | 18.4 |
| **4** | 180.51 | 12.09 | 48.4 | 1.09 | 4.4 | 0.00 | - | -2.98 | 47.2 |
| **6** | 177.14 | 12.01 | 42.4 | 0.93 | 3.3 | 0.00 | - | 15.38 | 54.3 |
| **8** | 173.71 | 12.23 | 38.5 | 1.08 | 3.4 | 0.00 | - | 18.44 | 58.1 |

*Table 15 Experimental data of reaction SB11. T = 90°C, $Q_{air}$ = 88.49 mL/min, $[Co]_0$ = 0.01 M, $[HMF]_0$ = 0.175 M, $[acetaldehyde]_0$ = 0.225 M, t = 8 h, weight loss = 6.7 wt%.*

| TIME (h) | [HMF] (mmol/L) | [DFF] (mmol/L) | $\sigma_{DFF}$ (%) | [FFCA] (mmol/L) | $\sigma_{FFCA}$ (%) | [FDCA] (mmol/L) | $\sigma_{FDCA}$ (%) | [X] (mmol/L) | $\sigma_X$ (%) |
|---|---|---|---|---|---|---|---|---|---|
| **0** | 174.70 | 0.00 | - | 0.00 | - | 0.00 | - | 0.00 | - |
| **0.17** | 186.36 | 0.53 | -4.5 | 0.00 | - | 0.00 | - | -12.19 | 104.5 |
| **0.33** | 178.98 | 2.57 | -60.2 | 0.04 | -1.0 | 0.00 | - | -6.88 | 161.2 |
| **0.5** | 168.50 | 3.98 | 64.3 | 0.34 | 5.5 | 0.00 | - | 1.87 | 30.2 |
| **0.75** | 159.41 | 6.93 | 45.3 | 0.75 | 4.9 | 0.00 | - | 7.61 | 49.8 |
| **1** | 148.39 | 11.87 | 45.1 | 1.46 | 5.6 | 0.00 | - | 12.98 | 49.3 |
| **2** | 90.20 | 32.27 | 38.2 | 5.85 | 6.9 | 0.00 | - | 46.37 | 54.9 |
| **4** | 19.11 | 57.09 | 36.7 | 16.36 | 10.5 | 2.34 | 1.5 | 79.80 | 51.3 |
| **6** | 4.95 | 50.96 | 30.0 | 26.13 | 15.4 | 5.56 | 3.3 | 87.11 | 51.3 |
| **8** | 0.89 | 35.46 | 20.4 | 31.04 | 17.9 | 23.97 | 13.8 | 83.34 | 47.9 |

*Table 16 Experimental data of reaction SB12. T = 90°C, $Q_{air}$ = 88.49 mL/min, $[Co]_0$ = 0.002 M, $[HMF]_0$ = 0.180 M, $[acetaldehyde]_0$ = 0.234 M, t = 8 h, weight loss = 7.7 wt%.*

| TIME (h) | [HMF] (mmol/L) | [DFF] (mmol/L) | $\sigma_{DFF}$ (%) | [FFCA] (mmol/L) | $\sigma_{FFCA}$ (%) | [FDCA] (mmol/L) | $\sigma_{FDCA}$ (%) | [X] (mmol/L) | $\sigma_X$ (%) |
|---|---|---|---|---|---|---|---|---|---|
| **0** | 180.22 | 0.00 | - | 0.00 | - | 0.00 | - | 0.00 | - |
| **0.17** | 176.84 | 0.91 | 26.9 | 0.00 | - | 0.00 | - | 2.47 | 73.1 |
| **0.33** | 173.00 | 3.60 | 49.9 | 0.51 | 7.0 | 0.00 | - | 3.12 | 43.1 |
| **0.5** | 167.12 | 4.76 | 36.3 | 0.57 | 4.4 | 0.00 | - | 7.77 | 59.3 |
| **0.75** | 155.93 | 8.68 | 35.7 | 0.74 | 3.0 | 0.00 | - | 14.87 | 61.2 |
| **1** | 151.17 | 11.50 | 39.6 | 1.09 | 3.8 | 0.00 | - | 16.45 | 56.6 |
| **2** | 127.07 | 16.97 | 31.9 | 1.91 | 3.6 | 0.00 | - | 34.28 | 64.5 |
| **4** | 98.68 | 25.77 | 31.6 | 3.31 | 4.1 | 0.00 | - | 52.45 | 64.3 |
| **6** | 79.26 | 30.77 | 30.5 | 3.81 | 3.8 | 0.00 | - | 66.38 | 65.8 |
| **8** | 62.37 | 35.56 | 30.2 | 4.80 | 4.1 | 0.20 | 0.2 | 77.29 | 65.6 |

*Table 17 Experimental data of reaction SB13. T = 90°C, $Q_{air}$ = 88.49 mL/min, $[Co]_0$ = 0.01 M, $[HMF]_0$ = 0.373 M, $[acetaldehyde]_0$ = 0.234 M, t = 8 h, weight loss = 6.2 wt%.*

| TIME (h) | [HMF] (mmol/L) | [DFF] (mmol/L) | $\sigma_{DFF}$ (%) | [FFCA] (mmol/L) | $\sigma_{FFCA}$ (%) | [FDCA] (mmol/L) | $\sigma_{FDCA}$ (%) | [X] (mmol/L) | $\sigma_X$ (%) |
|---|---|---|---|---|---|---|---|---|---|
| **0** | 372.57 | 0.75 | | 0.00 | - | 0.00 | - | -0.75 | |
| **0.17** | 376.19 | 1.14 | -31.7 | 0.00 | - | 0.00 | - | -4.76 | 131.7 |
| **0.33** | 368.56 | 3.34 | 83.4 | 0.24 | 6.1 | 0.00 | - | 0.42 | 10.6 |
| **0.5** | 357.97 | 5.36 | 36.7 | 0.10 | 0.7 | 0.00 | - | 9.14 | 62.6 |
| **0.75** | 354.18 | 10.08 | 54.8 | 1.12 | 6.1 | 0.00 | - | 7.19 | 39.1 |
| **1** | 359.10 | 16.81 | 124.7 | 1.77 | 13.1 | 0.00 | - | -5.10 | -37.9 |
| **2** | 298.45 | 49.04 | 66.2 | 5.43 | 7.3 | 0.00 | - | 19.65 | 26.5 |
| **4** | 168.82 | 110.14 | 54.1 | 19.40 | 9.5 | 0,75 | 0.4 | 73.45 | 36.1 |
| **6** | 128.97 | 169.40 | 69.5 | 41.31 | 17.0 | 0,74 | 0.3 | 32.16 | 13.2 |
| **8** | 94.36 | 197.46 | 71.0 | 61.29 | 22.0 | 9,29 | 3.3 | 10.17 | 3.7 |

*Table 18 Experimental data of reaction SB14. T = 90°C, $Q_{air}$ = 88.49 mL/min, $[Co]_0$ = 0.01 M, $[HMF]_0$ = 0.096 M, $[acetaldehyde]_0$ = 0.236 M, t = 8 h, weight loss = 7.3 wt%.*

| TIME (h) | [HMF] (mmol/L) | [DFF] (mmol/L) | $\sigma_{DFF}$ (%) | [FFCA] (mmol/L) | $\sigma_{FFCA}$ (%) | [FDCA] (mmol/L) | $\sigma_{FDCA}$ (%) | [X] (mmol/L) | $\sigma_X$ (%) |
|---|---|---|---|---|---|---|---|---|---|
| **0** | 95.98 | 0.00 | - | 0.00 | - | 0.00 | - | 0.00 | - |
| **0.17** | 98.23 | 0.57 | -25.2 | 0.00 | - | 0.00 | - | -2.82 | 125.2 |
| **0.33** | 94.31 | 2.27 | 135.5 | 0.00 | - | 0.00 | - | -0.59 | -35.5 |
| **0.5** | 86.45 | 3.97 | 41.7 | 0.19 | 2.0 | 0.00 | - | 5.37 | 56.3 |
| **0.75** | 72.53 | 7.52 | 32.1 | 0.79 | 3.4 | 0.00 | - | 15.14 | 64.5 |
| **1** | 54.91 | 13.11 | 31.9 | 1.92 | 4.7 | 0.00 | - | 26.04 | 63.4 |
| **2** | 14.38 | 28.59 | 35.0 | 6.65 | 8.1 | 0.62 | 0.8 | 45.74 | 56.8 |
| **4** | 4.87 | 30.66 | 33.7 | 10.05 | 11.0 | 1.88 | 2.1 | 48.52 | 56.1 |
| **6** | 1.78 | 23.94 | 25.4 | 12.58 | 13.4 | 1.84 | 2.0 | 55.84 | 59.3 |
| **8** | 0.72 | 21.06 | 22.1 | 14.70 | 15.4 | 7.04 | 7.4 | 52.46 | 55.1 |

### 3.2.2 Results autoclave

In Table 19 to 23 below, the results of the reactions in the autoclave are displayed. Per reaction the experimental conditions are presented in short. Only the concentration of Co is given; the catalyst molar ratio that was used in all reactions was (Co + Mn)/Br = 1:1.

*Table 19 Experimental data of reaction A15. $T_{set}$ = 125°C, p = 20 bar, $[Co]_0$ = 0.011 M, $[HMF]_0$ = 0.200 M, $[acetaldehyde]_0$ = 0 M, t = 6 h, weight loss = unknown.*

| TIME (h) | [HMF] (mmol/L) | [DFF] (mmol/L) | $\sigma_{DFF}$ (%) | [X] (mmol/L) | $\sigma_X$ (%) |
|---|---|---|---|---|---|
| **0** | 200.52 | 0.20 | | -0.20 | |
| **0.5** | 195.73 | 0.17 | 3.5 | 4.63 | 96.5 |
| **1** | 199.08 | 0.15 | 10.2 | 1.30 | 89.8 |
| **1.5** | 206.07 | 0.00 | - | -5.54 | 100.0 |
| **2** | 201.36 | 0.08 | -10.1 | -0.91 | 110.1 |
| **3** | 196.15 | 0.11 | 2.5 | 4.27 | 97.5 |
| **4** | 192.87 | 0.07 | 0.9 | 7.58 | 99.1 |
| **5** | 201.21 | 0.00 | - | -0.68 | 100.0 |
| **6** | 177.64 | 0.00 | - | 22.89 | 100.0 |

*Table 20 Experimental data of reaction A16. $T_{set}$ = 125°C, p = 20 bar, $[Co]_0$ = 0.01 M, $[HMF]_0$ = 0.197 M, $[acetaldehyde]_0$ = 0.237 M, t = 6.75 h, weight loss = unknown.*

| TIME (h) | [HMF] (mmol/L) | [DFF] (mmol/L) | $\sigma_{DFF}$ (%) | [FFCA] (mmol/L) | $\sigma_{FFCA}$ (%) | [X] (mmol/L) | $\sigma_X$ (%) |
|---|---|---|---|---|---|---|---|
| **0** | 197.13 | 0.00 | - | 0.00 | - | 0.00 | - |
| **0.5** | 116.62 | 23.89 | 29.7 | 1.18 | 1.5 | 55.43 | 68.9 |
| **1** | 60.30 | 23.15 | 16.9 | 1.17 | 0.9 | 112.50 | 82.2 |
| **1.5** | 58.46 | 22.25 | 16.0 | 1.25 | 0.9 | 115.17 | 83.1 |
| **2** | 57.72 | 20.21 | 14.5 | 1.25 | 0.9 | 117.95 | 84.6 |
| **3** | 55.99 | 20.17 | 14.3 | 1.31 | 0.9 | 119.67 | 84.8 |
| **4** | 54.92 | 18.51 | 13.0 | 1.26 | 0.9 | 122.43 | 86.1 |
| **5** | 56.08 | 17.74 | 12.6 | 1.34 | 1.0 | 121.96 | 86.5 |
| **6.75** | 54.39 | 16.97 | 11.9 | 1.27 | 0.9 | 124.50 | 87.2 |

*Table 21 Experimental data of reaction A17. $T_{set}$ = 125°C, p = 20 bar, $[Co]_0$ = 0.01 M, $[HMF]_0$ = 0.222 M, $[acetaldehyde]_0$ = 0.132 M, t = 6.5 h, weight loss = 9.3 wt%.*

| TIME (h) | [HMF] (mmol/L) | [DFF] (mmol/L) | $\sigma_{DFF}$ (%) | [FFCA] (mmol/L) | $\sigma_{FFCA}$ (%) | [FDCA] (mmol/L) | $\sigma_{FDCA}$ (%) | [X] (mmol/L) | $\sigma_X$ (%) |
|---|---|---|---|---|---|---|---|---|---|
| **0** | 221.76 | 0.17 | | 0.00 | - | 0.00 | - | -0.17 | |
| **0.25** | 179.76 | 13.12 | 31.5 | 0.51 | 1.2 | 0.00 | - | 28.04 | 67.3 |
| **0.5** | 57.90 | 38.19 | 23.3 | 2.67 | 1.6 | 0.00 | - | 122.95 | 75.1 |
| **0.75** | 102.46 | 25.99 | 21.8 | 3.68 | 3.1 | 0.00 | - | 89.49 | 75.2 |
| **1** | 112.23 | 27.44 | 25.1 | 4.42 | 4.0 | 0.00 | - | 77.46 | 71.0 |
| **1.5** | 98.82 | 26.42 | 21.5 | 4.05 | 3.3 | 0.25 | 0.2 | 91.93 | 75.1 |
| **2** | 90.88 | 26.60 | 20.4 | 4.08 | 3.1 | 0.28 | 0.2 | 99.57 | 76.4 |
| **3** | 77.32 | 26.31 | 18.3 | 4.01 | 2.8 | 0.31 | 0,2 | 113.35 | 78.9 |
| **4** | 79.85 | 26.09 | 18.5 | 4.33 | 3.1 | 0.33 | 0,2 | 110.52 | 78.5 |
| **6.5** | 58.10 | 24.70 | 15.2 | 3.90 | 2.4 | 0.31 | 0,2 | 133.96 | 82.6 |

*Table 22 Experimental data of reaction A18. $T_{set}$ = 75°C, p = 20 bar, $[Co]_0$ = 0.01 M, $[HMF]_0$ = 0.187 M, $[acetaldehyde]_0$ = 0.227 M, t = 6.5 h, weight loss = 6.4 wt%.*

| TIME (h) | [HMF] (mmol/L) | [DFF] (mmol/L) | $\sigma_{DFF}$ (%) | [FFCA] (mmol/L) | $\sigma_{FFCA}$ (%) | [X] (mmol/L) | $\sigma_X$ (%) |
|---|---|---|---|---|---|---|---|
| **0** | 186.64 | 0.00 | - | 0.00 | - | 0.00 | - |
| **0.33** | 182.47 | 0.00 | 0.0 | 0.00 | 0.0 | 4.17 | 100.0 |
| **0.5** | 191.48 | 0.74 | -15.4 | 0.11 | -2.2 | -5.69 | 117.6 |
| **0.75** | 169.14 | 2.02 | 11.5 | 0.17 | 1.0 | 15.32 | 87.5 |
| **1** | 166.14 | 3.40 | 16.6 | 0.29 | 1.4 | 16.80 | 82.0 |
| **1.5** | 159.46 | 3.86 | 14.2 | 0.38 | 1.4 | 22.94 | 84.4 |
| **2** | 150.48 | 5.06 | 14.0 | 0.57 | 1.6 | 30.53 | 84.4 |
| **3** | 134.33 | 6.58 | 12.6 | 0.84 | 1.6 | 44.89 | 85.8 |
| **4** | 119.98 | 9.51 | 14.3 | 1.40 | 2.1 | 55.75 | 83.6 |
| **6.5** | 108.28 | 16.32 | 20.8 | 2.81 | 3.6 | 59.23 | 75.6 |

*Table 23 Experimental data of reaction A19. $T_{set}$ = 75°C, p = 40 bar, $[Co]_0$ = 0.01 M, $[HMF]_0$ = 0.181 M, $[acetaldehyde]_0$ = 0.237 M, t = 6.5 h, weight loss = 1.7 wt%.*

| TIME (h) | [HMF] (mmol/L) | [DFF] (mmol/L) | $\sigma_{DFF}$ (%) | [FFCA] (mmol/L) | $\sigma_{FFCA}$ (%) | [FDCA] (mmol/L) | $\sigma_{FDCA}$ (%) | [X] (mmol/L) | $\sigma_X$ (%) |
|---|---|---|---|---|---|---|---|---|---|
| **0** | 180.65 | 0.15 | | 0.00 | - | 0.00 | - | -0.15 | |
| **0.25** | 182.88 | 0.10 | -4.6 | 0.00 | 0.0 | 0.00 | - | -2.34 | 104.6 |
| **0.5** | 132.77 | 17.11 | 35.7 | 0.69 | 1.4 | 0.00 | - | 30.08 | 62.8 |
| **0.75** | 69.52 | 33.91 | 30.5 | 2.32 | 2.1 | 0.00 | - | 74.91 | 67.4 |
| **1** | 52.63 | 34.56 | 27.0 | 2.68 | 2.1 | 0.00 | - | 90.78 | 70.9 |
| **1.5** | 45.40 | 34.54 | 25.5 | 3.10 | 2.3 | 0.00 | - | 97.60 | 72.2 |
| **2** | 40.72 | 35.82 | 25.6 | 3.74 | 2.7 | 0.00 | - | 100.37 | 71.7 |
| **3** | 31.28 | 36.10 | 24.2 | 4.76 | 3.2 | 0.52 | 0.3 | 107.99 | 72.3 |
| **4** | 23.91 | 31.95 | 20.4 | 5.59 | 3.6 | 0.74 | 0.5 | 118.46 | 75.6 |
| **6.5** | 16.52 | 35.92 | 21.9 | 7.72 | 4.7 | 1.45 | 0.9 | 119.05 | 72.5 |

### 3.2.3 Results microreactor

In Table 25 to 28 below the results of the reactions in the microreactor are displayed. Per reaction the experimental conditions are presented in short. Only the concentration of Co is given; the catalyst molar ratio that was used in all reactions was (Co + Mn)/Br = 1:1. Attention must be paid to the fact that the first column (time) in these tables has another meaning than in the previous tables with experimental data for the semi-batch reactor and the autoclave. For the microreactor dealt with here, these times are not the reaction time, but only the times at which the aliquot was collected. An aliquot was taken from the vessel with reaction mixture before the start of the reaction (i.e. time 0), then at the moment when the slug flow had reached the end of the microreactor (i.e. time 'start') and every half an hour after that (i.e. time 0.5 h, 1 h etc). After the flow has run several times the residence time in the microreactor, the reaction is expected to have reached a steady state. The compound concentrations in the aliquots collected afterwards should remain the same. Pictures were taken from the slug flow at steady state at the inlet and outlet of the microreactor; these are displayed in Figure 17 to 20.
Reaction time in a microreactor is equal to the residence time therein, which is a function of the reactor volume and flow rate according to equation (f5). This was calculated for all the reaction conditions that were performed in the microreactor.

$$t = \frac{V_{microreactor}}{Q_{air}+Q_{liquid}} \qquad (f5)$$

The air flow rate that was measured by the mass flow controller is the value for standard temperature and pressure. The operating conditions of the reactions are nonetheless not standard, so the measured flow rate has to be converted to the actual flow rate by taking account of the effect of pressure and temperature. According to the ideal gas law (equation (f6)), the pressure at the inlet of the capillary tube can be calculated if the actual air flow rate therein is known. The pressure *p* in the ideal gas law is expressed in Pa, volume *V* in $m^3$, amount of gas *n* in moles, temperature *T* in K and the gas constant *R* is then 8,31 J $K^{-1}$ $mol^{-1}$.

$$pV = nRT \qquad (f6)$$

This was addressed by calculating the ratio of the length of the air bubble to the combined length of the bubble and liquid slug as observed at the microreactor inlet since this is approximately equal to the gas void fraction φ that is in turn equal to the ratio of the actual gas flow rate to the total flow rate. That is,

$$\frac{L_{bubble}}{L_{liquid\ slug}+L_{bubble}} = \varphi = \frac{Q_{air,in}}{Q_{air,in}+Q_{liquid}} \qquad (f7)$$

The amount *n* and the gas constant *R* stay the same so the dependence in (f8) can be derived. The units that were used are mL/min for flow rate *Q*; *p* is in bar and *T* in °C.

$$\frac{Q_{air,in}}{Q_{air,STP}} = \frac{p_{STP}}{p_{in}} \cdot \frac{T+273}{T_{STP}+273} \qquad \text{(f8)}$$

Now the pressure at the inlet $p_{in}$ is known, the average pressure $p_{av}$ in the microreactor can be calculated, assuming the pressure at the outlet is 1 bar. Through the ideal gas law this can again be converted to the average actual air flow rate $Q_{air,av}$ that can be used to calculate the reaction time. That is,

$$\frac{Q_{air,av}}{Q_{air,STP}} = \frac{p_{STP}}{p_{av}} \cdot \frac{T+273}{T_{STP}+273} \qquad \text{(f9)}$$

$$t = \frac{V_{microreactor}}{Q_{air,,av}+Q_{liquid}} \qquad \text{(f10)}$$

The results of these calculations for the experiments in the microreactor are given in Table 24. It should be mentioned that $P_{STP}$ is 1 bar, $T_{STP}$ is 0°C and the microreactor volume is 5.03 mL.

*Table 24 Calculated values of actual air flow rate and reaction time.*

| **EXP. NO.** | | **M20** | **M21** | **M22** | **M23** |
|---|---|---|---|---|---|
| **$Q_{AIR,STP}$** | mL/min | 0.200 | 0.150 | 0.150 | 0.200 |
| **$Q_{LIQUID}$** | mL/min | 0.033 | 0.033 | 0.017 | 0.033 |
| **T** | °C | 70 | 70 | 70 | 90 |
| | | | | | |
| **φ** | - | 0.794 | 0.699 | 0.853 | 0.791 |
| **$Q_{AIR,IN}$** | mL/min | 0.129 | 0.077 | 0.097 | 0.126 |
| **$P_{IN}$** | bar | 1.95 | 2.43 | 1.95 | 2.11 |
| **$P_{AV}$** | bar | 1.48 | 1.72 | 1.48 | 1.56 |
| | | | | | |
| **$Q_{AIR,AV}$** | mL/min | 0.170 | 0.110 | 0.128 | 0.171 |
| **REACTION TIME** | min | 24.7 | 35.1 | 34.8 | 24.6 |

*Table 25 Experimental data of reaction M20. T = 70°C, φ = 0.794, $[Co]_0$ = 0.01 M, $[HMF]_0$ = 0.189 M, $[acetaldehyde]_0$ = 0.227 M, t = 24.7 min*

| TIME (h) | [HMF] (mmol/L) | [DFF] (mmol/L) | $\sigma_{DFF}$ (%) | [FFCA] (mmol/L) | $\sigma_{FFCA}$ (%) | [X] (mmol/L) | $\sigma_X$ (%) |
|---|---|---|---|---|---|---|---|
| **0** | 189.01 | 0.08 | | 0.00 | - | -0.08 | |
| **start** | 193.99 | 0.00 | 0.0 | 0.00 | 0.0 | -4.98 | 100.0 |
| **0.5** | 198.47 | 0.00 | 0.0 | 0.00 | 0.0 | -9.46 | 100.0 |
| **1** | 190.33 | 1.75 | -132.2 | 1.15 | -86.8 | -4.22 | 318.9 |
| **1.5** | 193.05 | 3.85 | -95.4 | 0.51 | -12.6 | -8.40 | 208.0 |
| **2** | 191.21 | 3.34 | -151.8 | 0.77 | -35.2 | -6.32 | 287.0 |
| **2.5** | 192.29 | 3.70 | -112.6 | 0.59 | -18.1 | -7.57 | 230.7 |
| **3** | 190.31 | 3.03 | -232.0 | 0.85 | -65.0 | -5.18 | 397.0 |
| **3.5** | 185.04 | 2.87 | 72.3 | 0.81 | 20.4 | 0.29 | 7.3 |
| **4** | 207.66 | 3.19 | -17.1 | 0.70 | -3.8 | -22.54 | 120.9 |

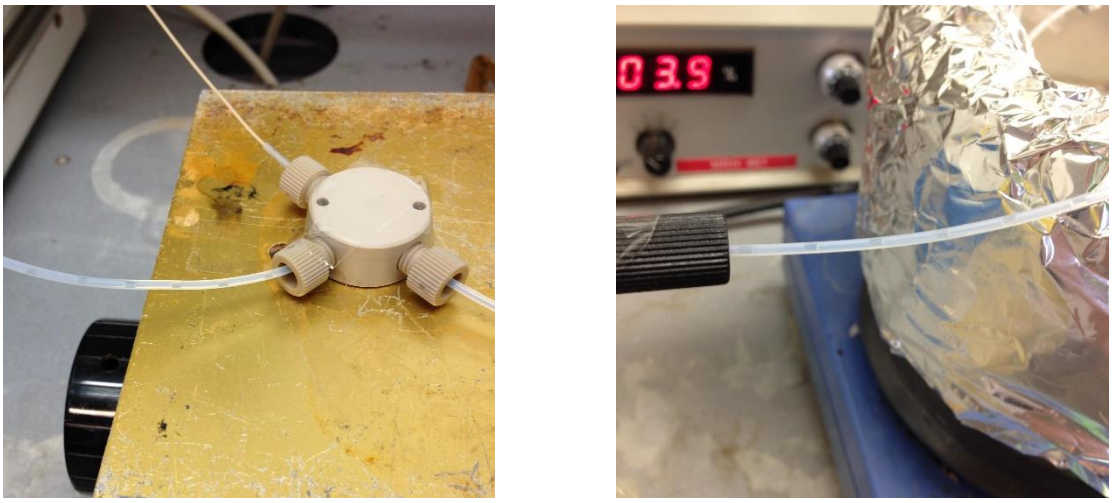

*(a)* *(b)*

*Figure 17 Slug flow during reaction M20 at the inlet (a) and outlet (b).*

*Table 26 Experimental data of reaction M21. T = 70°C, φ = 0.699, $[Co]_0$ = 0.01 M, $[HMF]_0$ = 0.198 M, $[acetaldehyde]_0$ = 0.227 M, t = 35.1 min*

| TIME (h) | [HMF] (mmol/L) | [DFF] (mmol/L) | $\sigma_{DFF}$ (%) | [FFCA] (mmol/L) | $\sigma_{FFCA}$ (%) | [X] (mmol/L) | $\sigma_X$ (%) |
|---|---|---|---|---|---|---|---|
| **0** | 197.91 | 0.00 | | 0.00 | | 0.00 | |
| **start** | 189.28 | 0.00 | 0.0 | 0.00 | 0.0 | 8.63 | 100.0 |
| **0.5** | 195.87 | 0.29 | 14.2 | 0.46 | 22.7 | 1.29 | 63.1 |
| **1** | 202.24 | 0.34 | -7.9 | 0.59 | -13.6 | -5.26 | 121.5 |
| **1.5** | 202.56 | 0.27 | -5.9 | 0.44 | -9.5 | -5.36 | 115.4 |
| **2** | 203.69 | 0.26 | -4.4 | 0.48 | -8.4 | -6.52 | 112.8 |
| **2.5** | 208.07 | 0.26 | -2.5 | 0.51 | -5.0 | -10.93 | 107.5 |
| **3** | 188.47 | 0.21 | 2.2 | 0.41 | 4.3 | 8.83 | 93.5 |
| **3.5** | 208.13 | 0.22 | -2.2 | 0.51 | -4.9 | -10.95 | 107.1 |

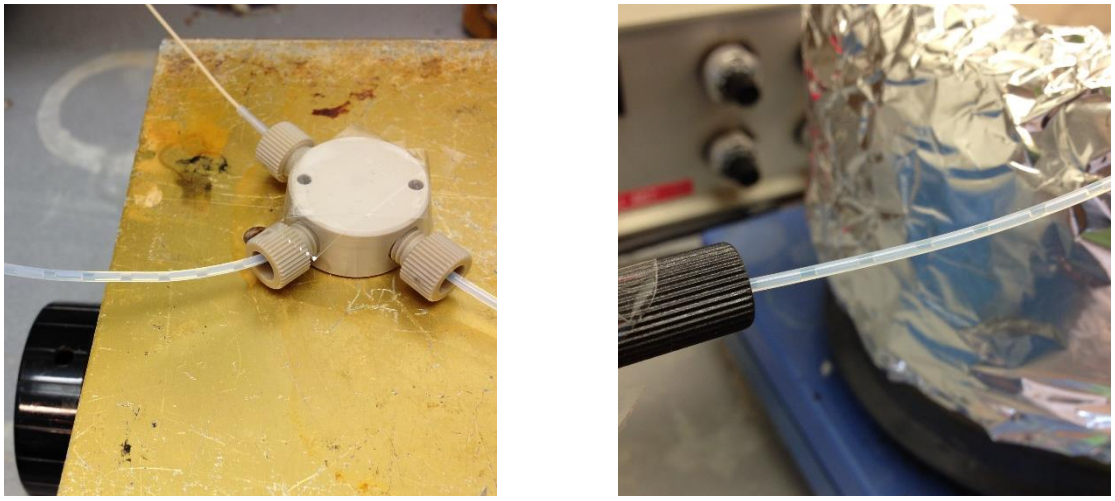

*(a)* *(b)*

*Figure 18 Slug flow during reaction M21 at the inlet (a) and outlet (b).*

*Table 27 Experimental data of reaction M22. T = 70°C, φ = 0.853, $[Co]_0$ = 0.01 M, $[HMF]_0$ = 0.211 M, $[acetaldehyde]_0$ = 0.227 M, t = 34.8 min*

| TIME (h) | [HMF] (mmol/L) | [DFF] (mmol/L) | $\sigma_{DFF}$ (%) | [FFCA] (mmol/L) | $\sigma_{FFCA}$ (%) | [X] (mmol/L) | $\sigma_X$ (%) |
|---|---|---|---|---|---|---|---|
| **0** | 211.40 | 0.00 | | 0.00 | | 0.00 | |
| **start** | 221.74 | 2.97 | -28.7 | 2.17 | -21.0 | -15.48 | 149.7 |
| **0.5** | 195.46 | 0.57 | 3.6 | 1.29 | 8.1 | 14.08 | 88.3 |
| **1** | 181.61 | 0.57 | 1.9 | 0.99 | 3.3 | 28.23 | 94.8 |
| **1.5** | 202.42 | 4.85 | 54.0 | 1.02 | 11.3 | 3.11 | 34.7 |
| **2** | 198.66 | 3.67 | 28.8 | 1.02 | 8.0 | 8.06 | 63.2 |
| **2.5** | 197.41 | 3.79 | 27.1 | 1.20 | 8.5 | 9.01 | 64.4 |
| **3** | 194.09 | 3.30 | 19.0 | 0.97 | 5.6 | 13.04 | 75.3 |
| **3.5** | 202.35 | 4.03 | 44.6 | 1.01 | 11.1 | 4.01 | 44.3 |
| **4** | 188.66 | 3.66 | 16.1 | 1.27 | 5.6 | 17.81 | 78.3 |

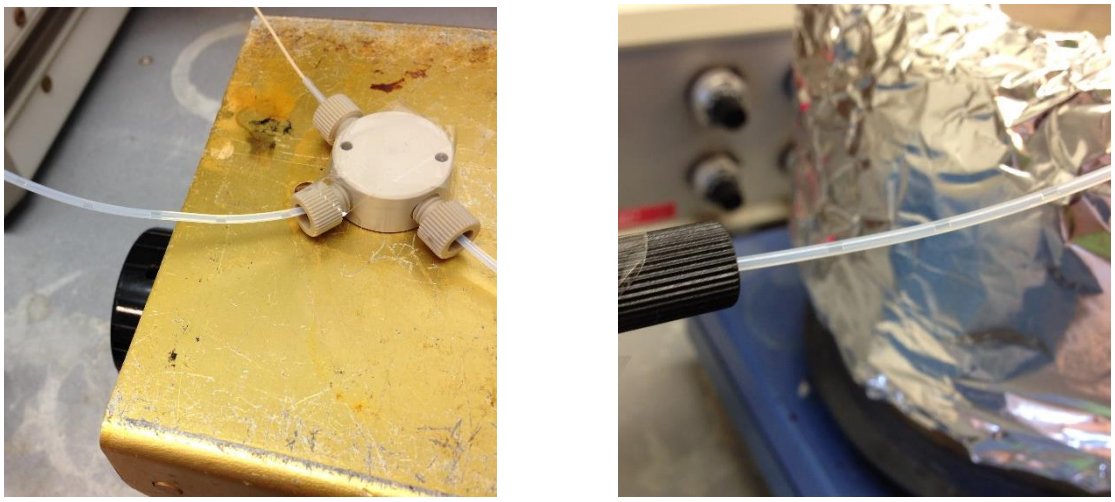

*(a)* *(b)*

*Figure 19 Slug flow during reaction M22 at the inlet (a) and outlet (b).*

*Table 28 Experimental data of reaction M23. T = 90°C, φ = 0.791, $[Co]_0$ = 0.01 M, $[HMF]_0$ = 0.185 M, $[acetaldehyde]_0$ = 0.245 M, t = 24.6 min*

| TIME (h) | [HMF] (mmol/L) | [DFF] (mmol/L) | $\sigma_{DFF}$ (%) | [FFCA] (mmol/L) | $\sigma_{FFCA}$ (%) | [X] (mmol/L) | $\sigma_X$ (%) |
|---|---|---|---|---|---|---|---|
| **0** | 184.84 | 0.00 | | 0.00 | | 0.00 | |
| **start** | 164.73 | 4.73 | 23.5 | 0.64 | 3.2 | 14.73 | 73.3 |
| **0.5** | 163.86 | 11.04 | 52.6 | 1.61 | 7.7 | 8.32 | 39.7 |
| **1** | 167.73 | 11.22 | 65.6 | 4.05 | 23.7 | 1.85 | 10.8 |
| **1.5** | 174.84 | 9.56 | 95.6 | 1.51 | 15.1 | -1.07 | -10.7 |
| **2** | 177.34 | 9.07 | 121.1 | 1.40 | 18.7 | -2.98 | -39.7 |
| **2.5** | 177.70 | 8.95 | 125,3 | 1.69 | 23.7 | -3.50 | -49.1 |
| **3** | 181.75 | 8.35 | 270.6 | 1.62 | 52.4 | -6.88 | -223.1 |
| **3.5** | 181.83 | 8.03 | 267.0 | 1.57 | 52.3 | -6.60 | -219.3 |
| **4** | 194.73 | 8.75 | -88.5 | 1.82 | -18.4 | -20.46 | 206.9 |

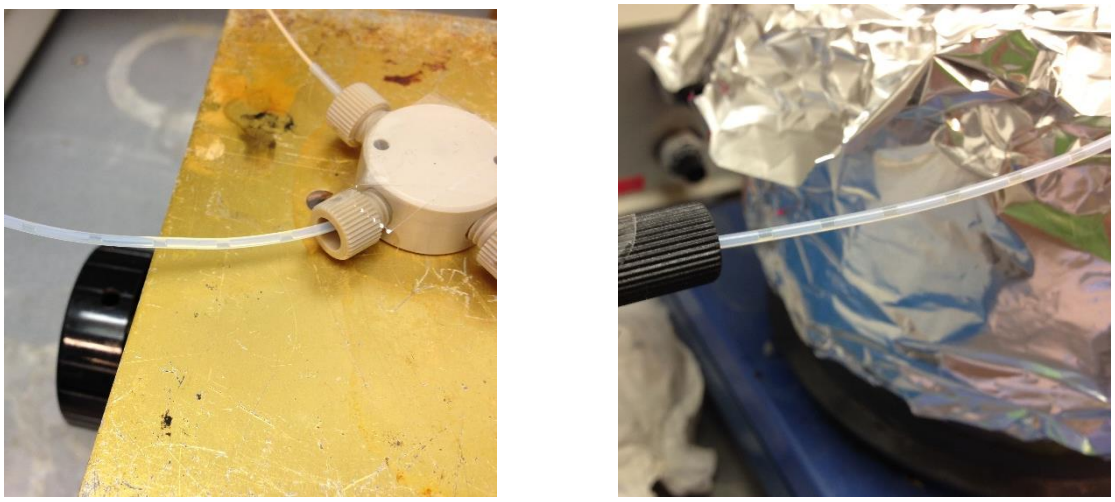

*(a)* *(b)*

*Figure 20 Slug flow during reaction M23 at the inlet (a) and outlet (b).*

# 4. DISCUSSION

In this chapter the results of the reactions that were performed in this research are discussed. First, some general remarks are made on how these results are interpreted.

As said in the previous chapter two different pathways are considered for the autoxidation reaction of HMF:

1) $\mathrm{HMF} \rightarrow \mathrm{DFF} \rightarrow \mathrm{FFCA} \rightarrow \mathrm{FDCA}$
2) $\mathrm{HMF} \rightarrow \text{side products (X)}$

The experimental results are first discussed based on two assumptions regarding the behaviour of the reaction:

a) The reaction rate is not limited by oxygen mass transfer from gas to liquid.
b) The reaction of HMF to the desired products (pathway 1) is first order in HMF.

This means that the reaction order in the dissolved oxygen is not considered according to assumption a (i.e., the dissolved oxygen concentration is constant and the reaction is approximated as pseudo-first order). The reaction rate $r_1$ of pathway 1 is given by equation (f11) that can be integrated into equation (f12). The conversion X is then given by (f13) and the temperature dependence of the pseudo-first order reaction rate constant, $k_1$, is shown in (f14).

$$r_1 = k_1[\mathrm{HMF}] \tag{f11}$$

$$[\mathrm{HMF}] = [\mathrm{HMF}]_0 e^{-k_1 t} \tag{f12}$$

$$X_{\mathrm{HMF}} = 1 - e^{-k_1 t} \tag{f13}$$

$$k_1 = k_0 e^{\frac{-E_A}{RT}} \tag{f14}$$

Assumption a and b were tested by performing reactions in three types of operations (batch, semi-batch and continuous) and varying several parameters (temperature, pressure, flow rate and HMF, acetaldehyde and catalyst concentration). In this way the requirements for the reaction to run efficiently could be determined and a general view on the mass transfer behaviour and the kinetics of the reaction was developed.

## 4.1 Requirements for functioning of the reaction

A blank reaction, without addition of catalyst and acetaldehyde (entry SB1: T = 90°C, $Q_{air}$ = 353.9 mL/min, $[Co]_0$ = 0 M, $[HMF]_0$ = 0.216 M), was performed to check whether anything happened with a solution of HMF in acetic acid upon heating and exposure to an air flow. The concentration of HMF stayed approximately the same, by taking measurement and sample preparation errors into account (max 4.3%), therefore it can be stated that HMF does not significantly react without the presence of a catalyst, see Figure 21. Literature states that this is the case for acetaldehyde as well (Bawn and Williamson 1950), this was however not experimentally checked in this research.

Not only a catalyst is necessary to oxidise HMF, also an initiator is needed. Reaction SB2 (T = 90°C, $Q_{air}$ > 353.9 mL/min, $[Co]_0$ = 0.030 M, $[HMF]_0$ = 0.155 M) was performed at atmospheric pressure, with catalyst but without acetaldehyde and this showed no product formation until after eight hours when a tiny peak is visible in the chromatogram for DFF and FFCA. Unfortunately the analysis of this reaction was done without internal standard so there is no data available on the actual HMF and product concentrations. Reaction A15 (T = 123°C, p = 20 bar, $[Co]_0$ = 0.011 M, $[HMF]_0$ = 0.200 M) was performed with similar reactant concentration and without acetaldehyde, but at 20 bar pressure. This reaction showed no product formation either after the six hours that the reaction was run. The difference in catalyst concentrations has only a small influence on the reaction performance, as will be explained in paragraph 4.1.2. Reaction A15 confirms, however, that an initiator such as acetaldehyde as is necessary to give the reaction a kick-start, even when catalyst is present in the mixture.

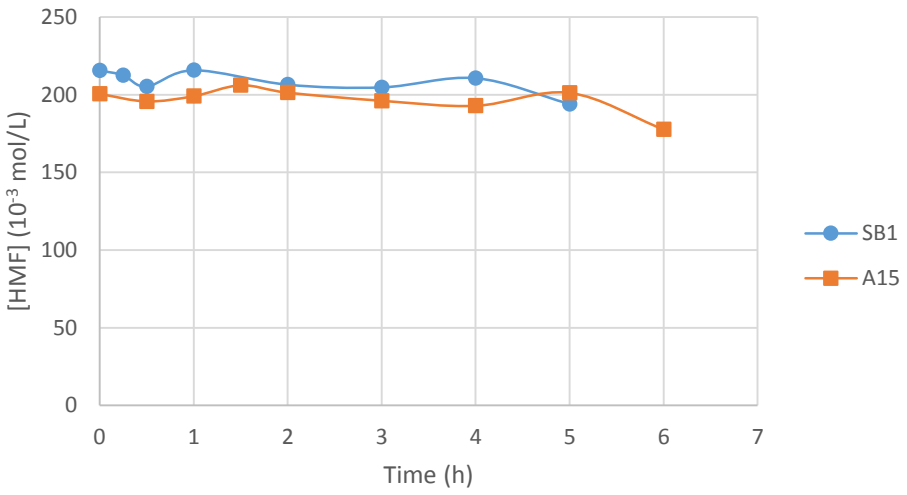


*Figure 21 Almost no HMF conversion or product formation occurred without addition of acetaldehyde in the time reactions SB1 (T = 90°C, $Q_{air}$ = 353.9 mL/min, $[Co]_0$ = 0 M, $[HMF]_0$ = 0.216 M) and A15 ($T_{set}$ = 125°C, p = 20 bar, $[Co]_0$ = 0.011 M, $[HMF]_0$ = 0.200 M) were run.*

### 4.1.1 Influence of acetaldehyde concentration

To test if a threshold for the initiator exists, the acetaldehyde concentration was varied in reactions SB3-5, A16 and A17 (0.226 M acetaldehyde in SB3, 0.119 M in SB4, 0.061 M in SB5, 0.237 M in A16 and 0.132 M in A17). It turned out that presence of acetaldehyde is essential for the reaction to proceed within hours under these conditions (SB: T = 90°C, $Q_{air}$ = 353.9 mL/min, $[Co]_0$ = 0.030 M; A: $T_{set}$ = 125°C, p = 20 bar, $[Co]_0$ = 0.010 M). Even a certain threshold had to be met, because no reaction had yet occurred at atmospheric pressure after three hours at an acetaldehyde concentration of 0.061 M (SB5), only at higher concentrations did the reaction occur. From this set of reactions it can be concluded that initiation is rate limiting, since a lower acetaldehyde concentration results in a lower reaction rate. This finding is supported by literature like was described in paragraph 1.1.3 (Bawn and Williamson 1950).

The earlier work of Bawn and Wiliamson (1950) taught us that autoxidation of acetaldehyde is linearly dependent on the acetaldehyde concentration, as is shown in Figure 22. This means that a reaction between acetaldehyde and oxygen does take place, even at low acetaldehyde concentrations. This statement is according to assumption a, that oxygen mass transfer is not limiting. It contradicts our findings, however. The fact that no HMF was converted in three hours at such low acetaldehyde concentration (reaction SB5) can best be explained by a too low HMF concentration. In that way the peracid radicals that are formed from acetaldehyde are terminated before even reaching an HMF molecule. This hypothesis can be tested by performing a reaction with that same low acetaldehyde concentration, but with a higher HMF concentration.

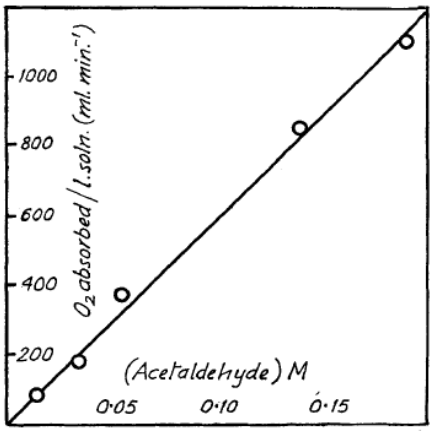


*Figure 22 Rate of oxygen consumption as a function of the acetaldehyde concentration. Adapted from (Bawn and Williamson 1950)*

In Figure 23 below the HMF conversion is displayed as a function of the reaction time for the reactions named above that showed product formation (entries SB3-5, A16 and A17). The initial HMF concentrations varied in these reactions, therefore the HMF conversion was plotted for easy comparison. A lower acetaldehyde concentration gives a slightly lower HMF conversion, due to the fact that less HMF molecules can be activated for oxidation if less peracetic acid is present. HMF

conversion is higher at 20 bar than at 1 bar at approximately the same acetaldehyde concentration because of higher oxygen concentration in the former case. Namely, according to the ideal gas law, the same volume contains more air (oxygen) at higher pressure. A higher oxygen concentration in the mixture results in a fast production rate of peracetic acid from acetaldehyde, subsequently contributing to higher rate of HMF oxidation. High acetaldehyde concentration (~0.23 M) was determined as the optimal concentration for the conditions used in this research, resulting in an acetaldehyde : HMF ratio of 1.29.

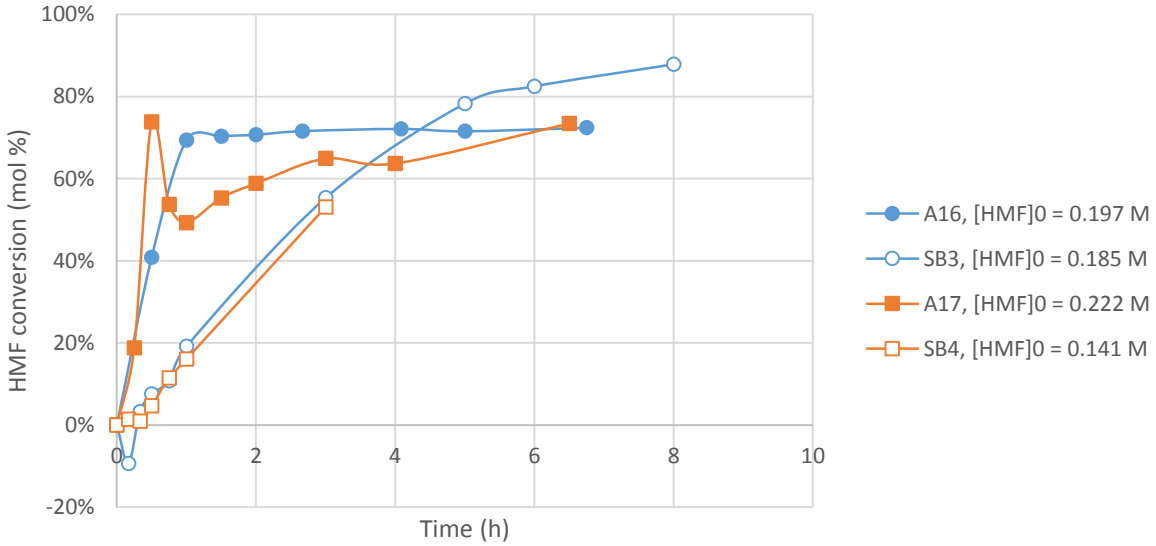


*Figure 23 HMF conversion of reactions SB3 and A16 at high (0.226 M, 0.237 M respectively) acetaldehyde concentration and SB4 and A17 at medium (0.119M, 0.132 M) acetaldehyde concentration, as a function of the reaction time. The fact that the HMF conversion reaches a maximum in the autoclave is addressed later in paragraph 4.3.2. SB: T = 90°C, $Q_{air}$ = 353.9 mL/min, $[Co]_0$ = 0.030 M; A: $T_{set}$ = 125°C, p = 20 bar, $[Co]_0$ = 0.010 M)*

### 4.1.2 Influence of catalyst concentration

Three different catalyst concentrations were tested (SB7: 0.03 M Co, SB11: 0.01 M Co, SB12: 0.002 M Co; T = 90°C, $Q_{air}$ = 88.49 mL/min, $[HMF]_0 \approx 0.184$ M) at high acetaldehyde concentration (~0.23 M). Only the concentration of Co is given; the catalyst molar ratio that was used in all reactions was (Co + Mn)/Br = 1:1. As was explained in paragraph 1.1.3, initiation of the reaction is dependent on the catalyst. Although only a trace of a trivalent metal is necessary to initiate the reaction, the chance of initiation increases with catalyst concentration. This explains the graph displayed in Figure 24 where it is clearly visible that a low catalyst concentration (0.002 M Co) obstructs good reaction rates and conversion. As catalyst concentration is increased to 0.010 M Co, the HMF conversion decreases much faster over time. This result is similar to that of Partenheimer (2000); they showed that for the same system, the rate of reaction increased 2.1 times when the catalyst concentration was doubled. Also in the patent of Grushin (2014) higher reaction rates were measured for an increase in catalyst concentration. The catalyst concentrations used in this

research lay within the same range as used by Partenheimer; Grushin used higher catalyst concentrations.
However, the HMF conversion decreases slightly slower when the catalyst concentration is tripled (reaction SB7 (0.03 M Co) as compared with reaction SB11 (0.01 M Co)), a result that was also obtained by Partenheimer. The catalyst tends to form dimeric complexes, a phenomenon that is more likely to happen at higher catalyst concentrations. This makes the catalyst less active.

As will be explained in paragraph 4.2.3 a higher catalyst concentration should account for better yield towards the desired products and therefore reactions with low catalyst concentrations should result in large formation of side products. In terms of weight loss of the reaction mixture this dependence was not experimentally proven, as is further explained below in paragraph 4.2.3. The selectivity towards X was, however, indeed highest at the lowest catalyst concentration, according to literature. It was slightly lower in reaction SB11 (0.010 M Co) compared to reaction SB7 (0.030 M Co), see Figure 25. An hypothesis was that increasing the catalyst concentration did not help to improve the product yields because the HMF concentration used was too low resulting in internal mass transfer limitations. Partenheimer, however, used similar catalyst concentrations with a higher HMF concentration and obtained the similar results. This shows that product yield is not limited by internal mass transfer and thus catalyst deactivation due to dimerization is a feasible explanation.
The final FDCA yield (13.7 mol%) obtained in reaction SB11 (0.010 M Co) was the highest achieved during this research. Along with that the DFF selectivity is visibly higher than in reaction SB7 (0.030 M Co) as is also shown in Figure 25. This is a result in accordance with the results of Partenheimer. The catalyst concentration of 0.010 M Co was determined as the optimal concentration for the conditions used in this research, resulting in a Co : HMF ratio of 0.06.

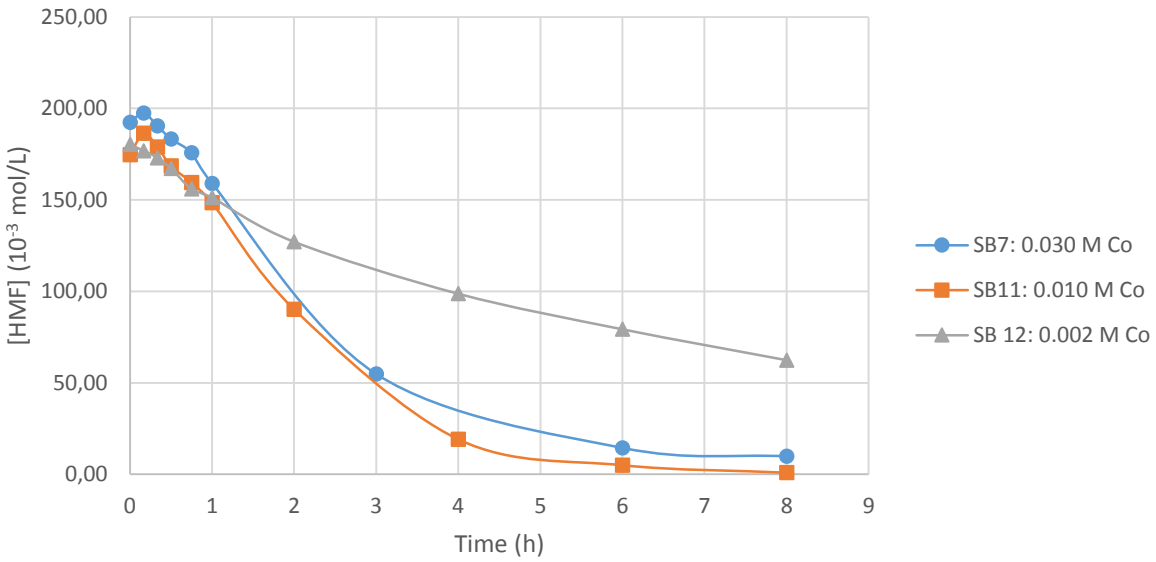


*Figure 24 HMF concentrations of reactions SB7, SB11 and SB12 as a function of the reaction time. T = 90°C, $Q_{air}$ = 88.49 mL/min, $[HMF]_0 \approx 0.184$ M, $[acetaldehyde]_0 \approx 0.23$ M.* Note: *the increase in HMF conversion at the beginning of the reaction is further explained in paragraph 4.2.2.*

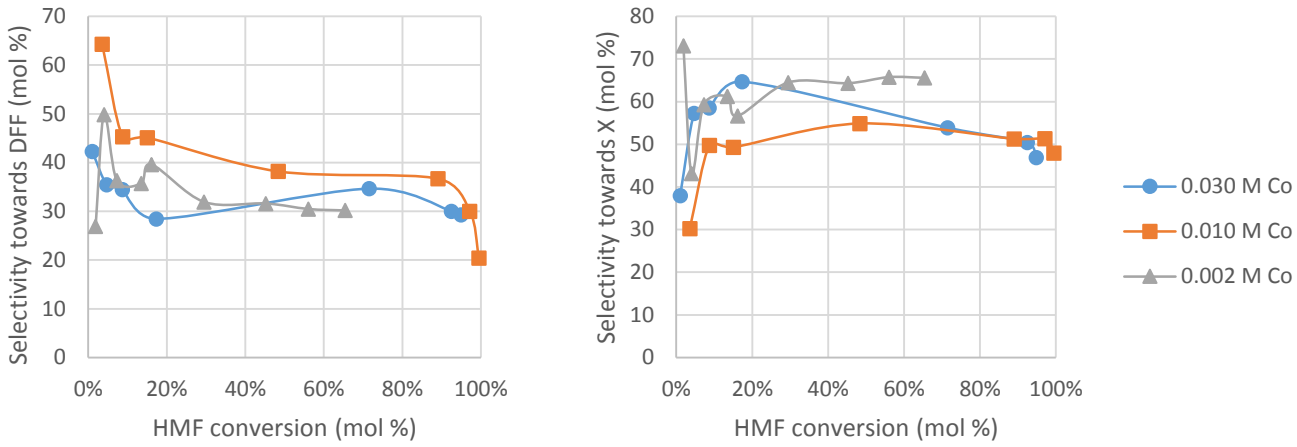


*(a)* *(b)*

*Figure 25 Selectivity towards DFF (a) and X (b) as a function of HMF conversion for reactions at different catalyst concentrations. Negative data points are not plotted since they have no value for the purpose of this research.*

## 4.2 Mass balance

As was briefly mentioned before, it was not possible to always close the mass balance for this research. Several explanations can be given supported by literature. Formation of additional oxidation products which could be identified so far is the most feasible explanation, since HMF is likely to be converted to more oxidation products than DFF, FFCA and FDCA (van Putten, et al. 2013).

### 4.2.1 AMF

As is shown in paragraph 3.1.1 the peaks of HMF and AMF have the same retention time. This means that separate integration of the HMF peak is not possible and calculation of the HMF concentration is hindered. In paragraph 3.1.2 it is shown that the response factor of AMF is lower than that of HMF, meaning that the peak area of HMF is affected negatively if AMF is formed and this results in a calculated HMF concentration that is too low. The AMF peak also displays a large tail, influencing the peaks appearing later in the chromatogram, see Figure 26. Although peak tailing is unfortunate, in this case it does make it easy to see whether AMF is present in the sample. AMF was in general only detected at later reaction times, thus at high HMF conversion. In Figure 26 the DFF peak is also visible: a clear large peak indicating that the reaction is in an advanced stage. If the “AMF tail” was visible in the chromatogram, the peaks were integrated according to the figure.
This might cause some inaccuracies in calculating the exact HMF concentration because only the response factor of HMF was used for calculations; the response factor of AMF was only determined to see the influence on HMF concentration calculations. To be able to calculate the amount of AMF formed during the reaction, a calibration should be performed on mixtures of HMF and AMF or the samples should be analysed by a method that is capable of distinguishing between AMF and HMF.

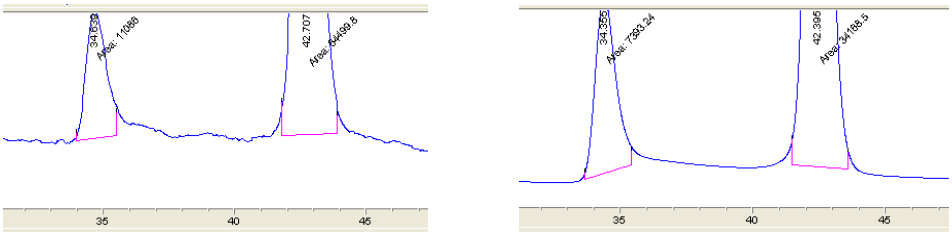


*(a)* *(b)*

*Figure 26 RID (a) and UV (b) chromatogram between RT 30-50 min at high HMF conversion (reaction SB13, t = 8h)*

### 4.2.2 HMF excess

In more than half of the reactions (reaction SB3, SB7-11 and SB14) that were performed in the semi-batch reactor, the HMF concentration appeared to increase at the beginning of the reaction. In reactions A18 and A19 in the autoclave, the "spike" was also observed. In Figure 27 a graph is displayed where a typical spike is visible for three of the four plotted reaction entries. In every reaction in the microreactor an increase in HMF concentration was determined, even after the reaction had run several times the reaction time in the microreactor. This results in data that does not make any sense; for example negative conversions, a negative concentration of side products X and negative selectivities towards the products. Since no additional HMF was added after starting the reaction, another explanation must be found. By introducing an air flow to the reaction mixture in the semi-batch reactor, it is likely that part of the solvent (i.e. acetic acid) evaporates into this air flow and leave out of the reactor although a reflux condenser was used, resulting in an increase in the concentration of the compounds in the mixture over time. As said before the concentrations of all the compounds were corrected for this weight loss, assuming it happened linearly over time, see Appendix III: Calculation example for weight loss compensation. A possibility is, however, that more solvent is evaporated at initiation of the air flow resulting in an relatively high concentration of HMF at the start of the reaction. The HMF "excess" should then be highest when the highest flow rate is used. Experimental data however do not confirm this statement, as can be seen in Figure 27. The reaction at 10% flow rate showed a significant spike while the reaction at 50% flow rate does not show a spike at all. The formation of AMF is not the cause of the spike either, since it is only detected at later reaction times, as is stated above.

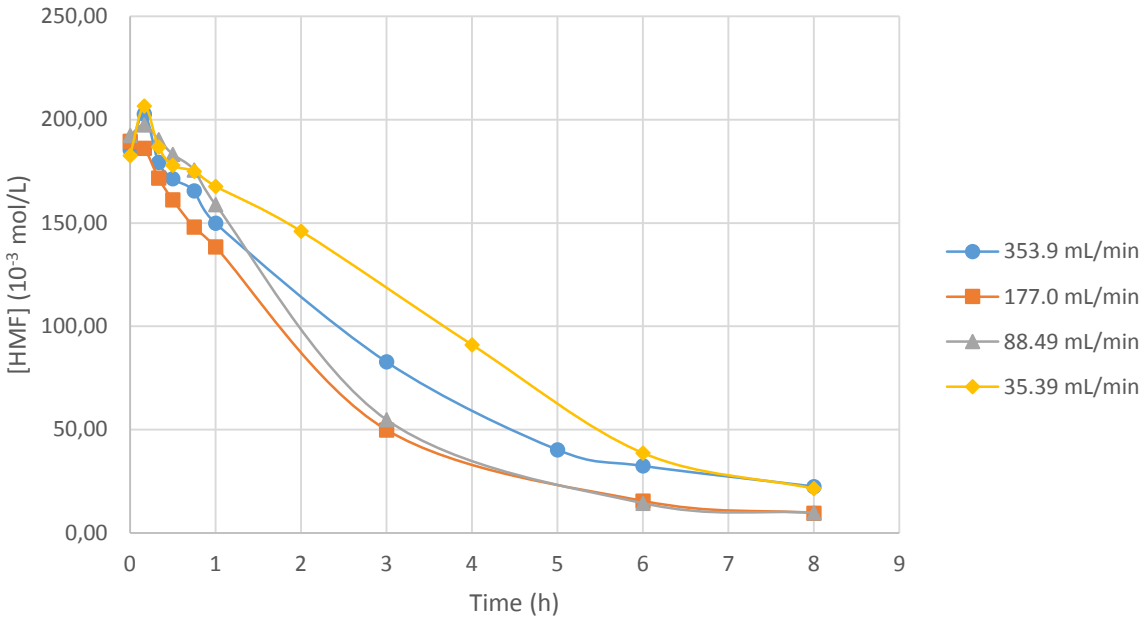


*Figure 27 HMF concentrations as a function of time at different air flow rates. Reactions SB3 (353.9 mL/min), SB6 (177.0 mL/min), SB7 (88.49 mL/min) and SB8 (35.39 mL/min) were compared. T = 90°C, $[Co]_0$ = 0.03 M, $[HMF]_0 \approx 0.197$ M, $[acetaldehyde]_0 \approx 0.24$ M*

A more probable explanation is that a product is formed that gives a response at the same retention time as HMF, but has a higher response factor. This product could have been 5-hydroxymethyl-2-furancarboxylic acid (HMFCA), a compound that is formed upon oxidation of the aldehyde group of HMF before oxidation of the alcohol group. HMFCA, however, emerges from the column at a lower retention time than HMF. Further research should be done to indicate if this "excess" is indeed caused by the formation of an additional oxidation product and what compound it is. Besides that the cause of forming this product should be identified, since the "excess" of HMF is not detected in all the reactions. In most of the performed reactions, HMF concentration before starting the reaction, measured by HPLC turned out to be higher than the concentration established by weighted amounts. This is partly caused by weighing errors and sample preparation errors, but it should be kept in mind that a product could have formed. In some cases the deviation is more than 10% and therefore this indicates an interesting topic for further research.

### 4.2.3 $CO_x$ formation

The formation of $CO_x$ is not accounted for in the mass balance since this was not measured during the reactions in this research. It is quite certain that this happens, as is extensively described in literature (Partenheimer and Grushin 2000, Partenheimer 2005, 2006, Kagan and Lubarsky 1934). The extent to which this happens in benzyl alcohol or aldehyde aerobic oxidation is negligible (< 0.01%) (Partenheimer 2005, 2006), but it becomes more significant when HMF is starting material. Due to the low resonance energy of HMF and its formyl functionality higher rates towards $CO_x$ formation are not surprising (Partenheimer and Grushin 2000).

A weight loss was indeed detected for all the reactions that were performed in the semi-batch reactor. This was assigned to evaporation of the solvent due to the air flow, since the blank reaction in the semi-batch reactor suffered from a 14.7% weight loss (SB1: T = 90°C, $Q_{air}$ = 353.9 mL/min). Nevertheless even at the lowest air flow rate (35.39 mL/min) a weight loss of 3.6% was measured and during the reactions in the autoclave a weight loss of the reaction mixture was also established. See Appendix III for an overview of the weight losses that were measured.

The weight loss in semi-batch operation ranged from 5.3% to 8.0% at an air flow rate of 88.49 mL/min (25% of full range flow rate of mass flow controller), values that are similar to the ones established by Partenheimer (2000) and were attributed to $CO_x$ formation. The air flow rate that was used is their work is not given, making a comparison unattainable. It is however an interesting result and suitable for further research.
In the same work of Partenheimer it was discovered that a higher catalyst concentration ([Co] > 0.01M) decreases the rate of reaction towards $CO_x$ formation. As was briefly mentioned in paragraph 4.1.2, this relationship was not confirmed in this research: at the same flow rates (88.49 mL/min; 25% full range) the reaction with the highest catalyst concentration (0.030 M Co; reaction SB7) that was tested suffered from a weight loss of 8.0% while the reaction with 0.010 M Co (reaction SB11) had only 6.7% weight loss. A reaction at the same or lower air flow rate with higher catalyst concentration should give more information on whether the weight loss might only be accounted for by the flow rate or if the catalyst could play a role here too.

### 4.2.4 Oligomers and other humins

A peak was visible in the chromatogram at retention time around 63 minutes, which increased during the reaction and therefore indicates formation of an additional compound. It was presumed that this was caused by an oligomer of HMF, such as a dimer. Oligomers of HMF can be formed upon homogeneous metal catalysed oxidation of HMF (van Putten, et al. 2013).

Formation of only one additional oxidation product does not account for the whole gap in the mass balance, since the area of the peak at RT 63 was not proportional to the gap. Oxidation of HMF tends to produce other humins as well, especially in acetic acid, that can also account for the gap in the mass balance. In some of the later reaction samples, a broad peak emerged at the beginning of the chromatogram, presumably belonging to a compound from the previous sample that had not yet left the column. In some cases, this peak seemed to increase, but accurate integration of the peak was difficult since it was so broad.

In the reaction samples peaks at RT 53 and RT 61 were always visible, especially at the beginning of the reaction, but they were absent in the calibration samples of HMF. This makes it likely that they were caused by an interaction of HMF with the catalyst. At various other retention times little peaks were visible in the chromatogram, indicating other unidentified products.

A change to an analytical method that can give information on the actual molecular structure will offer more clarity on the composition of the reaction mixture. A mass spectrometer can for example distinguish between AMF and HMF. A GC-MS was present, but is was chosen not to work with this analytical method since the metals present in the reaction mixture could clog the column of the gas chromatograph because they cannot be vaporised.

## 4.3 Mass transfer limitations

The mass transfer of oxygen from gas to liquid is not considered to be rate limiting for a first approximation, as was assumed at the beginning of this chapter. Oxygen mass transfer rate is dependent on the mass transfer coefficient ($k_L$) and the interfacial area ($a$). In this paragraph the extent to which this statement is correct is discussed.

### 4.3.1 Semi-batch operation: influence of air flow rate

As was mentioned in paragraphs 1.1.3 and 4.1.1 the acetaldehyde autoxidation is independent of the mass transfer of the oxygen from air to acetic acid at atmospheric pressure, since oxygen uptake can be measured as soon as the reaction is initiated (Bawn and Williamson 1950). The experimental setup used in their work was however not a bubble reactor like the one that was used in our research. They used a pear-shaped vessel with a piston rod to enable vigorous shaking. Oxygen was supplied by a thermostated gas burette that was connected to the vessel by a rubber tube. Oxygen supply is considered to be sufficient for efficient mass transfer.
Our semi-batch reactor can be considered as a single nozzle bubble column with small liquid volume, operated at atmospheric pressure. Lau et al. performed a study to the mass transfer of oxygen in different types of shallow bubble column reactors and concluded that the volumetric gas-liquid mass transfer coefficient ($k_La$) is lowest for our type of reactor compared to a perforated or porous plate bubble column reactor (Lau, Lee and Chen 2012). Improvement on gas-liquid mass transfer can thus be achieved by changing to another type of gas distribution to the mixture.

In this research, four different air flow rates were tested to determine the influence of oxygen mass transfer on the performance of the autoxidation reaction of HMF. If oxygen mass transfer is indeed not limiting in this reaction, the results should be the same for different flow rates. For similar reaction conditions (T = 90°C, $[Co]_0$ = 0.03 M, $[HMF]_0$ ≈ 0.197 M, $[acetaldehyde]_0$ ≈ 0.24 M,), flow rate was varied. Reactions SB3 (100%; 353.9 mL/min), SB6 (50%; 176.97 mL/min), SB7 (25%; 88.49 mL/min) and SB8 (10%; 35.39 mL/min) were used for comparison.

In reaction SB8 ($Q_{air}$ = 35.39 mL/min) a decrease in HMF conversion was measured, compared to the reactions with a higher flow rate, see Figure 27. This is an indication that mass transfer can become limiting compared to the reaction rate if the oxygen supply is low. The oxygen supply was calculated for the different reactions according to the ideal gas law ((f6), paragraph 3.2.3); the results are displayed in Table 29. It is clear from this table that the oxygen supply in reaction SB8 is

low compared to the amount of HMF present in the mixture, which is likely to incur a low mass transfer rate.

*Table 29 Oxygen supply for different air flow rates in the semi-batch reactor*

| EXP. NO. | | SB3 | SB6 | SB7 | SB8 |
|---|---|---|---|---|---|
| **$HMF_0$** | mmol | 9.27 | 9.48 | 9.62 | 9.13 |
| **AIR FLOW RATE** | mL/min | 354 | 177 | 88.5 | 35.4 |
| | | | | | |
| **OXYGEN SUPPLY** | mmol/min | 2.35 | 1.17 | 0.59 | 0.23 |
| | mmol in 30 minutes | 70.40 | 35.20 | 17.60 | 7.04 |

The fact that the reaction with the lowest air flow rate showed lower HMF conversion over time is according to literature: in the work of Chou and Lin it was shown that liquid phase oxidation of acetaldehyde is indeed controlled by mass transfer if the oxygen supply is low (Chou and Lin 1982). Also insufficient oxygen diffusion rate can deactivate the catalyst and cause the carbon radicals to dimerise and form humins (Partenheimer 1995). The selectivity towards X is indeed largest for the reaction at lowest flow rate, see Figure 28b. Since mass transfer rate is also dependent on the interfacial area, reactions with bubbles that are better dispersed in the mixture should be tested to confirm this statement. The perforated or porous plate bubble column reactor in the work of Lau et al gives better mass transfer results due to the fact that the bubbles are distributed better over the liquid mixture and interfacial area is enlarged. In a microreactor the interfacial area is very high and mass transfer limitations are greatly reduced so reaction rate limitations should decrease by operation in flow.

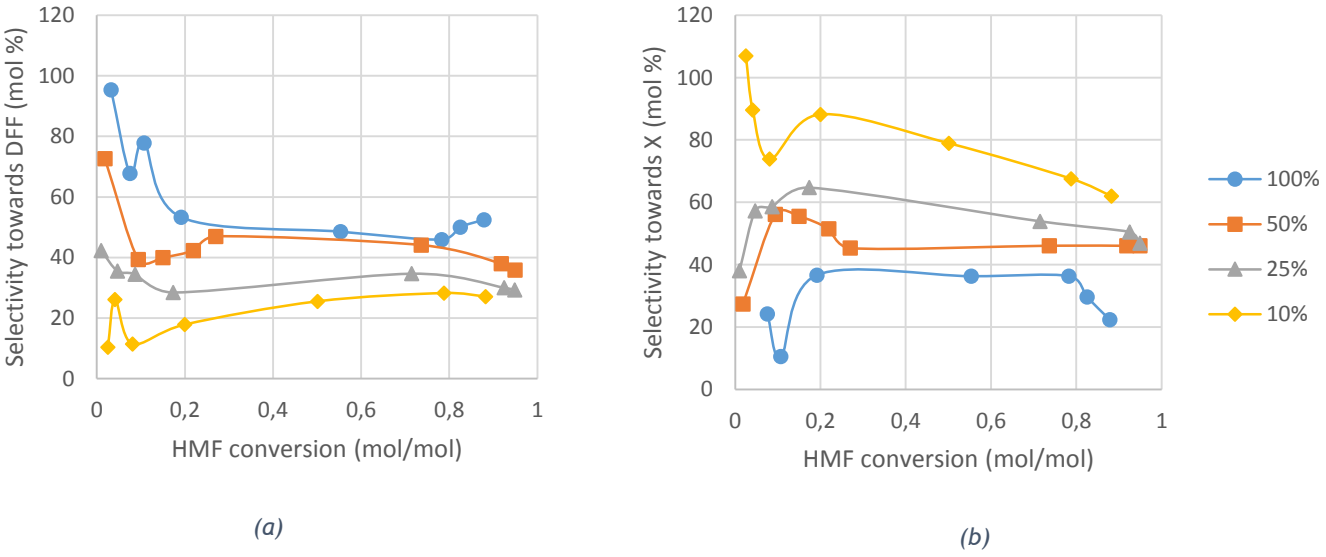


*Figure 28 Selectivity towards DFF (a) and X (b) as a function of HMF conversion in the reactions at different flow rates. Negative data points are not plotted since they have no value for the purpose of this research.*

Higher oxygen supply is at hand at higher air flow rates and $k_La$ is improved (Lau, Lee and Chen 2012), so in line with the reasoning that the highest flow rate is expected to give the highest reaction rate. Figure 27 showed us the contrary since the rate of reaction at 100% of full range flow rate was lower than that of the reactions at 25% and 50% full range flow rate. Cold flow experiments were performed at room temperature to determine the influence of flow rate on the bubble size. A three necked flask was filled with 50 mL water; air was introduced in the same manner as for the semi-batch experiments. Pictures were taken with fast shutter to catch the bubble size at the right time, see Figure 29. These experiments showed that bubble sizes indeed differed for different flow rates. It is clearly visible that the bubble sizes at 25% and 50% full range flow rates are similar while the bubble is much larger at 100% flow rate resulting in a low interfacial area which in turn tends to give a low mass transfer rate.

The importance of mixing should be emphasised as well. No stirrer was used during the experiments in the semi-batch reactor because the mixing caused by the air flow was considered to be sufficient. At low flow rate, however, the air flow becomes too small to enable good mixing. Combined with low $k_La$ at low air flow rate, this results in lowest HMF conversion in this set of experiments (entries 3 (353.9 mL/min), 6 (176.97 mL/min), 7 (88.49 mL/min) and 8 (35.39 mL/min)), as is clearly visible in Figure 27.

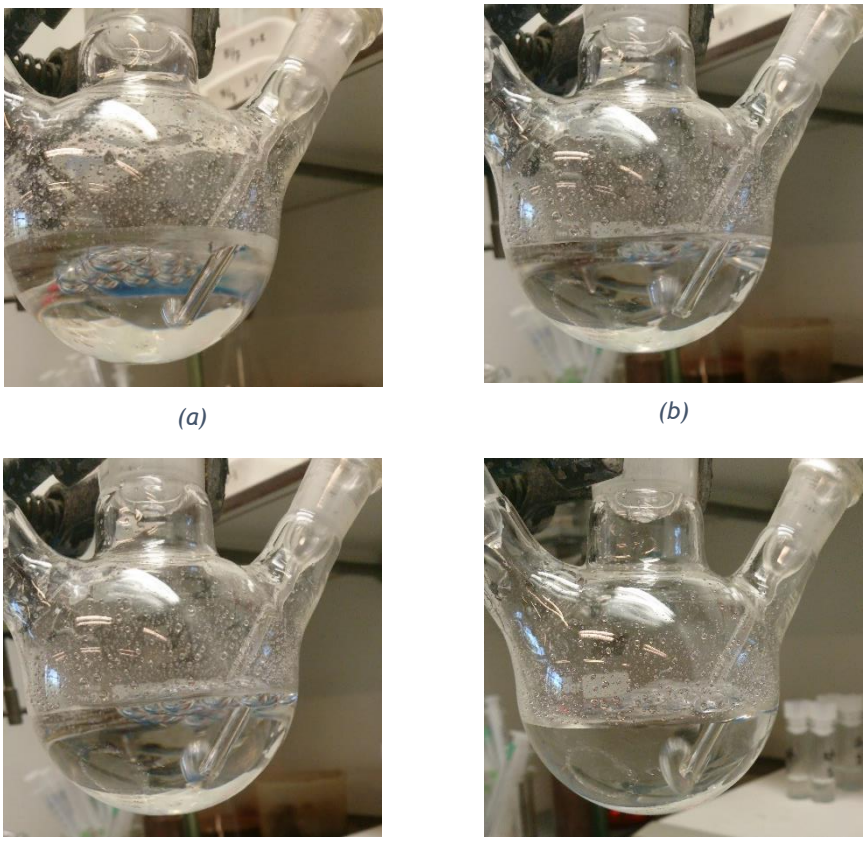

*(a)* *(b)*

*(c)* *(d)*

*Figure 29 Bubble sizes at (a) 10%; 35.39 mL/min (b) 25%; 88.49 mL/min (c) 50%;176.97 mL/min and (d) 100%; 353.9 mL/min.*

As was briefly mentioned above and is supported by literature the selectivity towards products X of pathway 2 is higher when oxygen supply is low (Partenheimer 1995). Like was explained above, the reaction at the highest air flow rate suffered from mass transfer limitations due to a low interfacial area. The selectivity towards X, however, is lowest compared to the other reactions and the selectivity towards DFF is highest, see Figure 28. This indicates that high oxygen supply is beneficial for the performance of the reaction in terms of selectivity toward the desired products. A reaction with enhanced interfacial area at a flow rate of 100% full range should be performed to check whether this is indeed beneficial for the reaction rate and gives similar or better product yields.

### 4.3.2 Batch operation: influence of pressure

Reactions A18 (p = 20 bar) and A19 (p = 40 bar) show the influence of pressure in a complete batch wise operation in the autoclave (T = 73°C, $[Co]_0$ = 0.010 M, $[HMF]_0 \approx 0.185$ M, $[acetaldehyde]_0 \approx 0.23$ M). The limitation of a batch wise operation of an oxidation reaction with air is the chance of depletion in oxygen since there is no continuous supply of air. Indeed, when the oxygen supply is calculated for the reactions in the autoclave, a conversion of 75% to FFCA turns out to be the maximum if 20 bar pressure is used. Operation at 40 bar pressure supplies enough oxygen to be able to oxidise all the HMF present completely to FDCA. At higher pressure, according to the ideal gas law ((f6), §3.2.3), the oxygen concentration in the gas is higher. Since the reaction mixture was not stirred during the reaction, oxygen mass transfer is the same as oxygen diffusion. The diffusion rate and thus the mass transfer rate is enhanced at high oxygen concentration.

*Table 30 Oxygen supply under different pressures in the autoclave. $X_{max}$ is the maximum conversion towards DFF or FFCA that can be reached under these conditions.*

| **EXP. NO.** | | **18** | **19** |
|---|---|---|---|
| **$HMF_0$** | mmol | 9.33 | 9.03 |
| **AIR VOLUME** | mL | 50 | 50 |
| **PRESSURE** | bar | 20 | 40 |
| | | | |
| **OXYGEN SUPPLY** | mmol | 7.01 | 14.03 |
| $X_{HMF\text{-}DFF,\ MAX}$ | mol/mol | 1 | 1 |
| $X_{HMF\text{-}FFCA,\ MAX}$ | mol/mol | 0.75 | 1 |

When the concentration of HMF is plotted against reaction time (Figure 30) one can clearly see that a low oxygen supply accounts for a low reaction rate, as was stated before and is according to literature (Chou and Lin 1982, Partenheimer 1995). Semi-batch operation is therefore preferred over batch operation to prevent depletion in oxygen and enable 100% HMF conversion. If an autoclave is used with continuous air flow, reactions at high temperature and pressure can be performed to mitigate mass transfer limitations. If continuous operation is used, the air flow rate must be chosen such that oxygen supply is sufficient.

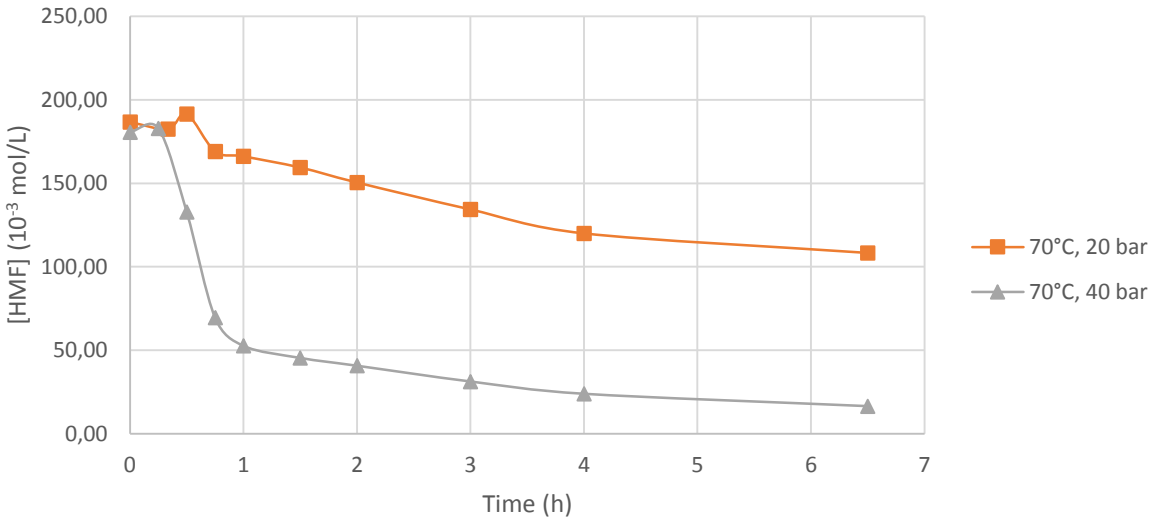


*Figure 30 HMF concentrations of reactions A18 (20 bar) and A19 (40 bar) as a function of the reaction time. $T_{set}$ = 125°C, $[Co]_0$ = 0.010 M, $[HMF]_0$ ≈ 0.185 M, $[acetaldehyde]_0$ ≈ 0.23 M*

## 4.4 Reaction kinetic limitations

The second assumption made at the beginning of this chapter considered the reaction of HMF to the desired products to be first order in HMF concentration. By performing reactions with different HMF concentrations, this was tested. The used air flow rate (88.49 mL/min) for this set of reactions was such that no mass transfer limitations occurred, as is shown in paragraph 4.3.1. Since the reaction rate constant is dependent on temperature, according to (f14) at the beginning of this chapter, the performance of the reaction at different temperatures was also investigated.

### 4.4.1 Influence of HMF concentration

From the experimental data of reactions with different initial HMF concentrations (SB11: 0.175 M in HMF, SB13: 0.373 M in HMF and SB14: 0.096 M in HMF) at similar reaction conditions (T = 90°C, $Q_{air}$ = 88.49 mL/min, $[Co]_0$ = 0.01 M, $[acetaldehyde]_0$ ≈ 0.23 M), the graph in Figure 31 was produced. The slopes of the three different lines seem similar at the slant part of the graph (i.e., over the first two hours), suggesting the rate of reaction is not dependent on HMF concentration under these conditions. The curve, however, also shows approximately an exponential decrease (i.e., at reaction time larger than 2 h), indicating indeed a first order dependence in HMF. To get an idea of what reaction order suits best, the rate constants for a zero, first and second order dependence in HMF were determined roughly. In this way the theoretical conversion could be calculated to see if it matched the experimental results. These calculations were made under the assumption that oxygen supply is sufficient: the reaction rate is independent of the oxygen concentration in the liquid. In Appendix IV: Calculations of the rate constants for different reaction orders, this is further explained. Further research on the kinetics of this reaction can provide us more information.

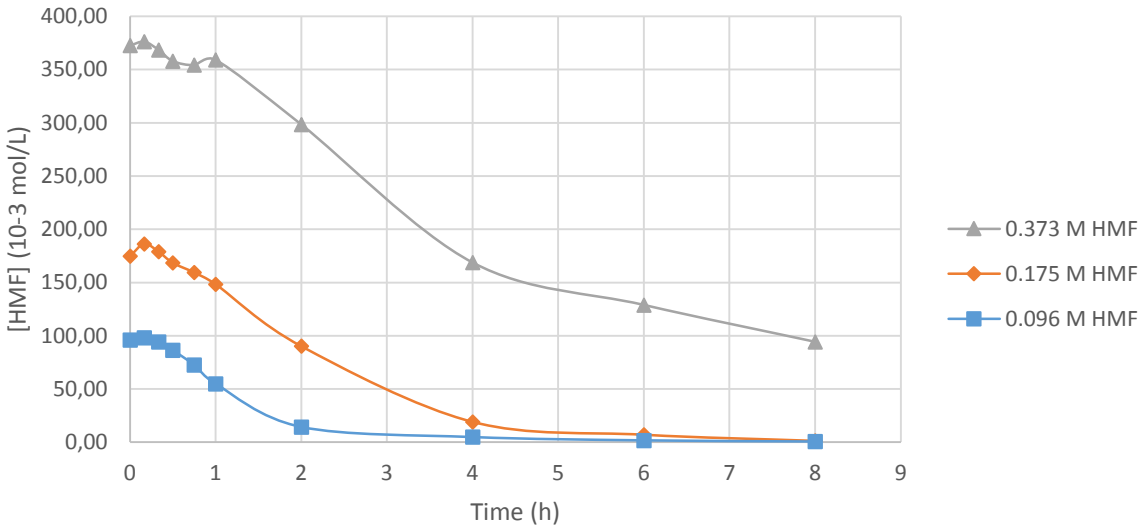


*Figure 31 HMF concentrations of reactions SB11 (0.175 M), SB13 (0.373 M) and SB14 (0.096 M) as a function of the reaction time. T = 90°C, $Q_{air}$ = 88.49 mL/min, $[Co]_0$ = 0.01 M, $[acetaldehyde]_0$ ≈ 0.23 M.*

To check whether assumption b is correct and the reaction rate is indeed first order in HMF, the conversion of HMF over time for three different initial concentrations of HMF is plotted in Figure 32. The theoretical first order conversions, calculated by (f13) in the beginning of this chapter are plotted in the same graph. Attention must be paid to the fact that the theoretical conversions calculated here are based on a combined reaction rate of pathway 1 towards the desired products and pathway 2 towards the side products. The reaction rate is given in equation (f15) that can be combined to equation (f16). That is,

$$r = k_{1,1}[HMF]^{\alpha} + k_{1,2}[HMF]^{\beta} \quad \text{(f15)}$$

$$r_1 = k_1[HMF]^{\gamma} \quad \text{(f16)}$$

In which $r$ is the combined reaction rate for both pathways with $k_{1,1}$ and $k_{1,2}$ as first order reaction rate constants for pathway 1 and 2, respectively. $\alpha$ and $\beta$ are the orders of the reactions towards the products and side products in HMF, respectively. $r_1$ is the apparent reaction rate with apparent reaction rate constant $k_1$ and apparent reaction order $\gamma$ in HMF.

At highest HMF concentration, the conversion shows most resemblance with the theory, meaning that the apparent reaction order is close to 1. The reaction rate is lowest at highest HMF concentration, because the oxygen supply is low compared to the HMF concentration. As was explained in paragraph 4.3.1, the reaction rate then becomes mass transfer controlled.

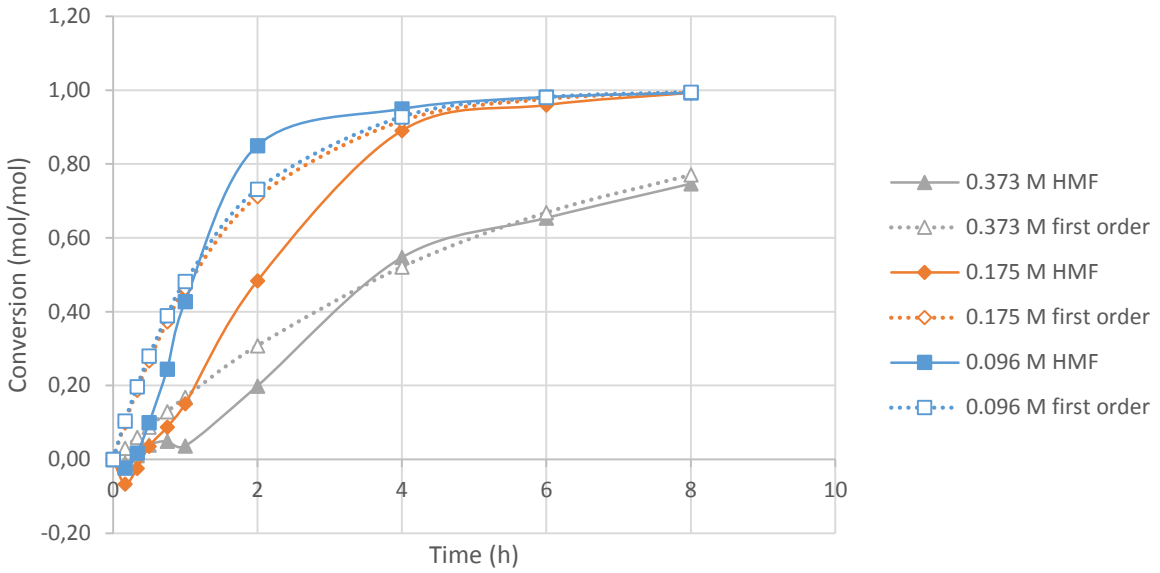


*Figure 32 HMF conversions of reactions SB11, SB13 and SB14 as a function of the reaction time. The dotted lines depict the apparent theoretical first order conversions. Reaction conditions are as specified in Figure 31.*

An interesting observation is that for the highest HMF concentration investigated (SB13: 0.373 M HMF), the concentration of and selectivity towards the side products X is lowest, see Figure 33. If the selectivity towards the side products ($\sigma_X$) is calculated by equation (f17), one can easily see that the order of pathway 1 must be higher than the order of pathway 2 to explain the experimental data. Reactions with even higher HMF concentrations should clarify this.

$$\sigma_X = \frac{k_{1,2}[HMF]^{\beta}}{k_{1,1}[HMF]^{\alpha}} = \frac{k_{1,2}}{k_{1,1}}[HMF]^{\beta-\alpha} \qquad \text{(f17)}$$

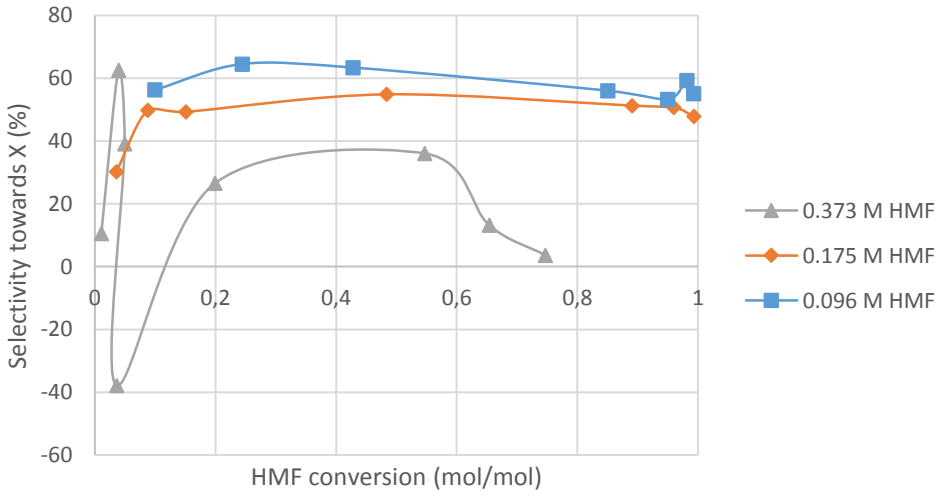


*Figure 33 Selectivity towards X as a function of HMF conversion.*

### 4.4.2 Influence of temperature

The results for the reactions at different temperatures are as expected, see Figure 34 and 35 According to equation (f14), a lower temperature gives a lower reaction rate and less HMF conversion, thus a minimum temperature is required for the reaction to perform well. This shows that when the oxygen supply is sufficient, the reaction tends to be kinetically controlled at lower temperatures. If oxygen mass transfer limitation is still important, the reaction tends to be in a regime controlled by mass transfer combined with kinetics.

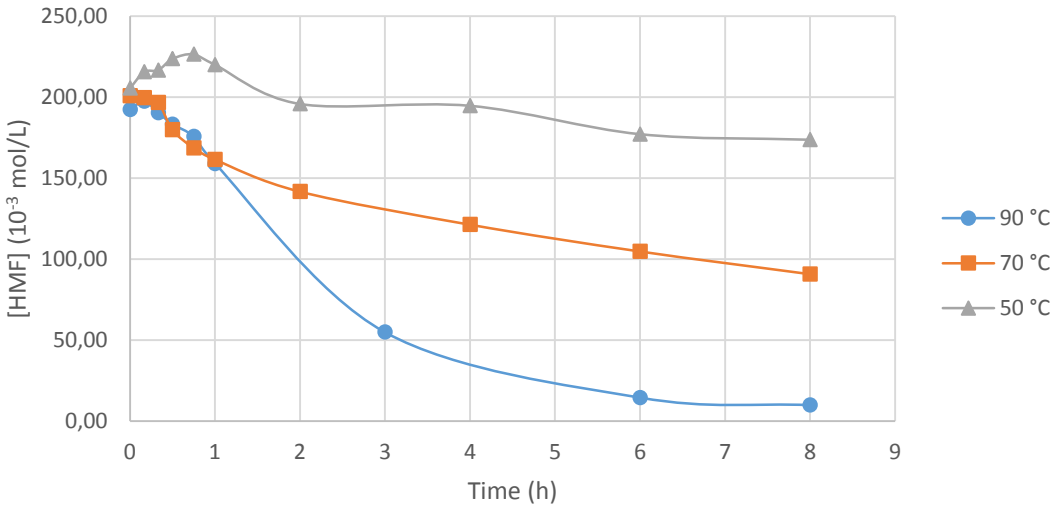


*Figure 34 HMF concentrations of reactions SB7 (90°C), SB9 (70°C) and SB10 (50°C) at atmospheric pressure as a function of the reaction time. $Q_{air}$ = 88.49 mL/min, $[Co]_0$ = 0.03 M, $[HMF]_0 \approx$ 0.20 M, $[acetaldehyde]_0 \approx$ 0.23 M.*

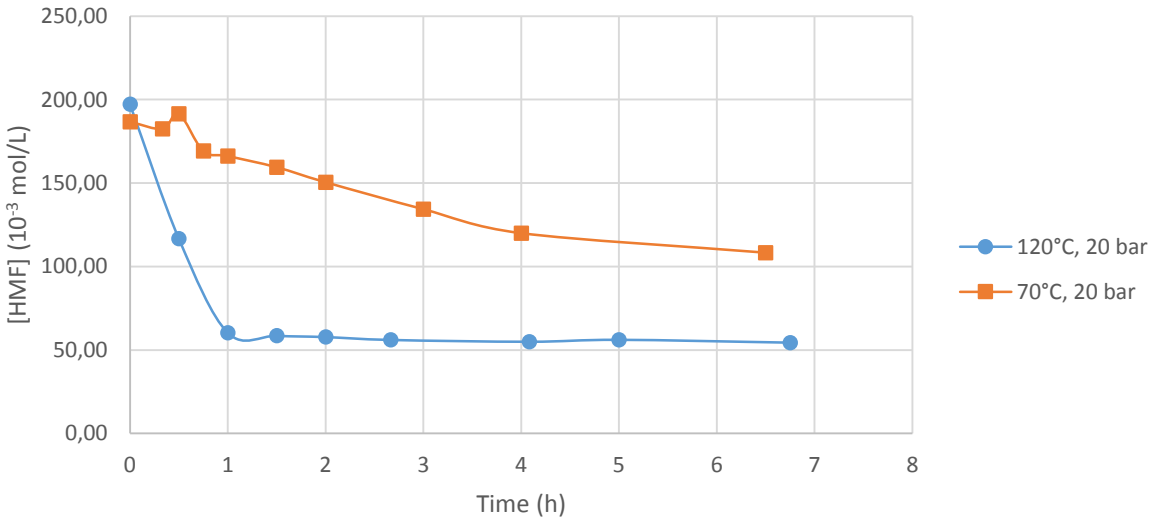


*Figure 35 HMF concentrations of reactions A16 (120°C) and A18 (70°C) at 20 bar as a function of reaction time. p = 20 bar, $[Co]_0$ = 0.01 M, $[HMF]_0 \approx$ 0.192 M, $[acetaldehyde]_0 \approx$ 0.232 M. The maximum HMF conversion in reaction A16 is 70%, which is already reached after one hour reaction time.*

## 4.5 Product yields

The decrease in HMF concentration and increase in desired product concentrations throughout the course of the reaction in semi-batch operation followed a path as was expected, see Figure 36 for a typical example. The DFF concentration remains almost constant from a certain point in the reaction, while FFCA and FDCA concentrations increase. This means that the DFF concentration is in "equilibrium" during part of the reaction: the amount of HMF converted to DFF is roughly the same as the amount of DFF converted to FFCA. This concentration profile can be observed in reactions with sufficient oxygen supply ($Q_{air}$ = 176.97 or 88.49 mL/min), high enough operation temperature of 90°C, sufficient acetaldehyde ($[acetaldehyde]_0 \approx 0.23$ M) and catalyst concentration (0.01 or 0.03 M Co) and medium or low HMF concentration ($[HMF]_0 < 0.20$ M).

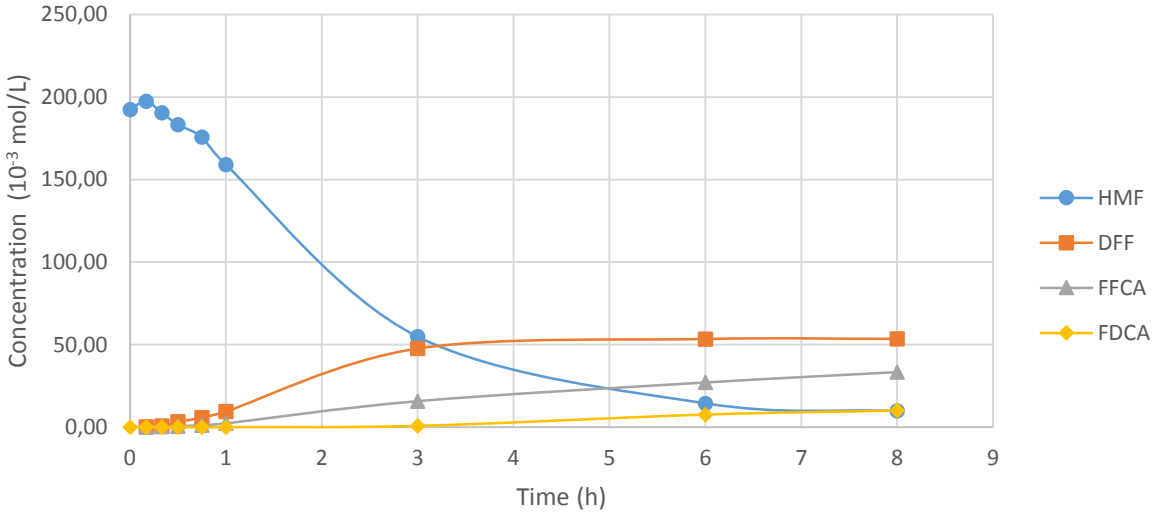


*Figure 36 Change in HMF, DFF, FFCA and FDCA concentration in reaction SB7 over time. T = 90°C, $Q_{air}$ = 88.49 mL/min, $[Co]_0$ = 0.03 M, $[HMF]_0$ = 0.192 M, $[acetaldehyde]_0$ = 0.232 M.*

The concentrations of the desired products were combined and plotted in the same graph as the concentration of side products. Not until after 6 hours the concentration of desired products exceeds that of the side products. Oxygen supply and HMF and catalyst concentration have an influence on the selectivity towards the desired product, as will be further outlines below.

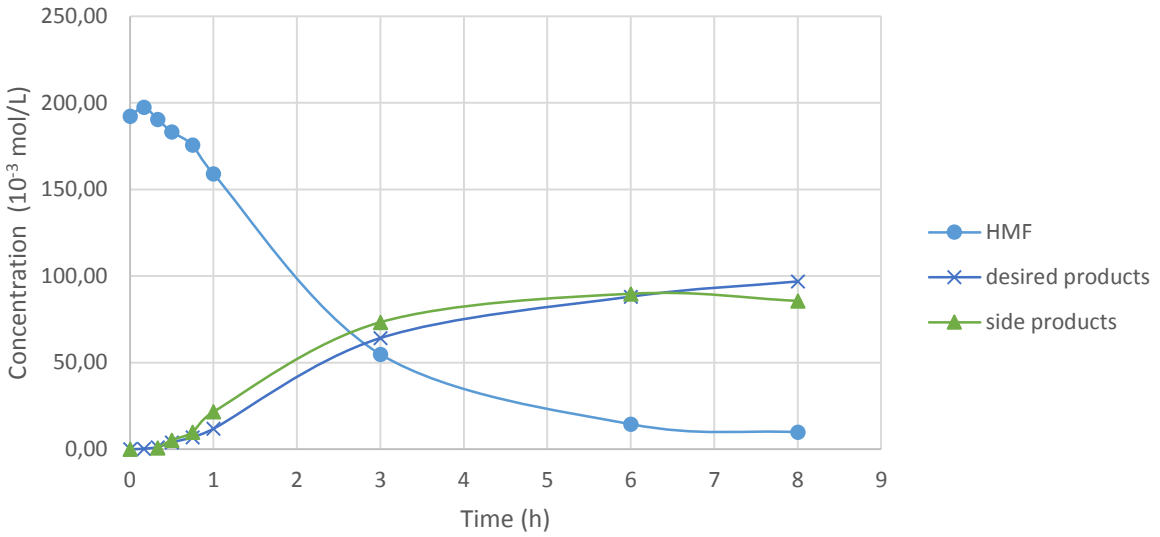


*Figure 37 Concentration profile of desired and side products as a function of reaction time. The reaction conditions are as described in Figure 36.*

Operation at a catalyst concentration of 0.01 M Co showed a maximum in DFF yield (32.7 %) around 4.5 h reaction time, indicating that the reaction had reached a further state in the same reaction time. With this catalyst concentration also the highest HMF conversion was achieved (99.5 %) in this research. From Figure 25 it is clear that a catalyst concentration of 0.01 M Co is favoured over a concentration of 0.03 M Co because it shows higher selectivity towards DFF and lower selectivity towards the side products.

In a reaction with the optimal catalyst concentration of 0.01 M Co, the maximum DFF yield (53 %) reached in this research, was achieved, at high HMF concentration (0.373 M HMF). In paragraph 4.4.1 it was explained that higher HMF concentration favours the formation of the desired products (Figure 33) and therefore it is logical that highest DFF yield is achieved in this experiment (SB13).

The maximum FFCA yield achieved in this research was 19.2 %, remarkably achieved in an experiment at high flow rate (353.9 mL/min) that had showed to be limited by mass transfer. The DFF yield (46.1 %) was also high in this experiment. As was explained in paragraph 4.3.1 high oxygen supply results in better selectivity towards the products.

## 4.6 Process intensification

As was discussed in the previous paragraphs the reaction rate of HMF to DFF and further oxidation products has shown to be mass transfer controlled at relatively lower oxygen supply in the semi-batch reactor (§4.3). At low temperatures and low initiator and catalyst concentrations, the reaction tends to be kinetically controlled (§4.1 and §4.4). In a microreactor, mass transfer limitations are greatly reduced (Jähnisch, et al. 2004), making it a very suitable reactor type for this reaction upon operation at a suitable temperature, and optimal initiator and catalyst concentration. Next to that, oxygen supply must be sufficient. The parameters that are important for increased yield of the desired products are, besides these, residence time and HMF concentration, as will be further outlined in this paragraph.

### 4.6.1 Minimum HMF conversion desired for optimal product yield

The selectivity towards the first oxidation product (DFF) is approximately constant between HMF conversions of 20% to 80% for all the reactions performed in semi-batch reactor and autoclave. See Figure 25a and Figure 28a for typical examples; in these figures the selectivity of DFF is plotted against the HMF conversion for several reaction entries. The selectivity towards the further oxidation products FFCA and FDCA increases with HMF conversion for all the reactions performed in semi-batch reactor and autoclave. For every aforementioned reaction it is true that the higher the HMF conversion, the higher the product concentrations in the reaction mixture. Nevertheless, a minimum of 20% HMF conversion is desired to achieve the best selectivity towards DFF. In addition to that the “excess” in HMF that was mentioned in paragraph 4.2.2, has then disappeared and does not interfere in the calculations.
Conversion is dependent on reaction time (according to (f13) at the beginning of this chapter) and therefore a minimum residence time in the microreactor must be assured to achieve a minimum HMF conversion of 20%. This minimum residence time is dependent on the HMF concentration: the higher the HMF concentration the longer it takes to achieve the minimal 20% conversion, see Figure 32. High HMF concentration on the other hand gives a lower selectivity towards X, which is also desired. Reaction time can be influenced by changing the length of the capillary and the air and liquid flow rates as well.

All in all a residence time of around 1 hour should be facilitated to ensure 20% HMF conversion at atmospheric pressure (Figure 23 and Figure 32). Unfortunately the present microreactor setup is limited by the length of the microreactor and flow rates of air and reaction mixture. For that reason a maximum residence time of 35 minutes could be achieved, see Table 31. In this table the conditions of the reactions discussed in this paragraph are summarised. Due to the HMF “excess” at low conversion, no clear conclusion can be derived from the change in HMF concentration over time in the reactions in the microreactor. Therefore it is decided to mainly focus on the product yields, which show nice results, see Figure 38. The yields displayed in the graphs are based on the DFF and FFCA concentrations after at least 2.5h running time to enable the reaction under slug flow in the

microreactor to stabilise. In all the performed reactions in the microreactor DFF and FFCA formation was detected; formation of FDCA was detected in none of the reactions.

*Table 31 Reaction conditions for the reactions that were compared for process intensification. In the right half of the table the yields of DFF and FFCA are given that were used to create the graph in Figure 39.The yields given for the microreactor are average values.*

| NO. | $[HMF]_0$ (M) | [Co] (M) | T (°C) | $Q_{AIR}$ (ML/MIN) | $Q_{LIQ.}$ (ML/MIN) | P (BAR) | TIME (MIN) | $\eta_{DFF}$ (mol %) | $\eta_{FFCA}$ (mol %) |
|---|---|---|---|---|---|---|---|---|---|
| **SB9** | 0.201 | 0.03 | 70 | 88.49 | - | 1.0 | 30 | 1.27 | 0.20 |
| **SB11** | 0.175 | 0.01 | 90 | 88.49 | - | 1.0 | 30 | 2.28 | 0.20 |
| **A16** | 0.197 | 0.01 | 125 | - | - | 20 | 30 | 12.12 | 0.60 |
| **A18** | 0.187 | 0.01 | 75 | - | - | 20 | 30 | 0.40 | 0.06 |
| **M20** | 0.189 | 0.01 | 70 | 0.129 | 0.033 | 1.48 | 24.7 | 1.71 | 0.39 |
| **M21** | 0.198 | 0.01 | 70 | 0.110 | 0.033 | 1.72 | 35.1 | 0.12 | 0.24 |
| **M22** | 0.211 | 0.01 | 70 | 0.097 | 0.017 | 1.48 | 34.8 | 1.74 | 0.52 |
| **M23** | 0.185 | 0.01 | 90 | 0.126 | 0.033 | 1.56 | 24.6 | 4.67 | 0.88 |

The residence time in the microreactor, that is equal to the reaction time, was varied by changing the gas and liquid flow rate. A longer residence time does not show any increase in DFF yield, FFCA yield is indeed increased. It is clear that at a reaction temperature of 90°C, the reaction performance is better than operation at 70°C in the capillary microreactor. The results for product yield of reaction M21 are out of the ordinary. This might be caused by the fact that the samples from reaction M21 were placed in the HPLC on one Friday afternoon and were not measured until Sunday night. The reaction samples have shown to degrade when they are left in the HPLC for a longer period of time. The reaction should be performed in duplicate to shown if this is indeed the cause.

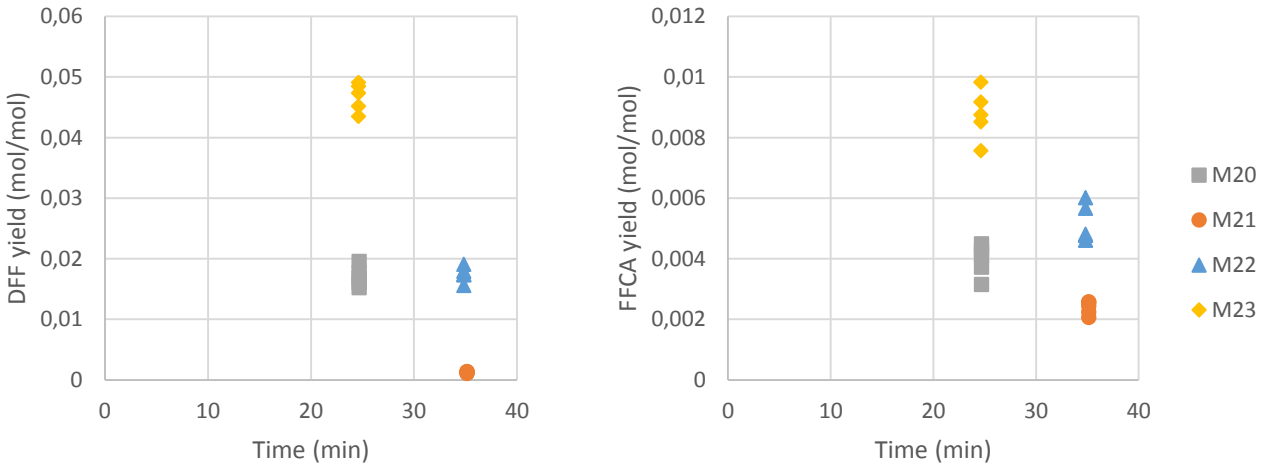


*(a)* *(b)*

*Figure 38 DFF (a) and FFCA (b) yield as a function of reaction time for reaction entries M20-23.*

### 4.6.2 Increased DFF and FFCA yield for operation in flow

Figure 39 gives a numerical and graphical overview of the increase in measured product yield when a reaction is performed in the microreactor compared to performance in the autoclave or semi-batch reactor under similar conditions. Medium (~70˚C) and high (90 or 125˚C) temperatures were tested in the different reactors (medium temperature: entry M20, A18 and SB9; high temperature: entry M23, A16 and SB11). In Table 31 the reaction conditions of these reactions are listed. The catalyst concentration in entry SB9 is higher than in entry SB11, but it was shown in paragraph 4.1.2 that the performance of the reaction is similar under these conditions.

The increase in yield is calculated according to equation (f8), based on the values displayed in Table 31 for similar reaction times. That is,

$$\Delta\eta = \frac{\eta_{M} - \eta_{A \text{ or } SB}}{\eta_{A \text{ or } SB}} \cdot 100\% \qquad \text{(f18)}$$

Where $\eta_M$ is the yield that is achieved in the microreactor and $\eta_{A\ or\ SB}$ is the yield after 30 minutes reaction time in the autoclave ($\eta_A$) or semi-batch reactor ($\eta_{SB}$).

| | DFF YIELD INCREASE | | FFCA YIELD INCREASE | |
|---|---|---|---|---|
| | medium T | high T | medium T | high T |
| **M towards A** | 327,78% | -61,47% | 578,13% | 46,17% |
| **M towards SB** | 34,17% | 104,77% | 93,95% | 348,13% |

*(a)*

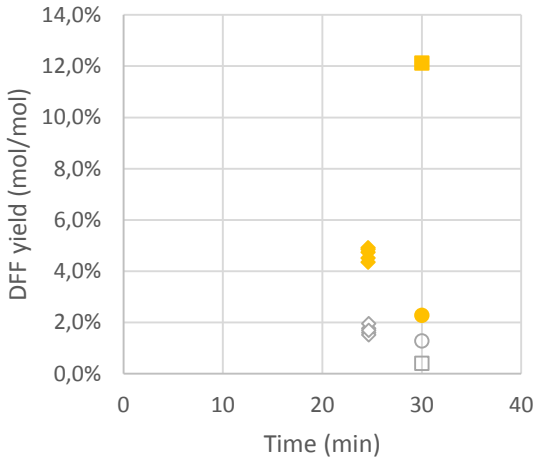


*(b)*

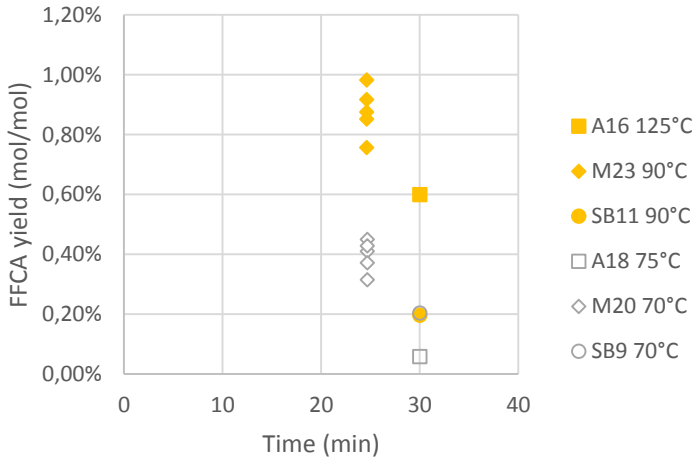


*(c)*

*Figure 39 Numerical (a) and graphical overview of the change in DFF (b) and FFCA (c) yield for the autoclave, microreactor and semi-batch reactor at medium (~70˚C) and high (90 or 125˚C) temperature. Entries SB9 (70˚C), A18 (75˚C) and M20 (70˚C) are used for medium temperature yield increase calculations in (a) and entries SB11 (90˚C), A16 (125˚C) and M23 (90˚C) for high temperature. The entries are as listed in Table 31. The temperature given for the autoclave is the set temperature of the hot plate.*

The product yields in the microreactor at medium temperature are better than in the semi-batch reactor and much better than in the autoclave. At high temperature the DFF yield in the autoclave exceeds that of the microreactor, because the temperature used in the autoclave was higher. Still, the FFCA yield is better in the microreactor. Again, higher yields than in semi-batch operation are achieved. This shows that oxygen mass transfer limitations play an important role and operation in a microreactor is therefore favoured, especially at lower operating temperatures. To enhance oxygen mass transfer even more, the pressure in the microreactor can be increased by installing a back pressure regulator at the outlet of the capillary.

Next to reduced mass transfer limitations, the microreactor offers reduced reaction times for reaction and kinetic studies due to easy change in conditions (i.e. variations in temperature and air and liquid flow rate). Temperature control in the microreactor is better compared to the autoclave since it takes around an hour for the reaction mixture to heat up in the autoclave. If it is desired to perform reactions at short residence time, operation in an autoclave is disfavoured. Using a microreactor is a safer operation mode than autoclave or semi-batch operation due to the small liquid volumes that are used, as was stated in paragraph 1.1.4 (Jähnisch, et al. 2004).

# 5. CONCLUSIONS

In this research the characteristics of the autoxidation reaction of HMF in acetic acid with a homogeneous Co/Mn/Br catalyst and acetaldehyde as initiator were explored. The aim was to investigate its potential to be intensified using a capillary microreactor. The behaviour of the reaction was primarily investigated in a semi-batch reactor (SB) at atmospheric pressure and in an autoclave (A). These results were compared to data obtained from fundamental experiments in the capillary microreactor (M).

Two reaction pathways were considered: the formation of DFF to subsequently FFCA and FDCA and the formation of unwanted side products X. The parameters that were varied in the performed reactions were acetaldehyde (A, SB), catalyst (SB) and HMF concentration (SB), temperature (A, M, SB), pressure (A) and flow rate (M, SB). The reactor type that was used for investigating the influence of these parameters is given in brackets.
A threshold for initiator and catalyst concentration had to be met in order to perform the reaction within hours. Varying HMF concentrations showed that the influence of side product formation on the overall reaction rate decreased with increasing HMF concentration. An increase in temperature resulted in an increase in reaction rate in all reactor types.

Although the reaction rate was not assumed to be limited by oxygen mass transfer from air to the liquid reaction mixture, experimental data showed the contrary. If oxygen supply is low, the reaction rate is indeed limited by mass transfer. Reactions performed at different air flow rates and at high HMF concentration in semi-batch operation and at different pressures in batch operation in an autoclave supplied proof for this statement: at low air flow rate, high HMF concentration or at low pressure the reaction rate decreased due to insufficient oxygen supply. In the semi-batch reactor this was caused by a decreased liquid mass transfer coefficient ($k_La$) due to small bubble sizes at low flow rate. In the autoclave insufficient oxygen supply was caused by a lower oxygen concentration in the gas phase at lower pressure and therefore slow molecular diffusion.
Mixing is an important aspect too: insufficient mixing causes low HMF conversion, especially when oxygen supply is low.

Since mass transfer limitations occurred at low oxygen supply, the reaction has potential to be intensified. The reaction rate can be increased upon operation in a microreactor. By changing air and liquid flow rates, a residence time of maximum 35 minutes in a 10 m capillary microreactor was achieved. This reaction time was insufficient to measure accurate HMF conversion and to achieve optimal DFF yield. Nonetheless, fundamental conclusions could be drawn to illustrate the effect of process intensification. For similar reaction time and conditions the DFF and FFCA yield showed an increase of respectively 34% and 94% at medium temperature (70°C), compared to the semi-batch

reactor. Compared to the autoclave under similar conditions and at 75°C set temperature, this increase was even 328% and 578%, respectively.

In order to enhance HMF conversion and product yields in the microreactor, the residence time should be increased to at least one hour. A better view on the actual effect of intensification can then be developed. The kinetic behaviour of the reaction is roughly explored in this research; a more detailed study should give more information on the reaction order in HMF for the two considered pathways. More detailed recommendations for further research are made in the next chapter.

# 6. RECOMMENDATIONS FOR FURTHER RESEARCH

Throughout chapter 4 some experiments came forth that can further support the claims that were made. These claims and experiments are listed below.

- Oxygen mass transfer is limiting at operation in semi-batch reactor at 100% (353.9 mL/min) because the interfacial area is small due to coalescence of the gas bubbles.
  *Experiment:* Performing the reaction at the same air flow rate with better dispersed liquid bubbles. If reaction rate is increased, gas to liquid mass transfer is enhanced due to increased interfacial area.

- Reaction rate in semi-batch operation is limited by internal mass transfer at low acetaldehyde concentration.
  *Experiment:* Performing the reaction at low acetaldehyde concentration and higher HMF concentration than used in this research. If reaction rate is increased, internal mass transfer is limiting.

- Selectivity towards desired products is increased at higher HMF concentration.
  *Experiment:* Performing the reaction with higher HMF concentrations than used in this research. If selectivity towards desired products is increased, the reaction order in HMF towards the desired products is higher than the reaction order in HMF towards unwanted side produtcs.

- The weight loss that was measured in the semi-batch reactor and the autoclave is caused by $CO_x$ formation and can be reduced by increased catalyst concentration.
  *Experiment:* Performing the reaction at 25% or 50% air flow rate (88.49 or 176.97 mL/min; for minimal mass transfer limitations) and higher catalyst concentration than used in this research. If weight loss is reduced, this can be accounted for by $CO_x$ formation.

Furthermore, a reaction in the autoclave at 90°C reaction temperature, instead of 125°C, should be performed to make a better comparison with the results of the reactions in the microreactor. Besides that, the reactions performed in the microreactor should be extended to collect more data. Increased residence time by lower flow rates or by using a longer capillary should result in higher HMF conversion and product yields. The advantages of operation in a microreactor are supported extra if more data are available.

Some general topics remained unclear during the course of this research and are suitable for future investigation, such as:

- *Closing the mass balance*: the composition of the reaction mixture should be clarified by further identification of side products formed. Mass spectrometry can give information on the structure of the unidentified compounds; the cause of the apparent "excess" in HMF at low HMF conversions can in that way be found. Formation of $CO_x$ should be measured, HMFCA formation should be investigated (e.g. by calibration of the compound) and another analytical method should be found that can distinguish between AMF and HMF to be able to close the mass balance.
- *Detailed kinetic studies*: determination of the reaction orders in HMF towards desired and side products and of the overall reaction order gives more information on the character of the reaction.

Changing the catalyst composition (i.e., addition of Zr) has proven to increase the selectivity towards the desired products (Partenheimer 2006). Variation in molar ratio of the used catalysts, e.g. increase in [Co], or addition of Zr should result in less formation of side products.

# REFERENCES


Bawn, C.E.H., and J.B. Williamson. “The oxidation of acetaldehyde in solution part I: The chemistry of the intermediate stages.” *Transactions of the Faraday Society*, 1950: 721-734.

Bawn, C.E.H., and J.B. Williamson. “The oxidation of acetaldehyde in solution part II: Kinetics and mechanism of the formation of peracetic acid.” *Transactions of the Faraday Society*, 1950: 735-743.

Bozell, Joseph J., and Gene R. Petersen. “Technology development for the production of biobased products from biorefinery carbohydrates - the US Department of Energy’s “Top 10” revisited.” *Green Chemistry*, 2010: 539-554.

Chou, Tse-Chuan, and Fwu-Shing Lin. “Effect of interface mass transfer on the liquid-phase oxidation of acetaldehyde.” *Chinese Journal of Chemistry*, 1982: 1295-1300.

Collinsona, S.R., and W. Thielemans. “The catalytic oxidation of biomass to new materials focusing on starch, cellulose and lignin.” *Coordination Chemistry Reviews*, 2010: 1854-1870.

Dam, Rene, Laszlo Sipos, Dirk Den Ouden, and Gert-Jan Gruter. “Furandicarboxylic acid (FDCA) a versatile building block for a very interesting class of polyesters.” In *Biobased Monomers, Polymers, and Materials*, by Patrick B. Smith and Richard A. Gross, 1-13. Washington DC: American Chemical Society, 2012.

Deuss, Peter J., Katalin Barta, and Johannes G. de Vries. “Homogeneous catalysis for the conversion of biomass and biomass-derived platform chemicals.” *Catalysis, Science & Technology*, 2014: 1174-1196.

Dolan, John. “HPLC Troubleshooting Guide.” *Advanced Chromatography Technologies Ltd.* 2012. http://www.ace-hplc.com (accessed July 7, 2015).

Gandini, Alessandro. “The irruption of polymers from renewable resources on the scene of macromolecular science and technology.” *Green Chemistry*, 2011: 1061-1083.

Geilen, Frank M.A., Barthel Engendahl, Andreas Harwardt, Wolfgang Marquardt, Jurgen Klankermayer, and Walter Leitner. “Selective and flexible transformation of biomass-derived platform chemicals by a multifunctional catalytic system.” *Angewandte Chemie International Edition*, 2010: 5510-5514.

Grushin, Vladimir, Leo Ernest Manzer, and Walt Partenheimer. Processes for preparing diacids, dialdehydes and polymers. USA Patent US 8,748,637 B2. 10 June 2014.

Jähnisch, Klaus, Volker Hessel, Holger Löwe, and Manfred Baerns. “Chemistry in Microstructured Reactors.” *Angewandte Chemie International Edition*, 2004: 406-446.

Kagan, M.J., and G.D. Lubarsky. “The intermediate stages of aldehyde oxidation I: The catalytic action of maganese catalyst in the various stages of the process of acetaldehyde oxidation.” *Journal of Physical Chemistry*, 1934: 837-846.

Kang, Eun-Sil, et al. “From lignocellulosic biomass to furans via 5-acetoxymethylfurfural as an alternative to 5-hydroxymethylfurfural.” *ChemSusChem*, 2015: 1179-1188.

Lau, Raymond, Pen Hui Venus Lee, and Tao Chen. “Mass transfer studies in shallow bubble column reactors.” *Chemical Engineering and Processing: Process Intesification*, 2012: 18-25.

Ma, Jiping, Zhongtian Du, Jie Xu, Qinghui Chu, and Yi Pang. “Efficient aerobic oxidation of 5-hydroxymethylfurfural to 2,5-diformylfuran, and synthesis of a fluorescent material.” *ChemSusChem*, 2011: 51-54.

Partenheimer, Walt. “Methodology and scope of metalbromide autoxidation of hydrocarbons.” *Catalysis Today*, 1995: 69-158.

Partenheimer, Walt. “The Complex Synergy of Water in Metal/Bromide Autoxidations.Part II. Effect of Water and Catalyst on the Aerobic Oxidation of Benzaldehydes and the Effect of Water on the Elementary Catalytic Pathways.” *Advanced Synthesis & Catalysis*, 2005: 580-590.

Partenheimer, Walt. “The high yield synthesis of benzaldehydes from benzylic alcohols using homogeneously catalyzed aerobic oxidation in acetic acid.” *Advanced Synthesis & Catalysis*, 2006: 559-568.

Partenheimer, Walt. “The structure of metal-bromide catalysts in acetic acid-water mixtures and its significance in autoxidation.” *Journal of Molecular Catalysis A: Chemical*, 2001: 29-33.

Partenheimer, Walt, and Vladimir Grushin. “Synthesis of 2,5-Diformylfuran and Furan-2,5-Dicarboxylic Acid by Catalytic Air-Oxidation of 5-Hydroxymethylfurfural. Unexpectedly Selective Aerobic Oxidation of Benzyl Alcohol to Benzaldehyde with Metal/Bromide Catalysts.” *Advanced Synthesis & Catalysis*, 2000: 102-111.

Resasco, Daniel E., Surapas Sitthisa, Jimmy Faria, Teerawit Prasomsri, and M. Pilar Ruiz. “Furfurals as chemical platform for biofuels production.” In *Heterogeneous Catalysis in Biomass to Chemicals and Fuels*, by David Kubička and Iva Kubičková, Chapter 5. Kerala, India: Research Signpost, 2011.

Saha, Basudeb, Saikat Duttaa, and Mahdi M. Abu-Omar. “Aerobic oxidation of 5-hydroxylmethylfurfural with homogeneous and nanoparticulate catalysts.” *Catalysis Science & Technology*, 2012: 79-81.

Sanborn, Alexandra. Oxidation of furfural compounds. United States Patent US 8,558,018 B2. 15 October 2013.

Teong, Siew Ping, Guangshun Yi, and Yugen Zhang. “Hydroxymethylfurfural production from bioresources: past, present and future.” *Green Chemistry*, 2014: 2015-2026.

Vaccaro, Luigi, Daniela Lanari, Assunta Marrocchia, and Giacomo Strappavecciaa. “Flow approaches towards sustainability.” *Green Chemistry*, 2014: 3680-3704.

van Putten, R.J., J.C. van der Waal, E. de Jong, C.B. Rasrendra, H.J. Heeres, and J.G. de Vries. “Hydroxymethylfurfural, a versatile platform chemical made from renewable resources.” *Chemical Reviews*, 2013: 1499-1597.

Vanoye, Laurent, et al. “A Safe and Efficient Flow Oxidation of Aldehydes with O2.” *Organic Letters*, 2013: 5978-5981.

Werpy, T., et al. *Top value added chemicals from biomass volume I: Results of screening for potential candidates from sugars and synthesis gas.* Oak Ridge: U.S. Department of Energy, 2004.

# APPENDIX I: AUTOXIDATION OF AN AROMATIC ALCOHOL

The mechanistic pathway of the oxidation of an aromatic alcohol group is similar to that of an aldehyde, as was explained in paragraph 1.1.3. The figure below gives the mechanism for phenol, but it works similarly for the alcohol group of HMF.

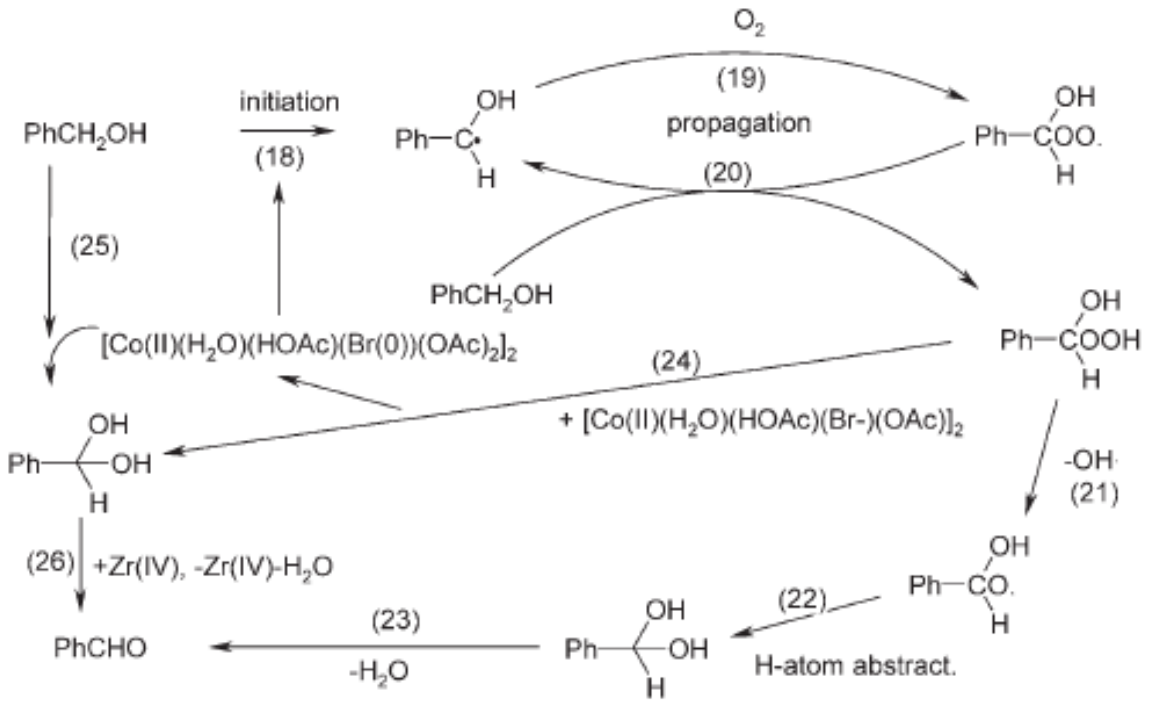


*Figure A-1 Mechanistic pathways of phenol oxidation. Adapted from (Partenheimer 2006).*

# APPENDIX II: EXPERIMENTAL DATA FOR CALIBRATION AND CALIBRATION CURVES

## HMF

*Table A-1 Experimental data for HMF calibration in HPLC.*

| | |
|---|---|
| CONCENTRATION STOCK SOLUTION | 40 g/L |
| SOLVENT | Acetic acid |
| CONCENTRATION IS SOLUTION | 20 g/L |
| SAMPLE VOLUME | 2000 µL |

| CONCENTRATION SAMPLE (g/L) | COMPOUND (µL) | IS (µL) | WATER (µL) |
|---|---|---|---|
| **0.0** | 0 | 100 | 1900 |
| **0.1** | 5 | 100 | 1895 |
| **0.25** | 12.5 | 100 | 1887.5 |
| **0.5** | 25 | 100 | 1875 |
| **0.75** | 37.5 | 100 | 1862.5 |
| **1.0** | 50 | 100 | 1850 |
| **1.2** | 60 | 100 | 1840 |
| **1.8** | 90 | 100 | 1810 |
| **2.0** | 100 | 100 | 1800 |
| **2.2** | 110 | 100 | 1790 |
| **2.8** | 140 | 100 | 1760 |
| **3.0** | 150 | 100 | 1750 |

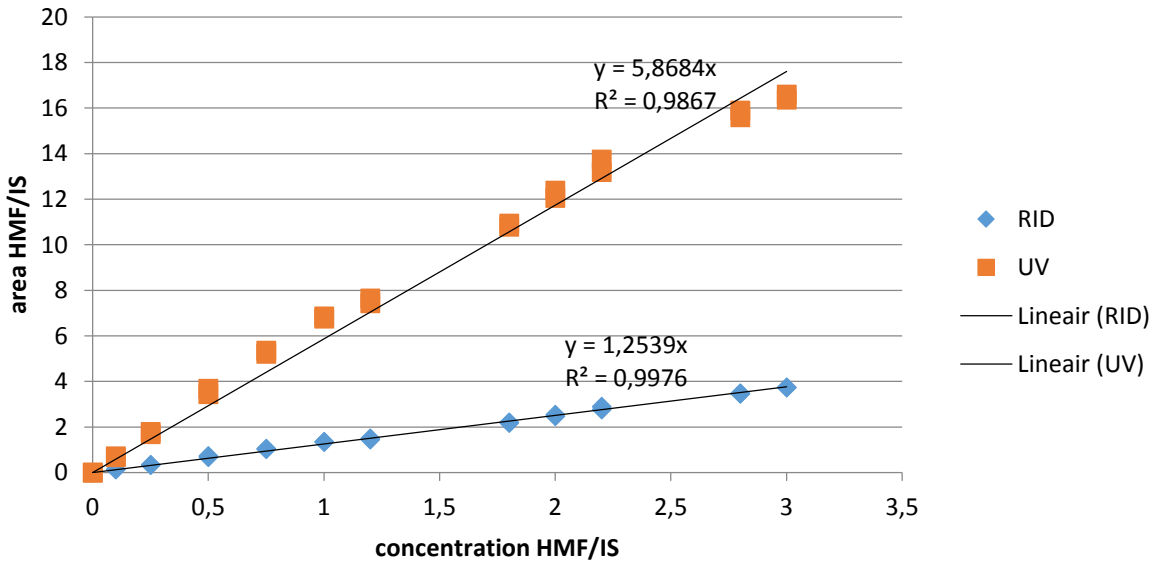


*Figure A-2 Calibration curve HMF calibration.*

## DFF

For the calibration of DFF, the stock solution of IS had to be diluted. This was performed in duplicate to preclude weighing errors. Three samples with the same concentration were therefore prepared and these indicated that the IS solution was diluted correctly. Since the pure DFF was delivered at 97% purity, an extra column is added to the table with the actual DFF concentration.

*Table A-2 Experimental data for DFF calibration in HPLC.*

| | |
|---|---|
| CONCENTRATION STOCK SOLUTION | 6 g/L |
| SOLVENT | Acetic acid |
| CONCENTRATION IS SOLUTION | 3 g/L |
| SAMPLE VOLUME | 300 µL |

| CONCENTRATION SAMPLE (g/L) | 97% pure | COMPOUND (µL) | IS (µL) | WATER (µL) |
|---|---|---|---|---|
| **0.0** | 0.00 | 0 | 100 | 200 |
| **0.1** | 0.10 | 5 | 100 | 195 |
| **0.25** | 0.24 | 12.5 | 100 | 187.5 |
| **0.5** | 0.49 | 25 | 100 | 175 |
| **0.75** | 0.73 | 37.5 | 100 | 162.5 |
| **1.0** | 0.97 | 50 | 100 | 150 |
| **1.5** | 1.46 | 75 | 100 | 125 |
| **2.0** | 1.94 | 100 | 100 | 100 |
| **2.5** | 2.43 | 125 | 100 | 75 |

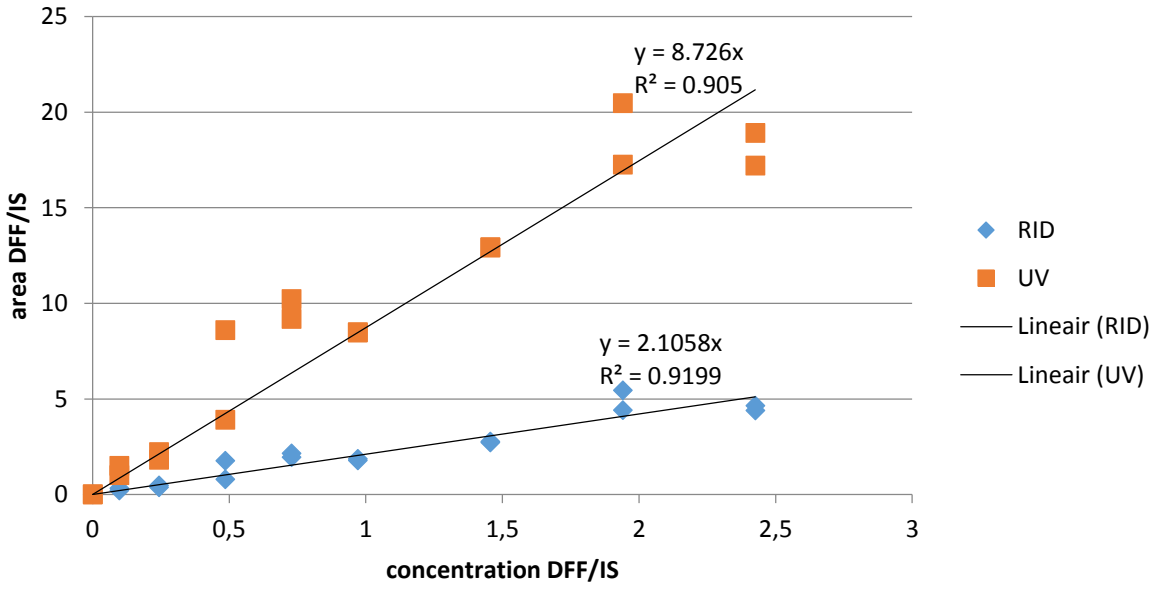


*Figure A-3 Calibration curve DFF calibration.*

## FFCA

The same dilution of the IS solution was used as the one for the DFF calibration so errors were already precluded and the samples could be made in duplicate instead of triplicate. The substance was not completely pure; it contained DFF and FDCA. The purity was determined by integration of these peaks in the calibration chromatograms and was determined to be 90.3%.

*Table A-3 Experimental data for FFCA calibration in HPLC. (1)*

| | |
|---|---|
| **CONCENTRATION STOCK SOLUTION** | 2.9 g/L |
| **SOLVENT** | 10% acetic acid in water |
| **CONCENTRATION IS SOLUTION** | 3 g/L |
| **SAMPLE VOLUME** | 300 µL |

| **CONCENTRATION SAMPLE** | | COMPOUND | IS | WATER |
|---|---|---|---|---|
| **(g/L)** | 90.3% pure | (µL) | (µL) | (µL) |
| **0.0** | 0.000 | 0 | 100 | 200 |
| **0.097** | 0,087 | 10 | 100 | 190 |
| **0.194** | 0,175 | 20 | 100 | 180 |
| **0.290** | 0,262 | 30 | 100 | 170 |
| **0.387** | 0,350 | 40 | 100 | 160 |
| **0.484** | 0,437 | 50 | 100 | 150 |
| **0.581** | 0,524 | 60 | 100 | 140 |
| **0.678** | 0,612 | 70 | 100 | 130 |
| **0.775** | 0,699 | 80 | 100 | 120 |

*Table A-4 Experimental data for FFCA calibration in HPLC. (2)*

| | |
|---|---|
| CONCENTRATION STOCK SOLUTION | 3 g/L |
| SOLVENT | 10% acetic acid in water |
| CONCENTRATION IS SOLUTION | 3 g/L |
| SAMPLE VOLUME | 300 µL |

| CONCENTRATION SAMPLE | | COMPOUND | IS | WATER |
|---|---|---|---|---|
| (g/L) | 90.3% pure | (µL) | (µL) | (µL) |
| **0.0** | 0.000 | 0 | 100 | 200 |
| **0.1** | 0.090 | 5 | 100 | 195 |
| **0.25** | 0.181 | 12.5 | 100 | 187.5 |
| **0.5** | 0.271 | 25 | 100 | 175 |
| **0.75** | 0.361 | 37.5 | 100 | 162.5 |
| **1.0** | 0.451 | 50 | 100 | 150 |
| **1.5** | 0.542 | 75 | 100 | 125 |
| **2.0** | 0.632 | 100 | 100 | 100 |
| **2.5** | 0.722 | 125 | 100 | 75 |

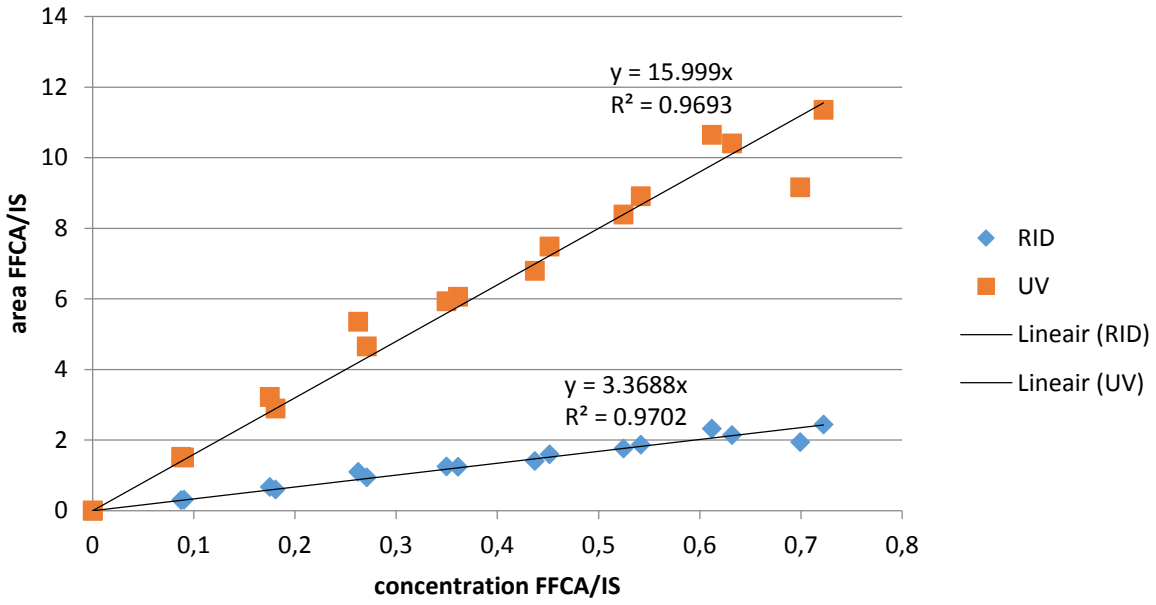


*Figure A-4 Calibration curve FFCA calibration.*

## FDCA

*Table A-5 Experimental data for FDCA calibration in HPLC.*

| | |
|---|---|
| CONCENTRATION STOCK SOLUTION | 1 g/L |
| SOLVENT | 10% acetic acid in water |
| CONCENTRATION IS SOLUTION | 20 g/L |
| SAMPLE VOLUME | 2000 µL |

| CONCENTRATION SAMPLE (g/L) | 97% pure | COMPOUND (µL) | IS (µL) | WATER (µL) |
|---|---|---|---|---|
| **0.0** | 0.00 | 0 | 100 | 1900 |
| **0.1** | 0.10 | 200 | 100 | 1700 |
| **0.2** | 0.19 | 400 | 100 | 1500 |
| **0.4** | 0.39 | 800 | 100 | 1100 |
| **0.6** | 0.58 | 1200 | 100 | 700 |
| **0.8** | 0.78 | 1600 | 100 | 300 |
| **0.9** | 0.87 | 1800 | 100 | 100 |

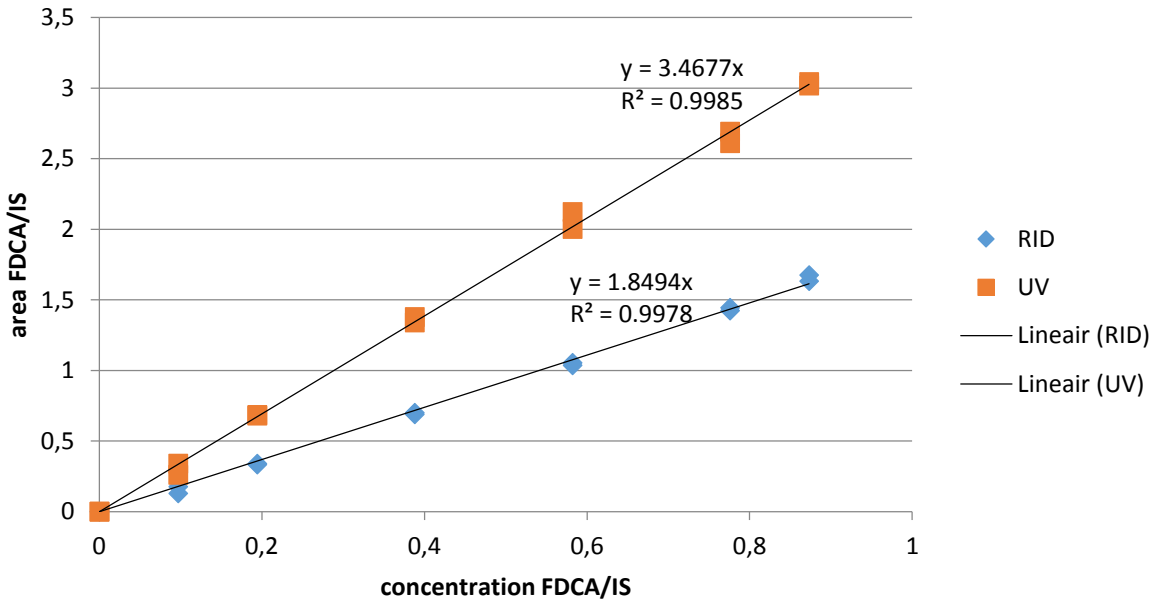


*Figure A-5 Calibration curve FDCA calibration.*

## AMF

The peak of AMF in the RID chromatogram as well as the UV chromatogram showed a huge shoulder. The peak was integrated until the point where the shoulder started, as was shown in Figure 26. If an AMF peak was observed in the chromatograms of one of the reaction samples, the same method was used.

*Table A-6 Experimental data for AMF calibration in HPLC.*

| | |
|---|---|
| **CONCENTRATION STOCK SOLUTION** | 5 g/L |
| **SOLVENT** | Acetic acid |
| **CONCENTRATION IS SOLUTION** | 20 g/L |
| **SAMPLE VOLUME** | 2000 µL |

| **CONCENTRATION SAMPLE** | | COMPOUND | IS | WATER |
|---|---|---|---|---|
| **(g/L)** | 97% pure | (µL) | (µL) | (µL) |
| **0.00** | 0.00 | 0 | 100 | 1900 |
| **0.25** | 0.24 | 100 | 100 | 1800 |
| **0.50** | 0.49 | 200 | 100 | 1700 |
| **0,75** | 0.73 | 300 | 100 | 1600 |
| **1.00** | 0.97 | 400 | 100 | 1500 |
| **1.25** | 1.21 | 500 | 100 | 1400 |
| **1.50** | 1.46 | 600 | 100 | 1300 |

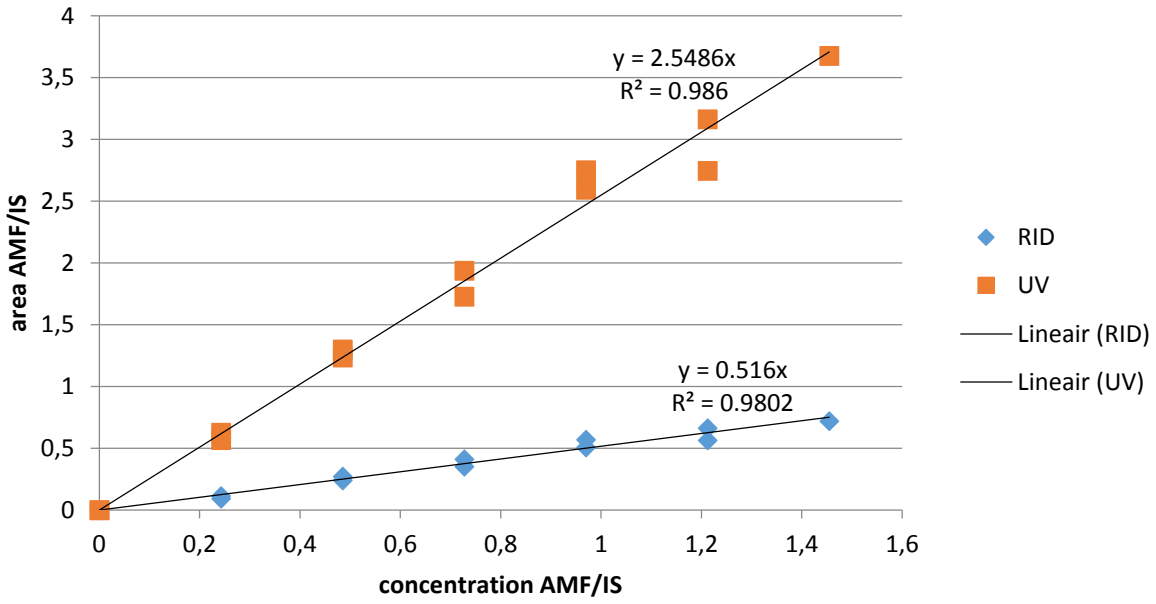


*Figure A-6 Calibration curve AMF calibration.*

# APPENDIX III: CALCULATION EXAMPLE FOR WEIGHT LOSS COMPENSATION

As mentioned several times throughout this thesis weight loss occurred in the reactions in the semi-batch reactor and the autoclave. It was assumed this was caused by solvent evaporation and that it happened linearly with time. The concentration of compound *i* at time *t* as measured by HPLC was compensated for this weight loss by multiplying it with compensation factor *C* according to equation (fA1). The compensated values are listed in Table 6-23 and Table 25-28 in chapter 3. *C* is calculated as 1 minus the weight loss at time *t*, in decimals, according to equation (fA2).

$$[\mathrm{i}]_{\mathrm{t,compensated}} = [\mathrm{i}]_{\mathrm{t,measured}} \cdot \mathrm{C} \qquad \text{(fA1)}$$

$$\mathrm{C} = 1 - \left(\frac{\text{weight loss}}{\mathrm{t_{total}}} \cdot \mathrm{t}\right) \qquad \text{(fA2)}$$

For example, the measured concentration of HMF after 5 hours in reaction 3 is 45.4 mmol/L. This reaction was run for 8 hours in total and suffered from a weight loss of 18.2%. The concentration, compensated for weight loss is then calculated as follows:

$$[\mathrm{HMF}]_{\mathrm{5h,compensated}} = 45.4\ \mathrm{mmol\ L^{-1}} \cdot \left[1 - \left(\frac{0.182}{8\ \mathrm{h}} \cdot 5\ \mathrm{h}\right)\right] = 40.3\ \mathrm{mmol\ L^{-1}}$$

In Table A-7 the weight losses that were measured for the reactions performed in the semi-batch reactor and the autoclave are listed. The total reaction time is given as well.

*Table A-7 Overview of the weight loss per reaction entry.*

| NO. | WEIGHT LOSS (%) | REACTION TIME (H) | FLOW RATE (ML/MIN) | NO. | WEIGHT LOSS (%) | REACTION TIME (H) | FLOW RATE (ML/MIN) |
|---|---|---|---|---|---|---|---|
| **SB1** | 14.7 | 5 | 353.9 | SB11 | 6.7 | 8 | 88.49 |
| **SB2** | no data | 8 | 353.9 | SB12 | 7.7 | 8 | 88.49 |
| **SB3** | 18.2 | 8 | 353.9 | SB13 | 6.2 | 8 | 88.49 |
| **SB4** | 7.2 | 3 | 353.9 | SB14 | 7.3 | 8 | 88.49 |
| **SB5** | 6.4 | 3 | 353.9 | A15 | no data | 6 | n/a |
| **SB6** | 9.9 | 8 | 176.97 | A16 | no data | 6.75 | n/a |
| **SB7** | 8.0 | 8 | 88.49 | A17 | 9.3 | 6.5 | n/a |
| **SB8** | 3.6 | 8 | 35.39 | A18 | 6.4 | 6.5 | n/a |
| **SB9** | 5.3 | 8 | 88.49 | A19 | 1.7 | 6.5 | n/a |
| **SB10** | 6.6 | 8 | 88.49 | | | | |

# APPENDIX IV: CALCULATIONS OF THE RATE CONSTANTS FOR DIFFERENT REACTION ORDERS

To roughly determine the order the reaction performed in this research, three different graphs were plotted to estimate the rate constant for zero, first and second order dependence in HMF, see below. The concentrations of HMF that these graphs are based on are given in Table 15, 17 and 18 in paragraph 3.2.1. Concentrations used in this appendix are always in mol/L. The rate constants that were found are displayed in Table A-8.

*Table A-8 Rate laws and reaction rate constants of reaction 10, 12 and 13 for different orders.*

| | **ZERO ORDER** | **FIRST ORDER** | **SECOND ORDER** |
|---|---|---|---|
| **Rate law** | $r_0 = k_0$ | $r_1 = k_1[HMF]$ | $r_2 = k_2[HMF]^2$ |
| **Integrated rate law** | $[HMF] = [HMF]_0 - k_0 t$ | $[HMF] = [HMF]_0\, e^{-k_1 t}$ | $\frac{1}{[HMF]} = \frac{1}{[HMF]_0} + k_2 t$ |
| **Rate constants** | | | |
| **0.096 M HMF** | 0.0705 M $s^{-1}$ | 0.6573 $s^{-1}$ | - |
| **0.175 M HMF** | 0.0582 M $s^{-1}$ | 0.6215 $s^{-1}$ | - |
| **0.373 M HMF** | 0.0636 M $s^{-1}$ | 0.1841 $s^{-1}$ | 0.9838 $M^{-1}$ $s^{-1}$ |

The rate constants were subsequently used to calculate the concentration and conversion for set times according to the integrated rate law. These values were plotted next to the conversion that was established experimentally to see if it matched, see Figure A-7.
The conversion calculated for zero order dependence is too low for all the reactions to match the results, so this is left out of the plot. Determination of the rate constant at second order dependence is only possible for reaction 13 with the highest initial HMF concentration. The conversion calculated by first order dependence matches best however for this reaction.
The experimentally established conversion of the other two reactions correspond to neither of the theoretical values, indicating a more complicated reaction order.

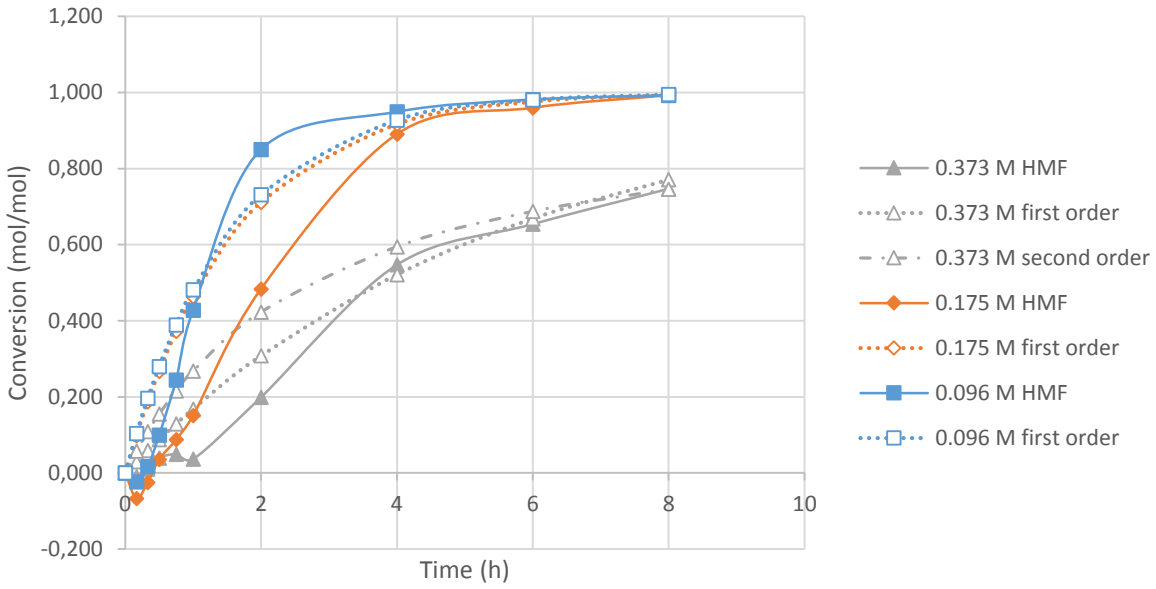


*Figure A-7 Experimental and theoretical conversion for different initial HMF concentrations.*

Zero order dependence: find $k_1$ by plotting [HMF] vs time; this should be linear with slope $-k_1$, see Figure A-8. For 0.096 M HMF the slope of the line between 0.75 and 1 h is used as a value for $k_1$; for 0.175 M HMF and 0.373 M HMF the slope between 1 and 2 h and 1 and 4 h was used respectively.

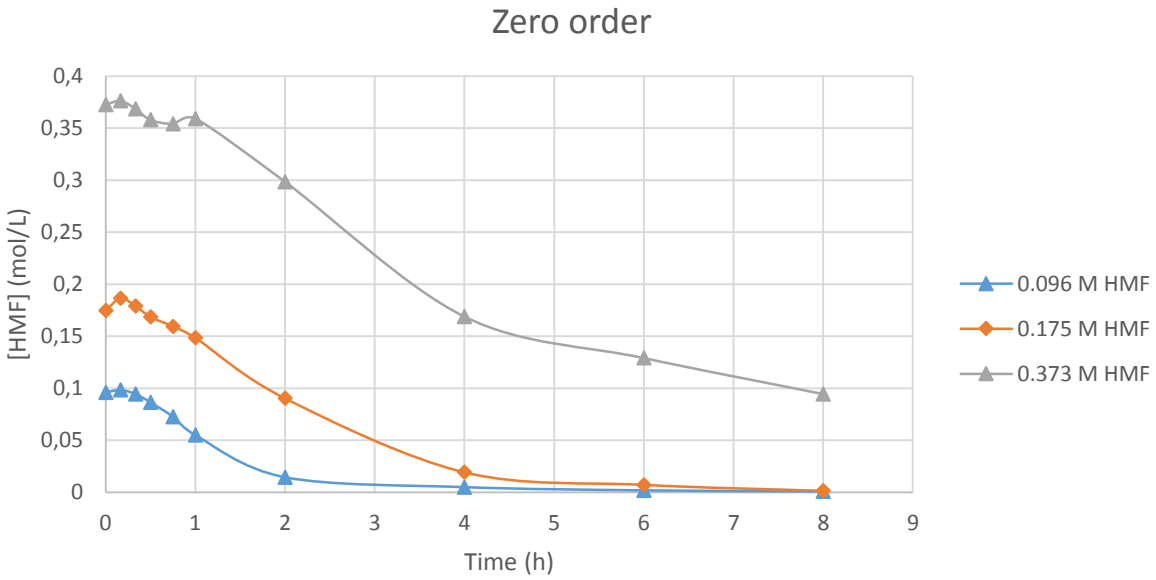


*Figure A-8 Determination of $k_0$ as zero order rate constant. HMF concentrations are adapted from Table 15, 17 and 18 in paragraph 3.2.2.*

First order dependence: find $k_1$ by plotting ln[HMF] vs time; this should be linear with slope $-k_1$, see Figure A-9.

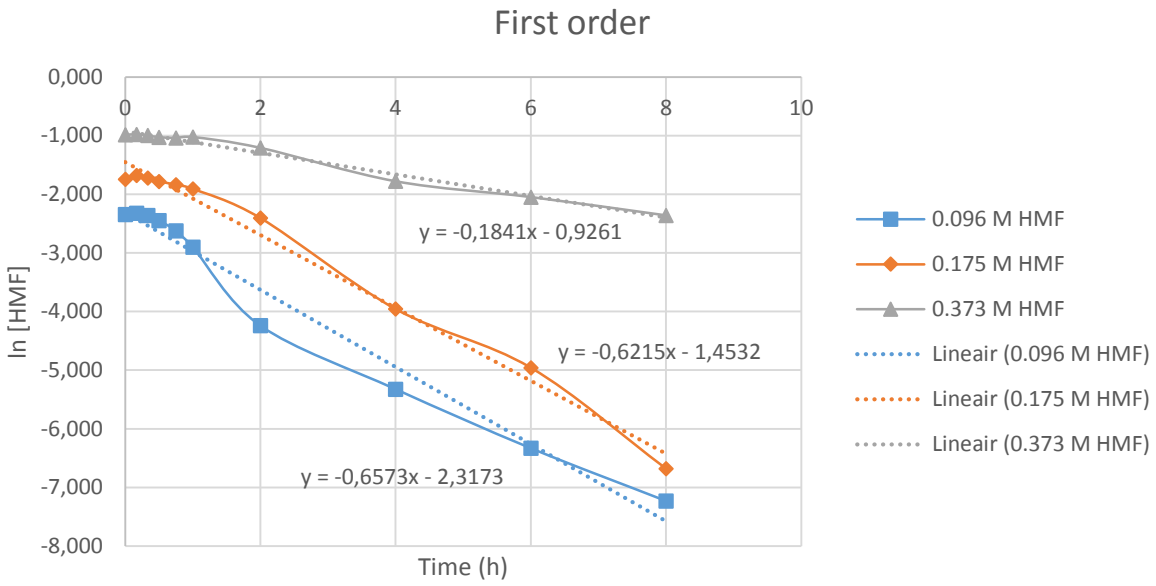


*Figure A-9 Determination of $k_1$ as first order rate constant. HMF concentrations are adapted from Table 15, 17 and 18 in paragraph 3.2.2.*

Second order dependence: find $k_1$ by plotting 1/[HMF] vs time; the curve should be linear with a slope of $k_2$, see Figure A-10. The graphs of 0.096 M HMF and 0.175 M HMF show exponential increase, meaning that second order is not possible in this case.

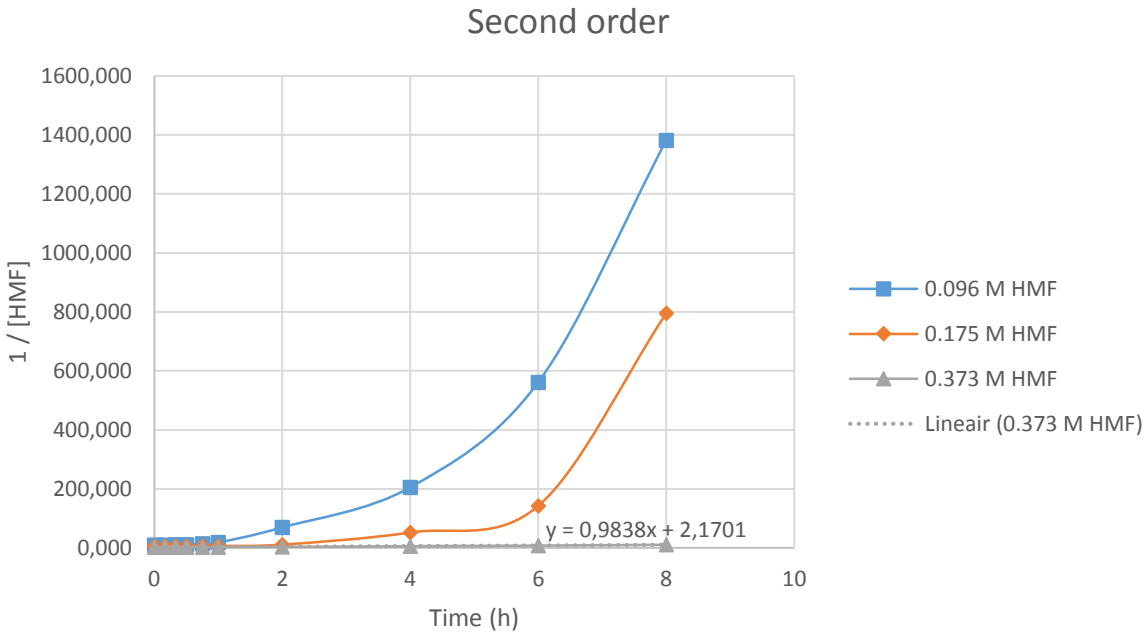


*Figure A-10 Determination of $k_2$ as second order rate constant. HMF concentrations are adapted from Table 15, 17 and 18 in paragraph 3.2.2.*